



Adsorption and determination of Lead in water and human urine samples based on $Zn_2(BDC)_2(DABCO)$ MOF as polycaprolactone nanocomposite by suspension micro solid phase extraction coupled to UV–Vis spectroscopy

Negar Motakef Kazemi^{a,*} and Masomeh Odar^b

^a Department of Medical Nanotechnology, Faculty of Advanced Sciences and Technology, Tehran Medical Sciences, Islamic Azad University, Tehran, Iran.

^b Department of Nanochemistry, Faculty of Pharmaceutical Chemistry, Tehran Medical Sciences, Islamic Azad University, Tehran, Iran

ARTICLE INFO:

Received 25 May 2021

Revised form 23 Jul 2021

Accepted 9 Aug 2021

Available online 28 Sep 2021

Keywords:

Lead,
Metal organic framework,
Polycaprolactone,
Nanocomposite,
Adsorption,
Suspension-micro-solid phase
extraction procedure

ABSTRACT

Today, the safety of water resource is the most important challenges which was reported by health and environment organizations. Water pollution can be created by hazardous contaminants of environmental pollutions. Lead as a heavy metal has carcinogenic effects in humans. Metal organic framework (MOF) is a highly porous material with different application. The $Zn_2(BDC)_2(DABCO)$ is a good candidate of MOF based on zinc metal (Zn-MOF) with potential adsorption/extraction. In this work, $Zn_2(BDC)_2(DABCO)$ MOF as polycaprolactone (PCL) nanocomposite were applied for lead adsorption/extraction from 50 mL of aqueous solution by ultra-assisted dispersive suspension-micro-solid phase extraction procedure (USA-S- μ -SPE) at pH=8. The samples were characterized by the FTIR, the XRD analysis, the FE-SEM and the BET surface area. The effect of parameters was investigated on lead absorption before determined by UV–Vis spectroscopy. The linear range, the detection limit (LOD) and enrichment factor of adsorbent were obtained 0.05-1 mg L⁻¹, 0.25 μ g L⁻¹ and 48.7, respectively ($r = 0.9992$, RSD%=3.65). The absorption capacity of $Zn_2(BDC)_2(DABCO)$ MOF for 50 mg L⁻¹ of standard lead solution were obtained 133.8 mg g⁻¹ for 0.25 g of adsorbent. The results indicate that this nanocomposite can have a good potential to develop different adsorbents.

1. Introduction

Heavy metals are considered one of the major pollutants with harmful effects on the environment and living organisms [1]. Lead is one of heavy metals with many industry applications. Lead element is a very strong poison and major environmental health problem. This non-biodegradable pollutant can be

caused detrimental effects on human health [2]. The world health organization (WHO) has identified lead as a hazardous material that needed to protect the health of workers, children and women of childbearing age. Threshold limit value (TLV) is the weighted average concentration of the risk factor in the atmosphere [1-3]. According to the results of workers in battery storage plants, TLV (working day of eight hours) was obtained about 0.1 mg m⁻³ and normal lead concentration in urine of workers was less than 50 μ g L⁻¹. The US Environmental

*Corresponding Author: [Negar Motakef Kazemi](mailto:Negar.Motakef.Kazemi@iaups.ac.ir)

Email: motakef@iaups.ac.ir

<https://doi.org/10.24200/amecj.v4.i03.145>

Protection Agency (EPA) has reported 5-100 $\mu\text{g L}^{-1}$ as a reference value in bottle and drinking water [3]. The lead effects on human health and causes the different diseases in humans such as, CNS defect, the nerve system damage, the renal/liver/bone dysfunction. The organic lead compound such as Triethyl and methyl lead with the Pb(II) as inorganic lead are toxic for the humans [3]. Lead emitted to environment with $(\text{C}_2\text{H}_5)_3/(\text{CH}_3)_3\text{-Pb}$ and Pb(II) forms and can be dispersed by oil/gasoline additives [4]. The organic lead is used in for industries, which can simply enter to human body by the skin and respiratory system. The organic lead with good hydrophobicity in organic solvent and foods has toxic effect in humans [5]. So, determination lead in water and human liquid samples (urine) is very important. Various methods have been developed to removal of each toxic heavy metal from water [6,7] such as the chemical precipitation [8], the ion exchange [9], the reverse osmosis [10], and the adsorbent process [11]. Recently, lead adsorbent from aqueous solution is a real challenge due to use widespread all over the world [12]. The adsorption process is the most efficient and extensive method for lead removal from wastewater [13]. The various adsorbents included, the graphene/graphene oxide [14], the nanofibers in different samples [15], the carbon nanotubes (CNTs) [16], the magnetic doped with carbon quantum dots(MDCQDs) [17], and the silica nanostructure [18] were widely used for lead extraction in water samples. Metal organic frameworks (MOFs) are a new class of porous coordination polymers with a variety of applications [19, 20]. They are formed of organic ligands as linkers and metal ions or clusters as metal centers [21, 22]. Recently, the MOFs have attracted a great attention because of unique properties [23, 24]. $\text{Zn}_2(\text{BDC})_2(\text{DABCO})$ MOF is metal organic framework based on zinc metal (Zn-MOF) by connection of Zn_4O units and 1,4-benzenedicarboxylate (BDC) and 1,4-diazabicyclo [2.2.2] octane (DABCO) ligands via self-assembly such as solution [25], solvothermal [26] and other methods. The common adsorbent compounds have expanded based on MOFs [27]. $\text{Zn}_2(\text{BDC})_2(\text{DABCO})$ MOF was loaded with various materials such as mercury [28], the gentamicin [29],

the Pd(II) [30], the methane [31], the azobenzene [32] and etc.

Easy separation of sorbent from the water is beneficial for reuse of materials and removal of heavy metals during treatment. Therefore, the adsorbents were developed based on magnetic [33-36] and polymer [33, 37] materials. Polycaprolactone is one of the most common polymers for the removal of heavy metals from aqueous solutions as hazardous, carcinogenic, and toxic pollutants. According to previous report, polycaprolactone nanofibrous were modified by clay mineral and zeolite nanoparticles for lead adsorption [38]. Also in another report, cyclodextrin-polycaprolactone titanium dioxide nanocomposites were used as a adsorbent for the removal of lead in aqueous waste samples [39]. The different techniques included, the graphite furnace coupled with atomic absorption spectrometry(GF-AAS) [40], the anodic stripping voltammetry (ASV) [41], the flame atomic absorption spectrometry (F-AAS) [42], the inductively coupled plasma atomic emission spectrometry (ICP- AES) [43] and the UV-Vis were used for lead determination in water samples. In present study, $\text{Zn}_2(\text{BDC})_2(\text{DABCO})$ MOF/PCL nanocomposites were prepared by a simple method and lead absorption was investigated by MOF and its nanocomposites from aqueous solution at optimized pH.

2. Experimental

2.1. Reagents and Materials

All reagents with high purity and analytical grade were purchased from Merck (Darmstadt, Germany). Ultra-pure water was used for the preparation of all reagent's solutions. Zinc acetate ehydrate ($\text{Zn}(\text{Oac})_2 \cdot 2\text{H}_2\text{O}$, CAS N:5970-45-6, Sigma, Germany), 1,4 benzenedicarboxylic acid (CAS N: 652-36-8, Sigma), 1,4-diazabicyclo [2.2.2] octane (CAS N: 280-57-9, Sigma), N,N-dimethylformamide anhydrous (DMF, CAS N: 68-12-2) were used for synthesis of MOF. The lead acetate salt and poly ϵ -Caprolactone (97%, CAS N: 502-44-3, Sigma, 1400 g mol⁻¹, molecular weight) were applied for preparation of lead and polymer solution respectively.

2.2. Sample preparations

For sampling, all glass tubes were washed with a 2.0 mol L⁻¹ HNO₃ solution for at least 12 h and rinsed 8 times with DW. The lead concentrations in humans have low concentration (ppb) in urine/water and even minor contamination for sampling and determination caused to effect on the accuracy of the results. By procedure, 50 mL of the urine samples were prepared from workers of batteries factories in Iran (Men, 25-55 age), based on ethical low. Clean and sterilized bottles were prepared for urine or water sampling. The water samples were prepared based on ASTM sampling and storage in 2% HNO₃.

2.3. MOF Synthesis

For preparation of Zn₂(BDC)₂(DABCO) MOF, Zn(OAc)₂·2H₂O (0.132 g, 2.0 mmol) to production of Zn²⁺ ions as a connector, BDC (0.1 g, 2.0 mmol) as a chelating ligand, and DABCO (0.035 g, 1.0 mmol) as a bridging ligand were added to 25 ml DMF as a solvent [28]. The reactants were sealed under reflux and stirred at 90 °C for 3 h. Then, the reaction mixture was cooled to room temperature, and filtered. The white crystals were washed with DMF to remove any metal and ligand remained,

and dried in a vacuum. DMF was removed from white crystals with a vacuum furnace at 150 °C for 5 h. Based on lead absorption, polycaprolactone nanocomposites cannot be prepared by solution casting method. In fact, the pores of MOF filled up with solvent and there is not any residual porosity for lead absorption. In this work, PCL nanocomposites were prepared by press method with different percentages of MOF for the first time. First, PCL polymer was dissolved in chloroform solvent under magnetic stirring. The final solution was transferred to the plate and allowed to dry. Then film surface was subjected to a hot press for 10 minutes. Finally, the certain amount of MOF powder was uniformly transferred to a cold press under the pressure on the film surface. Based on lead absorption, PCL nanocomposites with 5 and 10 percentage of MOF were shown better results and it was not possible to form a uniform nanocomposite with a higher percentage of MOF. Finally, the lead absorption was investigated in different values of lead concentrations, pH and temperature solution by MOF and its nanocomposite at different times. Figure 1 shows general procedure of Zn₂(BDC)₂(DABCO) MOF synthesis and lead adsorption by MOF.

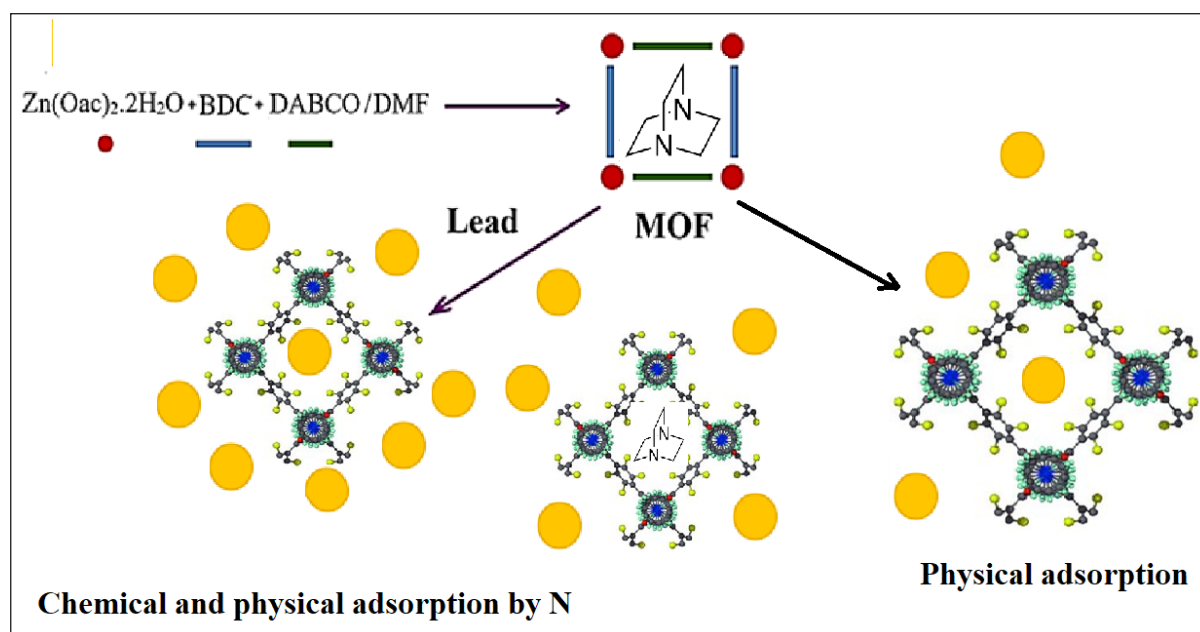


Fig. 1. General procedure for Zn₂(BDC)₂(DABCO) MOF synthesis and lead adsorption by MOF.

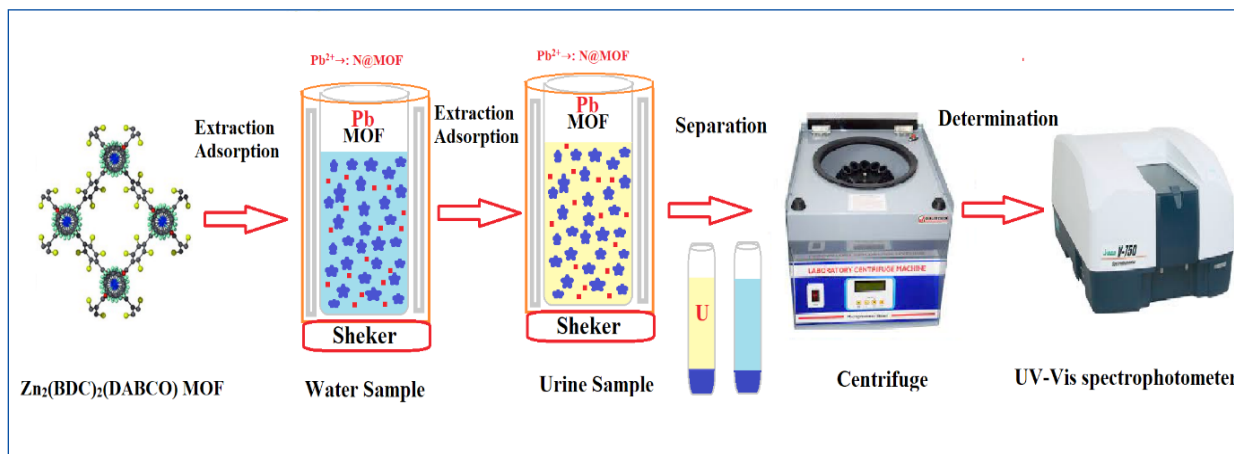


Fig. 2. Extraction/Adsorption procedure based on $Zn_2(BDC)_2(DABCO)$ MOF adsorbent for lead analysis

2.4. Characterization

FTIR spectra were recorded on a Shimadzu 460 spectrometer in a KBr matrix in the range of 400–4000 cm^{-1} . The crystalline structure of sample was investigated by X-ray diffraction utilizing Cu K α X-ray radiation with a voltage of 40 kV and a current of 30 mA by X'pert pro diffractometer (X'Pert Pro model, Panalytical, Peru). Field emission scanning electron microscope was employed to observe morphology and size (Sigma VP model, ZEISS, Germany). The surface area was determined using nitrogen gas sorption by MOF samples at 298 K and 0.88 atmosphere pressure (BEISORP Mini model, Microtrac Bel Corp, Japan). Lead adsorption was evaluated by UV–Vis spectroscopy (GENESYS 30 model, Thermo Scientific, America).

2.5. Extraction/Adsorption Procedure

By the USA-S- μ -SPE method, 50 mL of urine and water samples were used for extraction and determination lead ions by $Zn_2(BDC)_2(DABCO)$ MOF adsorbent. 0.25 g of $Zn_2(BDC)_2(DABCO)$ MOF added to urine/water or standard solution (0.05–1 $mg L^{-1}$) at pH=8. After sonication for 5.5 min, the Pb (II) ions were extracted/chemically adsorbed with the N group of the DABCO as a dative covalent bond in the optimized pH ($Pb^{2+} \rightarrow N \rightarrow MOF$). After centrifuging, the lead adsorbed on $Zn_2(BDC)_2(DABCO)$ MOF was separated from liquid phase in the bottom of the centrifuging tube (50 mL, 5.0 min; 3500 rpm). The liquid phase was

removed and the lead ions back-extracted from the $Zn_2(BDC)_2(DABCO)$ MOF in acidic pH (HNO_3 , 0.2M, 0.5 mL). The remained solution determined by UV-Vis after diluted with 0.5 mL of DW (Fig. 2). The calibration curve for lead in the standards solutions was prepared based on a LLOQ and ULOQ range with (0.05–1 $mg L^{-1}$) and without a preconcentration procedure (2–50 $mg L^{-1}$) and finally, the enrichment factor (EF) calculated by slope of the two calibration curves (m_1/m_2).

3. Results and discussions

3.1. FTIR spectra for MOF

The FTIR absorption spectra of the samples were recorded in the range of 400–4000 cm^{-1} with KBr pellets. FTIR spectra of MOF were presented before and after lead adsorption (Fig. 3). The C–H aromatic bands are shown at 3423 cm^{-1} . The IR bands of N–H and O–H stretching vibrations are characteristic at 3300 cm^{-1} . The aliphatic C–H asymmetric stretching is assigned at 2958 cm^{-1} . The O–H...O valance stretching vibration band is reported at 2600 cm^{-1} . The high intensity peak of C=O stretching is assigned at 1635 cm^{-1} for $Zn_2(BDC)_2(DABCO)$ MOF. The bands of aromatic C=C stretching are shown at 1593 cm^{-1} . The high intensity peak of C=O carboxylic group is specified at 1390 cm^{-1} . The peaks of obtained results has similar to the previous report [20, 25, 26]. The bands between 800 and 500 cm^{-1} are ascribed to Pb(II) adsorptions that according to the previous reports [44].

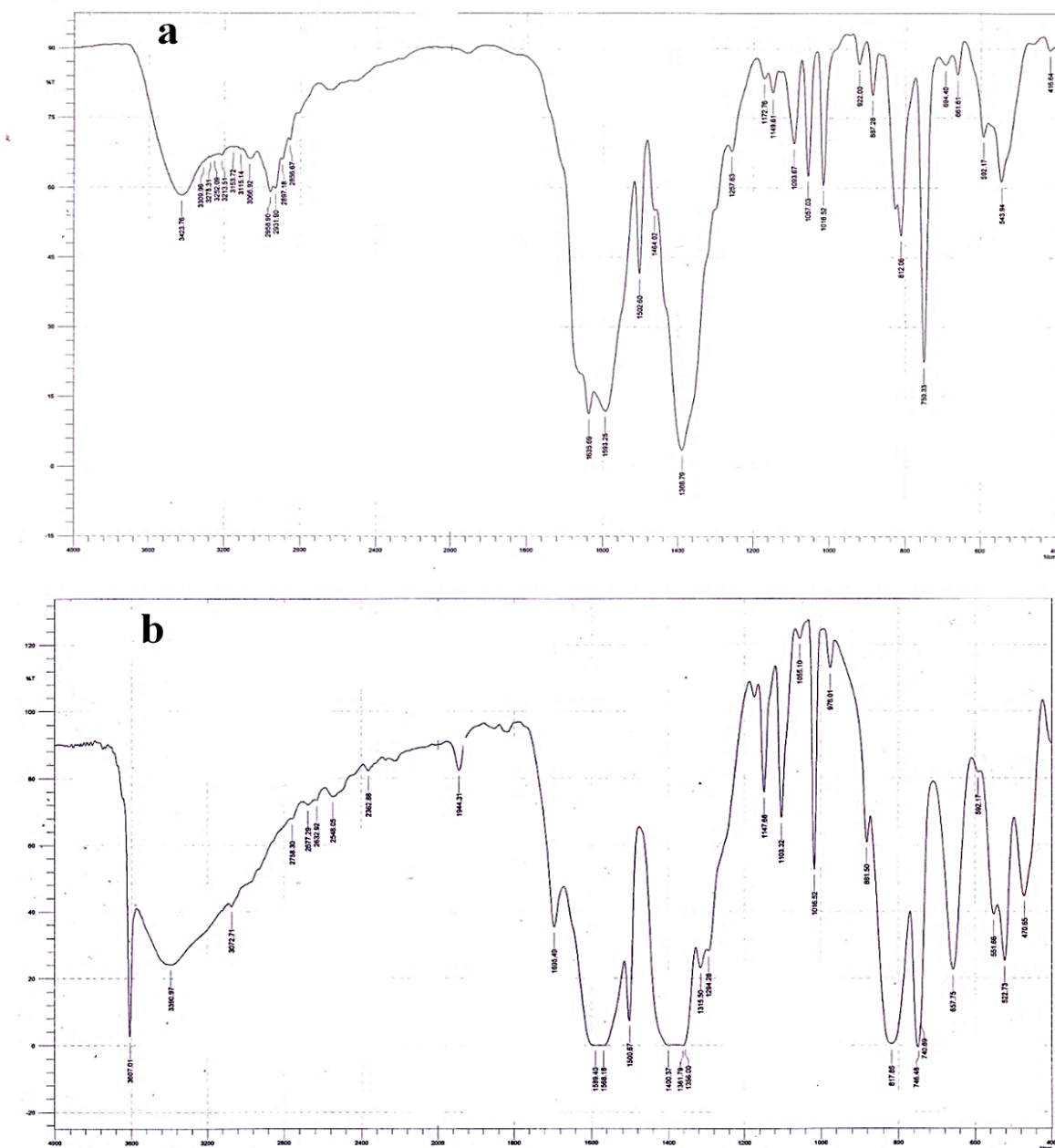


Fig. 3. FTIR spectra of MOF a) before and b) after lead adsorption.

3.2. XRD analysis

The XRD pattern of samples was measured in 2θ range $5\text{--}50^\circ$ that used to identify the crystalline structure (Fig. 4). The XRD pattern of MOF is similar to a previously reported pattern [25, 28] and its crystalline structure is preserved after the

absorption based on the previous report [27]. The XRD of PCL was approved the crystalline structure according to the previous report with two characteristic peaks [45]. The high percentage of polymer in the nanocomposite was caused no observation of MOF characteristic peaks.

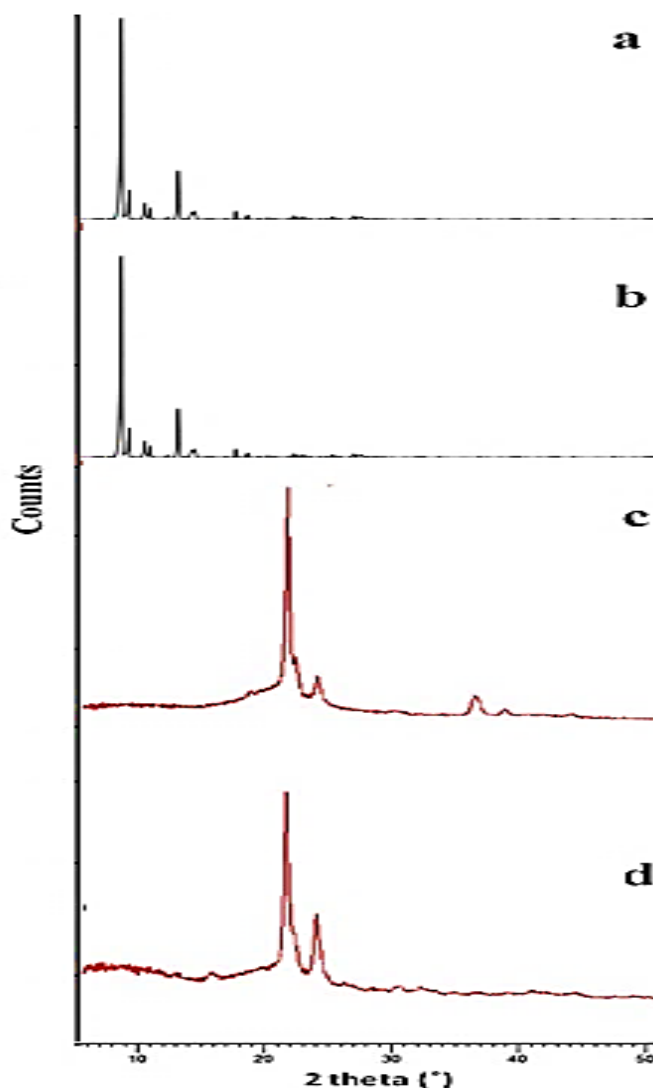


Fig. 4. XRD Pattern of **a)** MOF, **b)** MOF after lead adsorption, **c)** PCL polymer and **d)** MOF/PCL nanocomposite

3.3. FE-SEM images

The FE-SEM images were shown for MOF before and after lead adsorption (Fig. 5). SEM results were shown MOF nanoparticles with size of between 40-90 nm (before lead adsorption) and less than 100 nm (after lead adsorption). Lead absorption was caused the increase of particle size due to phenomenon of swelling. This result presented for the first time.

3.4. The Brunauer–Emmett–Teller (BET) analysis

The Brunauer–Emmett–Teller (BET) analysis was used for determination of surface area of MOF by N_2 adsorption before and after lead adsorption (Fig. 6). The surface area of MOF was decreased with lead adsorption from $762 \text{ m}^2 \text{ g}^{-1}$ to $21 \text{ m}^2 \text{ g}^{-1}$. The results indicate that there is almost no porosity after absorption and approximately the pores filled up lead.

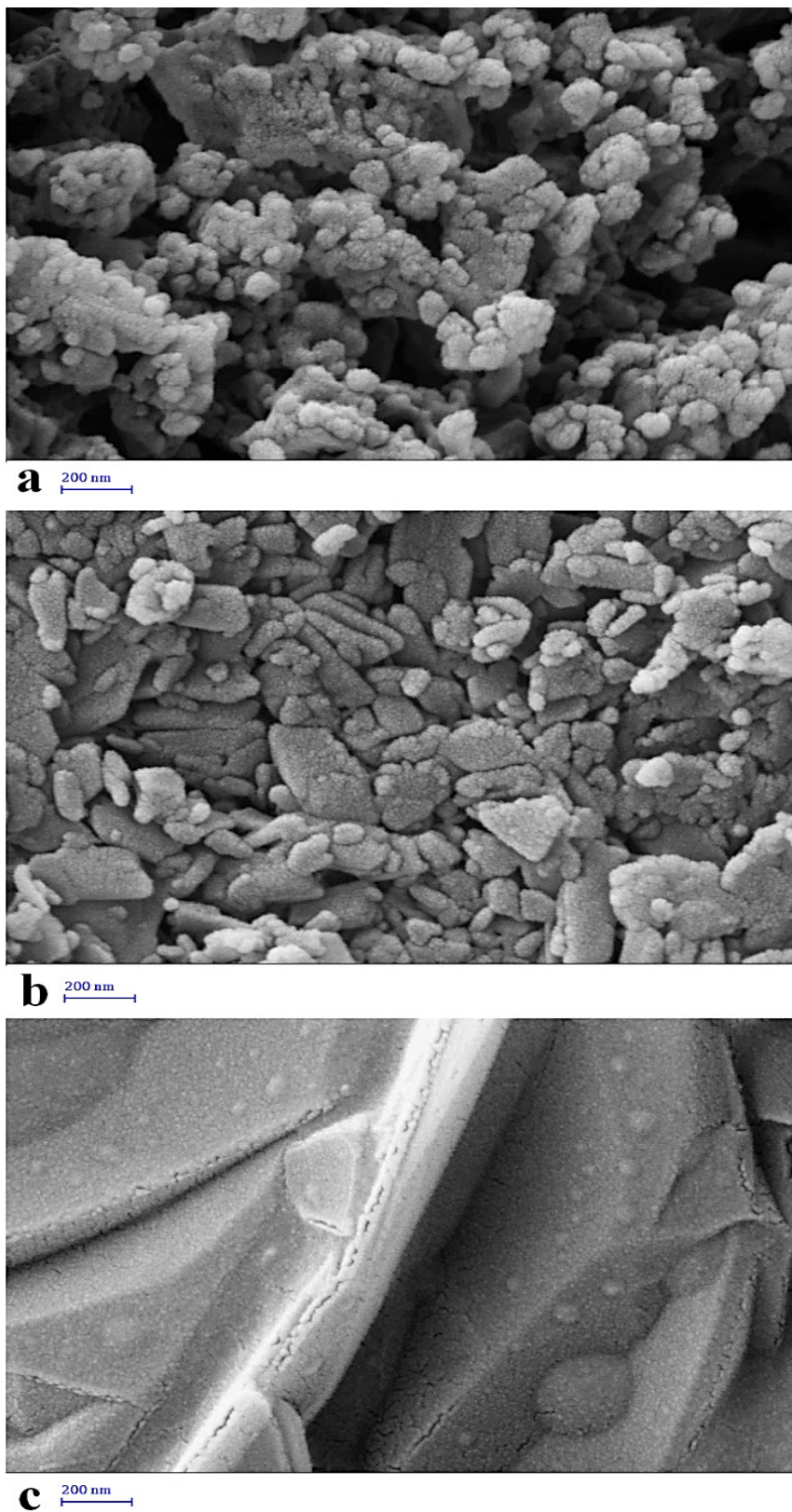


Fig. 5. FE-SEM images of **a)** MOF before lead adsorption before, **b)** MOF after lead adsorption, and **c)** MOF/PCL nanocomposite in 200 nm scale bare.

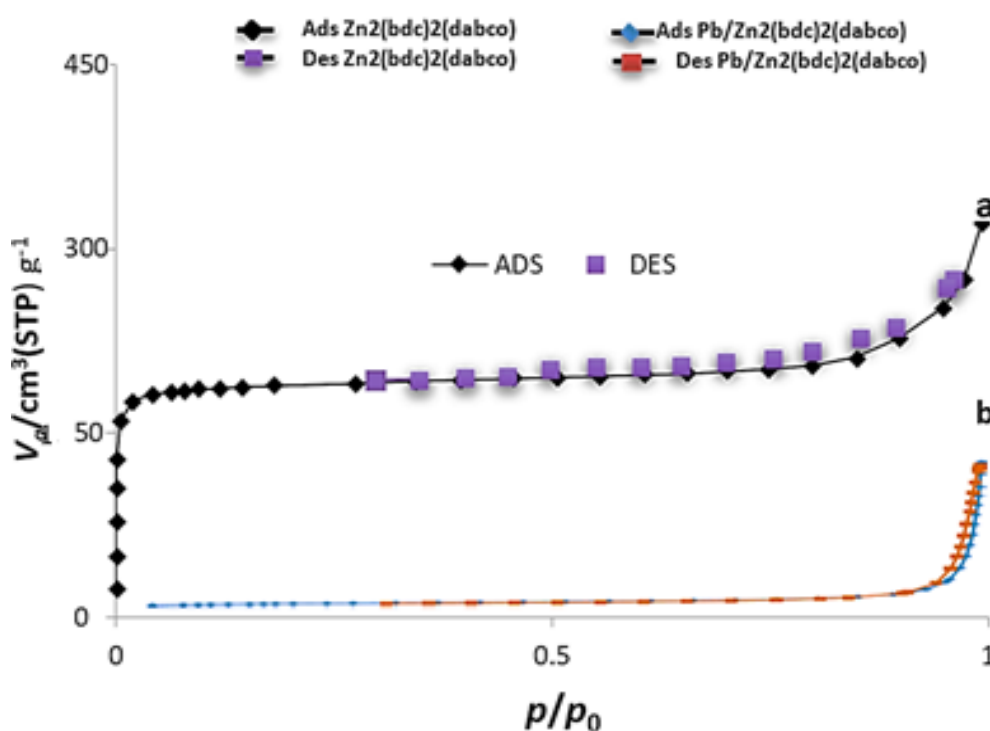


Fig. 6. The absorption/desorption N_2 curve related to MOF a) before and b) after lead adsorption.

3.5. Optimization study

The lead absorption was investigated by UV-Vis spectroscopy. The calibration curve of lead was examined at $\lambda_{\max} = 208$ nm with concentration of 0.1, 0.2, 0.4, 0.6, and 0.8 ppm (Fig. 7a). Lead adsorption diagram was investigated by different MOF amount including 0.1, 0.25, and 0.5 g for lead concentration at 0.6 ppm at various times (Fig. 7 b). Based on the result, the increase of MOF amount was resulted to the increase of lead adsorption due to increase of surface area.

The lead absorption was evaluated in different lead concentrations by MOF and its nanocomposite at different times (Fig. 8a). The lead concentrations were included 0.4, 0.4, 0.8, and 1.0 ppm for absorption investigation of 0.25 g MOF. The increase of lead concentration was resulted to increase of adsorption by MOF. The absorption of MOF/PCL nanocomposite was examined at a constant concentration of 0.6 ppm for lead solution (Fig. 8b). According to nanocomposite result, the increase of MOF percentage was resulted to increase of lead absorption. In fact, the increase of MOF was created the higher lead absorption due to increase of surface area.

Lead adsorption was studied in different pH of solution including acidic (pH=2), neutral, and basic (pH=10) for 0.25 g MOF with 0.6 ppm of lead concentration and 10% nanocomposite with 0.6 ppm of lead concentration (Fig. 9). The higher pH was caused more surface active sites, a competition between positive charges (Pb), and increase lead adsorption through the electrostatic force of attraction. However, the optimum pH in ranging from 7.5 to 8.5 for the divalent lead ions caused to preservation of MOF stability for efficiency improvement of chemical adsorption based on nitrogen dative bond more than 95% and have less than 32 % at pH 3-5 by physical adsorption.

Lead adsorption was evaluated in various temperature including 25 (ambient), 40, 60, and 80 °C for 0.25 g MOF and 10% nanocomposite with 0.6 ppm of lead concentration (Fig. 10). The increase of temperature was resulted to increase of lead adsorption because of kinetic energy and Brownian motion. Based on the previous report, temperature is directly related to the potential for adsorption by sorbent [19].

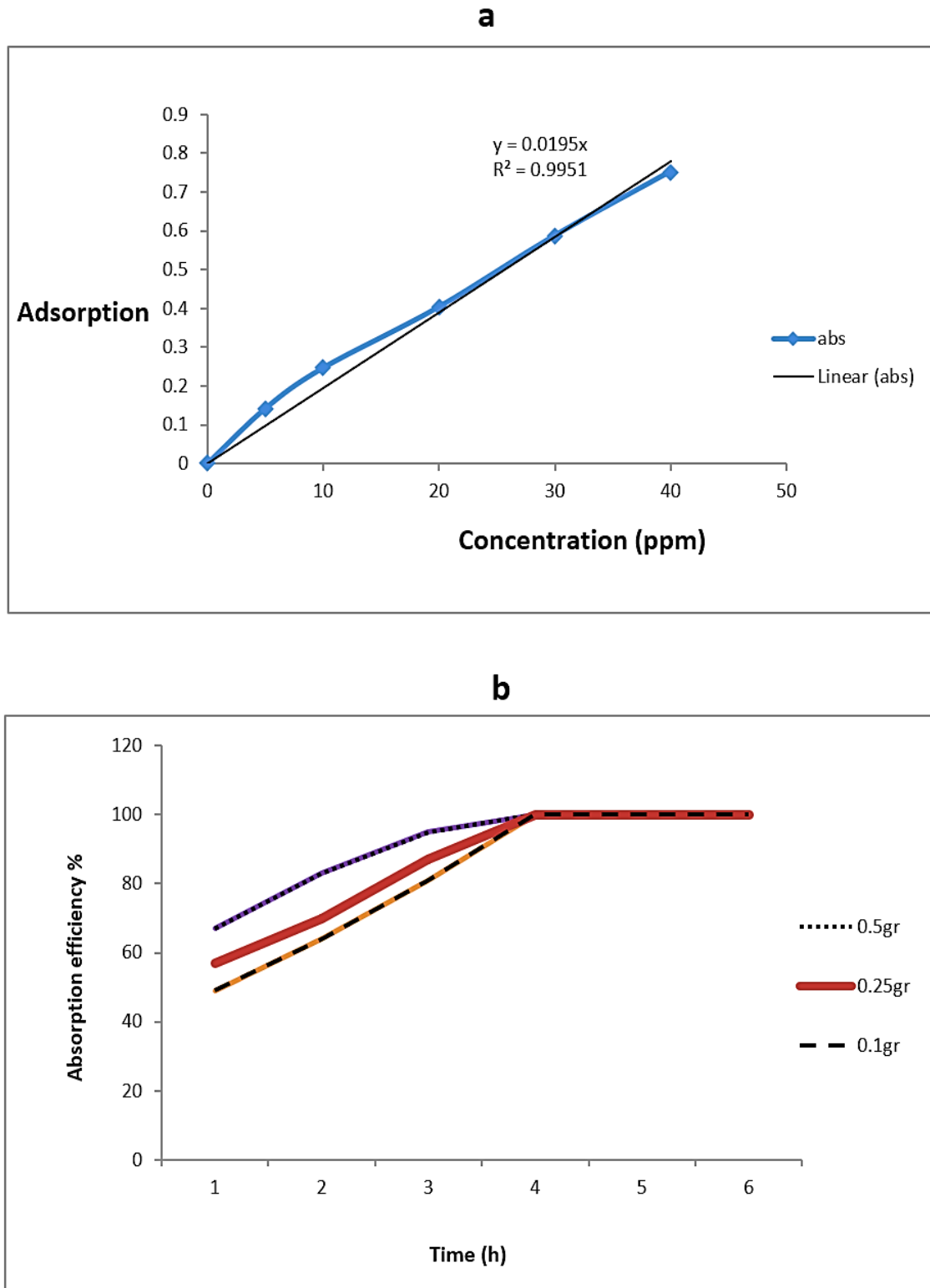


Fig. 7. a) The calibration curve of lead and **b)** the diagram of lead adsorption in different MOF amount

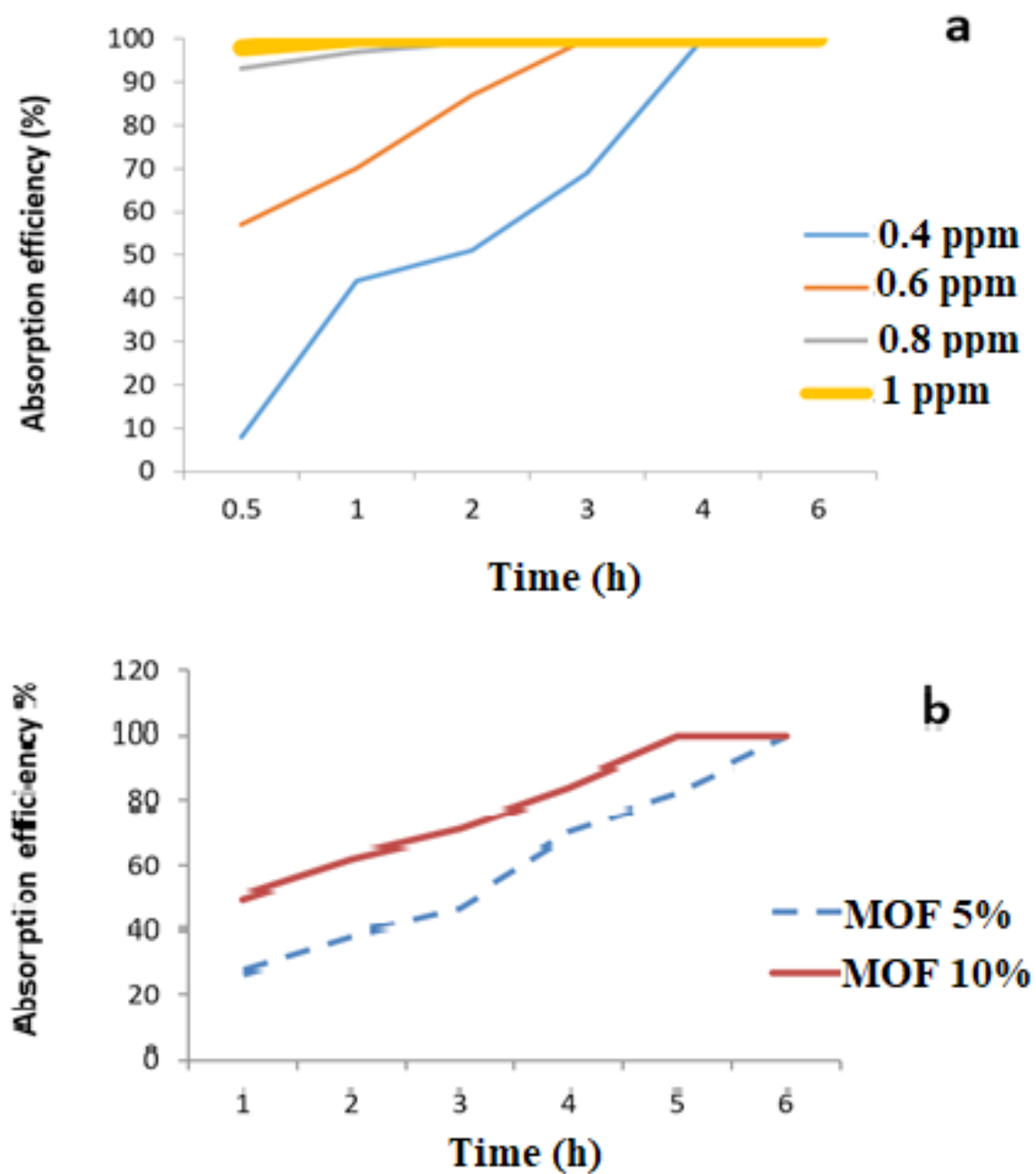


Fig. 8. The diagram of lead adsorption by **a)** MOF and **b)** MOF/PCL nanocomposite in different lead concentrations

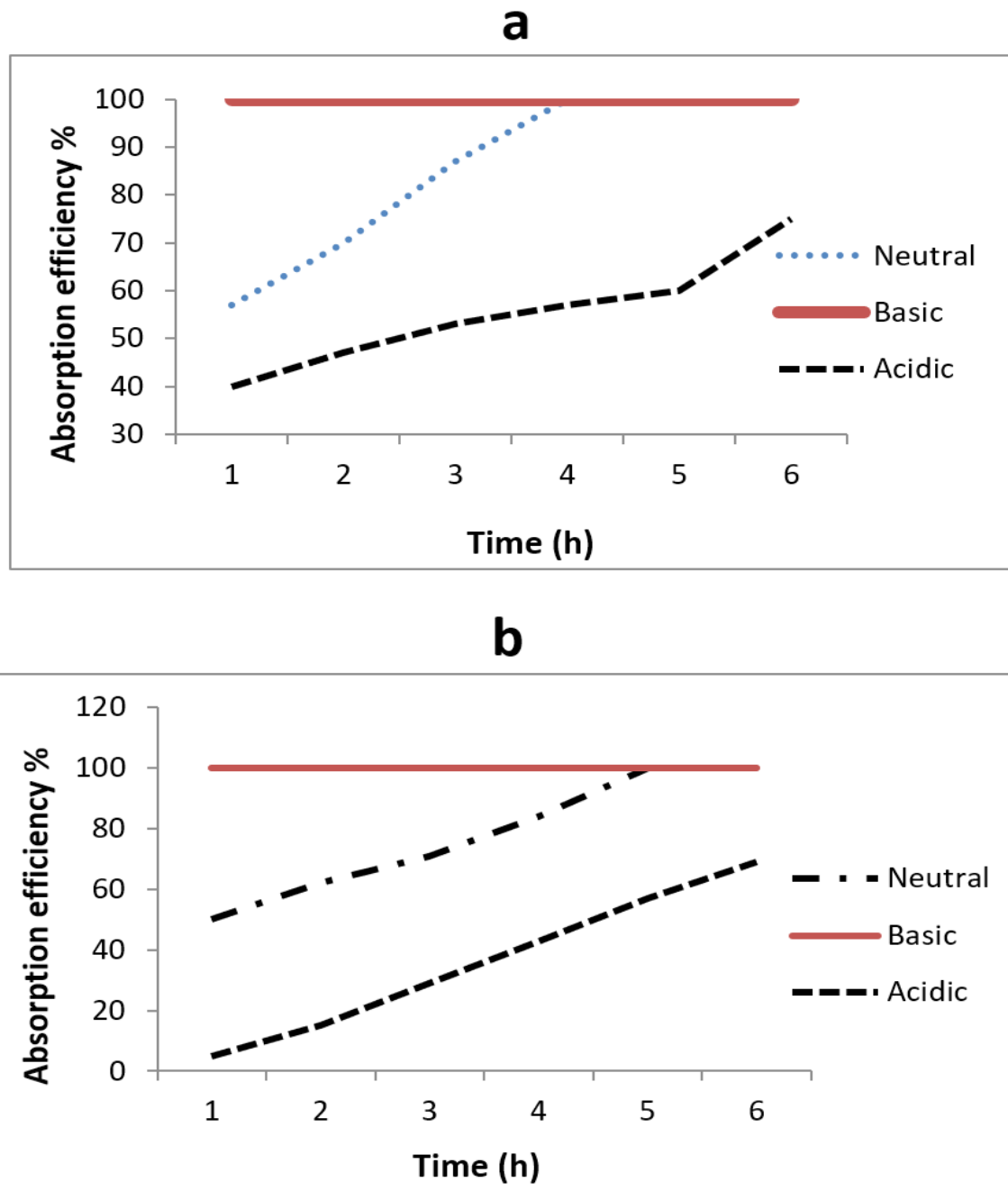


Fig. 9. The diagram of lead adsorption by **a)** MOF and **b)** MOF/PCL nanocomposite in different pH.

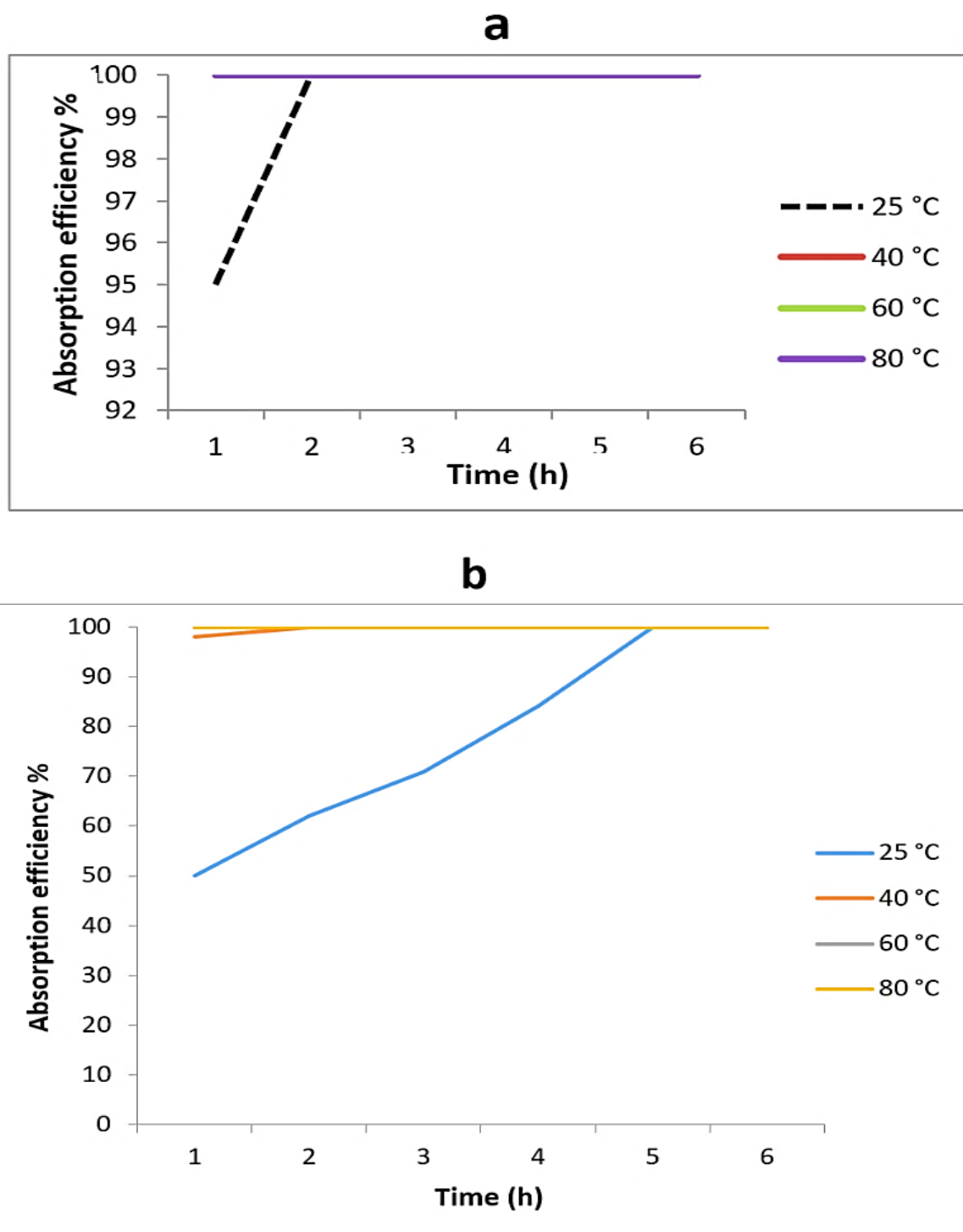


Fig. 10. The diagram of lead adsorption by **a)** MOF and **b)** MOF/PCL nanocomposite in different temperature.

3.6. Validation of USA-S- μ -SPE / UV-Vis

By the USA-S- μ -SPE method, 50 mL of urine and water samples were used for extraction and determination lead ions by 0.25 g of MOF adsorbent (0.05-1.0 mg L⁻¹, 100-1000 μ g L⁻¹, pH=8). The validated results were achieved for real samples by spiking of the standard solution of lead (Pb) to 50 mL of samples. The recoveries of spiked samples showed that the method was acceptable results for lead extraction and determination in urine and water samples. (Table 1) Also, the mean lead concentrations for five wastewater samples in paint factory, Karaj were obtained (325.4 \pm 13.8, n=5) by the ET-AAS which was near to the USA-S- μ -SPE/UV-Vis procedure (320.6 \pm 15.2, n=5) as 98.4 % recovery. The results confirmed the accuracy and precision of methodology for lead adsorption by MOF.

4. Conclusions

In this research, the MOF and MOF/PCL

nanocomposite were used for lead adsorption. The effect of different parameter including pH and temperature of solution, Zn₂(BDC)₂(DABCO) MOF and concentration of sorbent was shown on lead adsorption by MOF and its PCL nanocomposite. The results presented that MOF and its PCL nanocomposite can represent an economical source of lead sorbent from aqueous solution to develop environmental applications. The future prospects can be developed great application of this nanocomposites.

The working range and the relative standard deviation range (RSD%) for proposed procedure were obtained 0.05-5 mg L⁻¹ and 2.13-5.24, respectively ($r = 0.9992$). The absorption capacity of Zn₂(BDC)₂(DABCO) MOF for standard lead solution were ranged from 121.5 to 148.7 mg g⁻¹ in optimized conditions. The method was validated by the F-AAS.

Table 1. Validation of USA-S- μ -SPE/UV-Vis method for Pb(II) determination in urine and water samples based on Zn₂(BDC)₂(DABCO) MOF adsorbent by spiking real samples

Sample*	Added (μ g L ⁻¹)	*Found (μ g L ⁻¹)	Recovery (%)
Well Water	---	178.9 \pm 7.2	---
	150	323.5 \pm 15.6	96.4
Waste water	---	397.8 \pm 17.7	---
	500	903.6 \pm 41.5	101.2
Waste water	---	492.1 \pm 22.3	---
	500	986.3 \pm 44.6	98.8
Urine	---	62.4 \pm 2.8	---
	50	110.8 \pm 4.7	96.8
Drinking water	---	ND	---
	50	48.6 \pm 2.1	97.2
Urine	---	55.8 \pm 2.4	---
	50	107.1 \pm 3.3	102.6

*Mean of three determinations of samples \pm confidence interval (P = 0.95, n = 10) ND: Not detected

5. Acknowledgements

The Authors gratefully acknowledge the research council of Islamic Azad University and Department of Medical Nanotechnology, Faculty of Advanced Sciences and Technology, Tehran Medical Sciences, Islamic Azad University, Tehran, Iran.

6. References

- [1] P.B. Tchounwou, C.G. Yedjou, A.K. Patlolla, D.J. Sutton, Heavy metals toxicity and the environment, *EXS J.*, 101 (2012) 133–164.
- [2] A. Latif Wani, A. Ara, J. Ahmad Usmani, Lead toxicity: a review, *Interdiscip. Toxicol.*, 8 (2015) 55–64.
- [3] G. Flora, D. Gupta, A. Tiwari, Toxicity of lead: a review with recent updates, *Interdiscip. Toxicol.*, 5 (2012) 47–58.
- [4] M. Kosnett, Heavy metal intoxication and chelators, *Basic and clinical pharmacology*, 10th ed, New York: McGraw-Hill, (2007) 945–957.
- [5] Agency for Toxic Substances and Disease Registry (ATSDR), Toxicological profile for Lead, Atlanta, GA: U.S. Department of Health and Human Services, Public Health Service, 2019.
- [6] R. Arora, Adsorption of heavy metals—a review, *Mater. Today*, 18 (2019) 4745–4750.
- [7] J. Yang, B. Hou, J. Wang, B. Tian, J. Bi, N. Wang, X. Li, X. Huang, Nanomaterials for the removal of heavy metals from wastewater, *Nanomater.*, 9 (2019) 424. <https://doi.org/10.3390/nano9030424>
- [8] M.J. González-Muñoz, M.A. Rodríguez, S. Luque, J.R. Álvarez, Recovery of heavy metals from metal industry wastewaters by chemical precipitation and nanofiltration, *Desalination*, 200 (2006) 742–744.
- [9] MY. Vilensky, B. Berkowitz, A. Warshawsky, In-situ remediation of groundwater contaminated by heavy- and transition-metal ions by selective ion-exchange methods, *Environ. Sci. Technol.*, 36 (2002) 1851–1855.
- [10] M.G. Khedr, Nanofiltration and low energy reverse osmosis for rejection of radioactive isotopes and heavy metal cations from drinking water sources, *Desalination Water Treat.*, 2 (2009) 342–350.
- [11] S.B. Wang, H.W. Wu, Environmental-benign utilization of fly ash as low-cost adsorbents, *J. Hazard. Mater.*, 136 (2006) 482–501.
- [12] M. Odar, N. Motakef Kazemi, Nanohydroxyapatite and its polycaprolactone nanocomposite for lead sorbent from aqueous solution, *Nanomed. Res. J.*, (2020) Accepted.
- [13] A. Alghamdi, AB. Al-Odayni, W. Sharaf Saeed, A. Al-Kahtani, FA. Alharthi, T. Aouak, Efficient adsorption of lead (II) from aqueous phase solutions using polypyrrole-based activated carbon, *Materials*, 12 (2019) 2020.
- [14] B. Feist, M. Pilch, J. Nycz, Graphene oxide chemically modified with 5-amino-1, 10-phenanthroline as sorbent for separation and preconcentration of trace amount of lead (II), *Microchim. Acta*, 186 (2019) 91.
- [15] M.R. Karim, M.O. Aijaz, N.H. Alharth, H.F. Alharbi, F.S. Al-Mubaddel, M.R. Awual, Composite nanofibers membranes of poly (vinyl alcohol)/chitosan for selective lead (II) and cadmium (II) ions removal from wastewater, *Ecotoxicol. Environ. Safe.*, 169 (2019) 479–486.
- [16] E. Kazemi, S. Dadfarnia, A.M. Haji Shabani, P.S. Hashemi, Synthesis of 2-mercaptobenzothiazole/magnetic nanoparticles modified multi-walled carbon nanotubes for simultaneous solid-phase microextraction of cadmium and lead, *Int. J. Environ. Anal. Chem.*, 97 (2017) 743–755.
- [17] M. Mashkani, A. Mehdinia, A. Jabbari, Y. Bide, M.R. Nabid, Preconcentration and extraction of lead ions in vegetable and water samples by N-doped carbon quantum dot conjugated with Fe₃O₄ as a green and facial adsorbent, *Food Chem.*, 239 (2018) 1019–1026.
- [18] H. Shirkhanloo, S.D. Ahranjani, A lead analysis based on amine functionalized bimodal mesoporous silica nanoparticles in human biological samples by ultrasound

- assisted-ionic liquid trap-micro solid phase extraction, *J. pharm. Biomed. Anal.*, 157 (2018) 1-9.
- [19] F. Ataei, D. Dorrnian, N. Motakef-Kazemi, Bismuth-based metal-organic framework prepared by pulsed laser ablation method in liquid, *J. Theor. Appl. Phys.*, 14 (2020) 1-8.
- [20] N. Motakef-Kazemi, M. Rashidian, S. Taghizadeh Dabbagh, M. Yaqoubi, Synthesis and characterization of bismuth oxide nanoparticle by thermal decomposition of bismuth-based MOF and evaluation of its nanocomposite, *Iran. J. Chem. Chem. Eng.*, 40 (2021) 11-19.
- [21] F. Ataei, D. Dorrnian, N. Motakef-Kazemi, Synthesis of MOF-5 nanostructures by laser ablation method in liquid and evaluation of its properties, *J. Mater. Sci.: Mater. Electron.*, 32 (2021) 3819-3833.
- [22] B. Miri, N. Motakef-Kazemi, S.A. Shojaosadati, A. Morsali, Application of a nanoporous metal organic framework based on iron carboxylate as drug delivery system, *Iran. J. Pharm. Res.*, 17 (2018) 1164-1171.
- [23] H. Li, M. Eddaoudi, M. O'Keeffe, O. Yaghi, Design and synthesis of an exceptionally stable and highly porous metal-organic framework, *Nature*, 402 (1999) 276-279.
- [24] S. Hajiashrafi, N. Motakef-Kazemi, Preparation and evaluation of ZnO nanoparticles by thermal decomposition of MOF-5, *Heliyon*, 5 (2019) e02152.
- [25] N. Motakef-Kazemi, S.A. Shojaosadati, A. Morsali, In situ synthesis of a drug-loaded MOF at room temperature, *Micropor. Mesopor. Mater.*, 186 (2014) 73-79.
- [26] N. Motakef-Kazemi, S.A. Shojaosadati, A. Morsali, Evaluation of the effect of nanoporous nanorods Zn₂(bdc)₂(dabco) dimension on ibuprofen loading and release, *J. Iran. Chem. Soc.*, 13 (2016) 1205-1212.
- [27] M.R. Mehmandoust, N. Motakef-Kazemi, F. Ashouri, Nitrate adsorption from aqueous solution by metal-organic framework MOF-5, *Iran. J. Sci. Technol. A*, 43 (2019) 443-449.
- [28] N. Motakef-Kazemi, A novel sorbent based on metal-organic framework for mercury separation from human serum samples by ultrasound assisted-ionic liquid-solid phase microextraction, *Anal. Methods Environ. Chem. J.*, 2 (2019) 67-78.
- [29] H. Nabipour, B. Soltani, N. Ahmadi Nasab, Gentamicin loaded Zn₂(bdc)₂(dabco) frameworks as efficient materials for drug delivery and antibacterial activity, *J. Inorg. Organomet. Polymer Mater.*, 28 (2018) 1206-1213.
- [30] K. Xie, Y. He, Q. Zhao, J. Shang, Q. Gu, GG. Qiao, PA. Webley, Pd(0) loaded Zn₂(azoBDC)₂(dabco) as a heterogeneous catalyst, *Cryst. Eng. Comm.*, 19 (2017) 4182-4186.
- [31] I. Senkovska, S. Kaskel, High pressure methane adsorption in the metal-organic frameworks Cu₃(btc)₂, Zn₂(bdc)₂dabco, and Cr₃F(H₂O)₂O(bdc)₃, *Micropor. Mesopor. Mat.*, 112 (2008) 108-115.
- [32] A. Schneemann, V. Bon, I. Schwedler, I. Senkovska, S. Kaskel, R.A. Fischer, Flexible metal-organic frameworks, *Chem. Soc. Rev.*, 43 (2014) 6062-6096.
- [33] N.S. Behbahani, K. Rostamizadeh, M.R. Yaftian, A. Zamani, H. Ahmadi, Covalently modified magnetite nanoparticles with PEG: Preparation and characterization as nano-adsorbent for removal of lead from wastewater, *J. Environ. Health Sci.*, 12 (2014) 103.
- [34] R. Ricco, K. Konstas, MJ. Styles, J.J. Richardson, R. Babarao, K. Suzuki, P. Scopece, P. Falcaro, Lead(II) uptake by aluminium based magnetic framework composites (MFCs) in water, *J. Mater. Chem. A*, 3 (2015) 19822-19831.
- [35] Y. Wang, J. Xie, Y. Wu, H. Gea, Z. Hu, Preparation of a functionalized magnetic metal-organic framework sorbent for the extraction of lead prior to electrothermal atomic absorption spectrometer analysis, *J. Mater. Chem. A*, 1 (2013) 8782-8789.

- [36] J. Shen, N. Wang, Y. Guang Wang, D. Yu, Xk. Ouyang, Efficient adsorption of Pb(II) from aqueous solutions by metal organic framework (Zn-BDC) coated magnetic montmorillonite, *Polymers*, 10 (2018) 1383.
- [37] Y.L.F. Musico, C.M. Santos, M.L.P. Dalida, D.F. Rodrigues, Improved removal of lead(II) from water using a polymer-based graphene oxide nanocomposite, *J. Mater. Chem. A*, 1 (2013) 3789–3796.
- [38] M. Irandoost, M. Pezeshki-Modaress, V. Javanbakht, Removal of lead from aqueous solution with nanofibrous nanocomposite of polycaprolactone adsorbent modified by nanoclay and nanozeolite, *J. Water Process Eng.*, 32 (2019) 100981.
- [39] KM. Seema, BB. Mamba, J. Njuguna, RZ. Bakhtizin, AK. Mishra, Removal of lead (II) from aqueous waste using (CD-PCL-TiO₂) bio-nanocomposites, *Int. J. Biol. Macromol.*, 109 (2018) 136-142.
- [40] H.R. Cadorim, M. Schneider, J. Hinz, F. Luvizon, A.N. Dias, E. Carasek, B. Welz, Effective and high-throughput analytical methodology for the determination of lead and cadmium in water samples by disposable pipette extraction coupled with high-resolution continuum source graphite furnace atomic absorption spectrometry (HR-CS GF AAS), *Anal. Lett.*, 52 (2019) 2133-2149.
- [41] N. Mouhamed, K. Cheikhou, G.E.M. Rokhy, D.M. Bagha, M.-D.C. Guèye, T. Tzedakis, Determination of lead in water by linear sweep anodic stripping voltammetry (LSASV) at unmodified carbon paste electrode: optimization of operating parameters, *Am. J. Anal. Chem.*, 9 (2018) 171.
- [42] H. Shirkhanloo, A. Khaligh, H.Z. Mousavi, A. Rashidi, Graphene oxide-packed micro-column solid-phase extraction combined with flame atomic absorption spectrometry for determination of lead (II) and nickel (II) in water samples, *Int. J. Environ. Anal. Chem.*, 95 (2015) 16-32.
- [43] S. Azimi, Z. Eshaghi, A magnetized nanoparticle based solid-phase extraction procedure followed by inductively coupled plasma atomic emission spectrometry to determine arsenic, lead and cadmium in water, milk, Indian rice and red tea, *Bull. Environ. Contam. Toxicol.*, 98 (2017) 830-836.
- [44] Y. Huang, S. Lia, J. Chen, X. Zhang, Y. Chen, Adsorption of Pb(II) on mesoporous activated carbons fabricated from water hyacinth using H₃PO₄ activation: Adsorption capacity kinetic and isotherm studies, *Appl. Surf. Sci.*, 293 (2014) 160– 168.
- [45] M. Borjigin, C. Eskridge, R. Niamat, B. Strouse, P. Bialk, E.B. Kmiec, Electrospun fiber membranes enable proliferation of genetically modified cells, *Int. J. Nanomed.*, 8 (2013) 855–864.



Cobalt separation from water and food samples based on penicillamine ionic liquid and dispersive liquid-liquid microextraction before determination by AT-FAAS

Yaghoob Pourshojaei ^{a,*} and Alireza Nasiri ^b

^a Department of Medicinal Chemistry, Faculty of Pharmacy, Kerman University of Medical Sciences, Kerman, Iran.

^b Environmental Health Engineering Research Center, Kerman University of Medical Sciences, Postal code: 7619813159, Kerman, Iran

ARTICLE INFO:

Received 11 Jun 2021

Revised form 8 Aug 2021

Accepted 30 Aug 2021

Available online 28 Sep 2021

Keywords:

Cobalt,
Water and food,
Penicillamine,
Ionic liquid,
Ultra-assisted dispersive liquid-liquid microextraction,
Atom trap flame atomic absorption spectrometry

ABSTRACT

The cobalt compounds have adverse health effect on human and caused to damage of the DNA cells, neurological and endocrine systems. Therefore, the separation and determination of cobalt in water and food samples must be considered. In this research, the (2S)-2-amino-3-methyl-3-sulfanylbutanoic acid (penicillamine) as a chelating agent mixed with ionic liquid (OMIM PF₆) /acetone and used for extraction of cobalt from 50 mL of water samples by ultra-assisted dispersive liquid-liquid microextraction (USA-DLLME) at pH=6. Based on procedure, the samples were shaken for 5 min (25°C) and after complexation of cobalt ions by thiol and amine group of penicillamine, the ionic liquid phase separated in the bottom of the conical tube by centrifuging for 3.0 min. The upper liquid phase was vacuumed by the auto-sampler and the Co²⁺ ions back extracted from the ionic liquid/ penicillamine in acidic pH. Finally, the cobalt concentration in remained solution was determined by atom trap flame atomic absorption spectrometry (AT-FAAS). The main parameters such as the sample volume, the penicillamine amount, the ionic liquid amount and the shaking time were optimized. The linear range, the detection limit (LOD) and enrichment factor were obtained 1.5-62 μg L⁻¹, 0.38 μg L⁻¹ and 98.5, respectively (*r* = 0.9995, RSD%=2.2). The procedure was validated by ET-AAS analysis.

1. Introduction

Cobalt compounds exist in two valence forms include cobalt (Co II, cobaltous, Co²⁺ and Co III, cobaltic, Co³⁺), the other forms have not environmentally available. Also, the other cobalt compounds have toxic effect in the environment and the human body by extra exposure [1]. The people is exposed to cobalt through inhalation of air and food and drinking water. Cobalt ions enter to environment from numerous

industrial factories such as heavy metals activity process, the grinding, the mining and paint [2]. Furthermore, it can be used for a medical process for the medicine Company. The cobalt compounds are widely dispersed in air with a low concentration less than 2.0 ng m⁻³ [3, 4]. Cobalt has a low concentration range between 0.1-5 μg L⁻¹ in drinking water. The cobalt concentration in river, the groundwater, the ocean water has an average value about 0.3 μg L⁻¹ [5]. Feng et al reported the concentrations of cobalt in the groundwater had lower than 0.01 mg L⁻¹ which is lower than other heavy metals [6]. Lim *et al* showed an applied model for the heavy metals such cobalt in

*Corresponding Author: Yaghoob Pourshojaei

Email: pourshojaei@yahoo.com

<https://doi.org/10.24200/amecj.v4.i03.148>

wastewater based on fly ash near landfills [7]. United States Environmental Protection Agency (EPA) reported that the cobalt levels in sediment and surface water were $80 \mu\text{g g}^{-1}$ and $86 \mu\text{g L}^{-1}$, respectively [2]. Food analysis in dietary cobalt intake such as vegetables, cereals and fish is very important way to control cobalt toxicity in human body which is especially significant in children [8]. Besides, the skin contact is a main way that cobalt was entered to human body. Cobalt as an essential metal exists in the human body and the maximum amount of it generally concentrated in the liver. Cobalt in eggs has biological role in vitamin B12 and named cyanocobalamin [9]. It uses in structure of vitamin B₁₂ and produce the red blood cells in bones and define from anemia in body [9]. Cobalt toxicity cause several health problems such as cardiomyopathy, nerve/thyroid problems, hearing and visual impairment, neuropathy, tinnitus and glomerulonephritis [10, 11]. Therefore, the accurate results for determination of cobalt must be considered by a new technology. The normal concentration of cobalt is equal to 1.0 ng mL^{-1} for environmental or occupational exposure and more than this value cause to toxicity. The sources of cobalt can be entering to human body from occupational/environmental/food exposures. The blood Co concentration is $100 \mu\text{g L}^{-1}$ and more than $300 \mu\text{g L}^{-1}$ cause toxicity in human [12, 13]. The penicillamine a chelating agent, is a trifunctional compound, containing of a thioalcohol, a carboxylic acid, and an amine that was used for the treatment of Wilson's disease, kidney stones, rheumatoid arthritis, and removal of heavy metal. Based on disorder of copper metabolism, copper accumulated in human body and the penicillamine extracted extra copper from body but, it can be removed the other essential metals from body [14, 15]. Many analytical methods such as electrothermal atomic absorption spectrometry (ET-AAS) [16], the flame atomic absorption spectrometry (F-AAS) [17] and the inductively coupled plasma optical emission/mass spectrometry (ICP-OES, ICP-MS) [18] have previously used for the determination of cobalt in various water and food samples. Moreover, analytical techniques based on the above instruments cannot

enough to use for solving the difficulty matrices. For this purpose, the procedures must be developed for the separation and preconcentration of cobalt from samples. There are many methodologies for extraction cobalt from difficulty matrixes including, the magnetic solid phase extraction (MSPE) [19], dispersive micro-solid phase extraction (D- μ -SPE) [20], the liquid-liquid extraction (LLE), the dispersive liquid-liquid microextraction (DLLME) [21], the electrochemistry methods (ECM) [22], the cloud point extraction (CPE) [23] and the precipitation [24]. Recently, the ultra-assisted dispersive liquid-liquid microextraction (USA-DLLME) [25] has been used as one of the most practical methods for the separation of metal ions. The main advantages of USA-DLLME to other techniques are simple separation, high preconcentration, fast analysis, low time, high recovery and good enrichment factor (EF). The ionic liquid as green solvent plays critical role for collection of ligand and metals from samples into two phases; a IL/ligand phase and liquid phase of water samples. Metal ions can be extracted from aqueous solution into the small-volume IL/ligand phase with hydrophobicity, the more density than water samples and low solubility in water. In this study, the mixture of (2S)-2-amino-3-methyl-3-sulfanylbutanoic acid (penicillamine)/ (OMIM PF₆)/acetone have been used for extraction of cobalt from water samples by USA-DLLME at pH=6. The thiol and amine groups of penicillamine play an important role in the coordination of metals and have a strong complex with the cobalt ions [26]. In this study, this ligand was used as an ion carrier and as a chelating agent to cobalt ions accompanied with ionic liquid

2. Experimental

2.1. Instrumental Analysis

The cobalt (Co) value in water and digested food samples was determined by AT-FAAS (GBC, Aus). The air-acetylene was used for cobalt measurement by AT-FAAS. The atom trap accessory as SQT-AT devices is placed on the burner. In order to improve sensitivity, the upper end of a tubular flame was directed into a SQT which the source beam was passed. SQT-AT devices cause to increase the sensitivity of absorption

(ABS) per concentration before analysis. The limits of detection (LOD) were obtained at 0.05 and 0.13 mg L⁻¹ for the AT-FAAS and FAAS, respectively. The HCL was adjusted by screws up to maximum energy. The AT-FAAS for cobalt determination was tuned by wavelength of 240.7 nm (7 mA). The aspiration of samples into FAAS was done by the auto-sampler (0.5-1 mL). The linear range for AT-FAAS was 0.15-6.0 mg L⁻¹ for cobalt analysis. The working range for the AT-FAAS and F-AAS was obtained at 0.15-15 and 0.4-15 mg L⁻¹ for cobalt, respectively. Graphite furnace accessory coupled to an atomic absorption spectrophotometer (GBC) was used for validation of cobalt in digested food and water samples. The pH of the samples was adjusted by favorite buffer solutions (Sigma, Germany) and determined by the Metrohm pH meter (Swiss). The phosphate buffers (Na₂HPO₄ and NaH₂PO₄) were used to adjust the pH from 6.0 to 8.0.

2.2. Reagents and Materials

The ultra-pure H₂SO₄, HCl, NaOH and HNO₃ solutions for cobalt analysis in food and water samples were prepared from Sigma Aldrich (Germany). The calibration solutions of Co(II) were made by dissolving 1.0 g of cobalt nitrate (Co(NO₃)₂) in 1 L of deionized water (DW) solution (2% HNO₃). The linear ranges of cobalt were daily prepared by standard solutions (1g L⁻¹, 1000 mg L⁻¹) and diluted by DW (Millipore, USA). All of the laboratory glassware was cleaned with nitric acid (5% v/v) and washed with DW for 10 times. ionic liquid of 1-hexyl-3-methylimidazolium hexafluorophosphate (HMIM PF₆, CAS N: 304680-35-1), 1-Methyl-3-octylimidazolium hexafluorophosphate ([OMIM][PF₆], CAS N: 304680-36-2), 1-methyl-3-octylimidazolium hexafluorophosphate ([OMIM][PF₆], [BMIM][PF₆], CAS N: 304680-36-2), and 1-ethyl-3-methylimidazolium hexafluorophosphate ([EMIM][PF₆], CAS N: 155371-19-0), acetone (CAS N: 67-64-1) and the penicillamine (CAS N: 52-66-4) were purchased from Sigma, Germany. The reagents of Na₂HPO₄ and NaH₂PO₄ (CAS N: 7558-79-4, 99.95%; CAS N: 7558-80-7, 99%) were prepared from the Sigma Aldrich, Germany.

2.3. Preparation of water and food samples

All food samples (Rice, Spinach, Broccoli, and Onion) were pulverized and then ground/ dried/ homogenized before analysis. Finally, the powder samples are converted to a uniform size and then place in the oven at 90 °C for 3 h. After adding DW to food samples, the homogenization of sample was digested with microwave (Antom Paar, multi-wave) based on book catalog procedure. The food samples were digested at optimum conditions (200 °C, 500 ps UV radiation). First, 1.0 g of food powder samples were placed in PTFE tube with surrounding ceramic tube of microwave and then, 5 mL of HNO₃ with 1 mL of H₂O₂ solution were added to samples. The powder samples were digested for 58 min and diluted with DW up to 50 mL before determination of cobalt by the USA-DLLME at pH=6. By microwave, the all cobalt forms in foods (organic foods) convert to Co(II) by induced oxygen combustion and total cobalt can be determined in food samples. All water samples prepared based on filtration (200 nm) and acidified with HNO₃ (2%) by the ASTM sampling method for water and storage in PE tube at -4°C.

2.4. Procedure of cobalt extraction

The Co(II) ions were separated and preconcentrated based on the complexation of cobalt-penicillamine in water and food samples by the USA-DLLME procedure (Fig.1). Also, the total cobalt in food samples was determined based on penicillamine ligand by the AT-AAS. The penicillamine (0.12 g) dispersed into 180 mg of hydrophobic ionic liquid ([HMIM][PF₆] and 0.5 mL acetone and then, the mixture of ligand/([HMIM][PF₆]/acetone was injected into 50 mL of water or standard solution of cobalt (1.5-62 µg L⁻¹) by a syringe at pH=6. After sonication of samples for 5.0 min, the Co(II) ions were complexed by the thiol group of penicillamine ligand at pH of 6 [Co(II)←:SH—(2S)-2-amino-3-methyl-3-sulfanylbutanoic acid]. After the extraction process, the Co-ligand was trapped in the hydrophobic [HMIM][PF₆] at the bottom of a conical PE tube by centrifuging for 5 min (3500 rpm). The upper liquid phase was

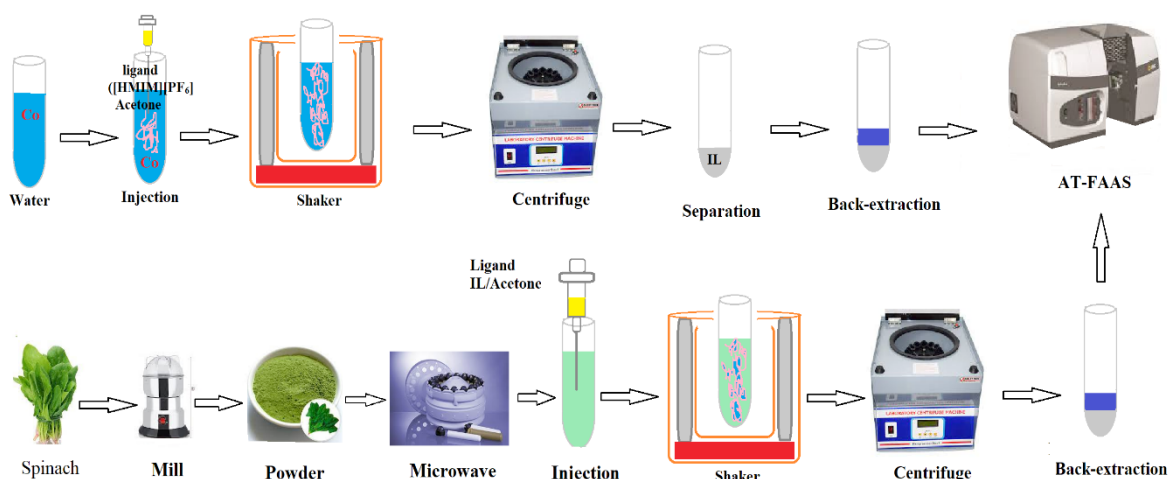
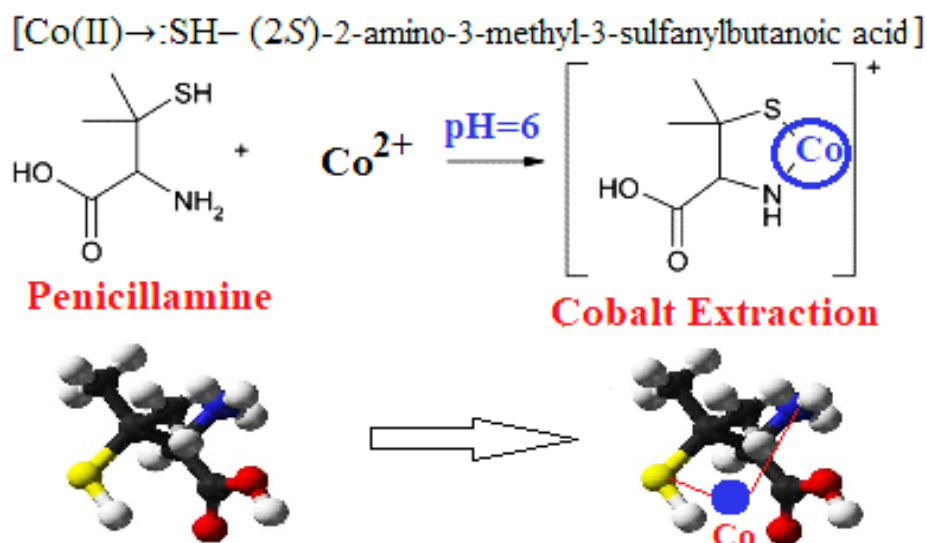


Fig.1. Cobalt extraction based on the complexation of penicillamine in water and food samples by the USA-DLLME procedure

evacuated and the Co ions were back-extracted from ligand/([HMIM][PF₆]) into an aqueous phase by 0.25 mL of HNO₃ (0.5M) and diluted with DW up to 0.5 mL. Finally, the Co concentration in the remaining solution was determined by the AT-FAAS. In addition, 1.0 g of food powder was added to HNO₃/H₂O₂ solution (5:1) in the PTFE vials and samples were digested at 58 min based on the induced oxygen combustion/UV radiation. The digested food samples are diluted with DW up to 50 mL before cobalt analysis by the AT-F-AAS based on same procedure by ligand/([HMIM][PF₆])/acetone at pH=6.

3. Results and Discussion

By the USA-DLLME procedure, the preconcentration/separation of Co (II) ions in water samples was occurred for different cobalt concentrations as a lower range (1.5 µg L⁻¹) and upper range (62 µg L⁻¹) by the penicillamine ligand. Moreover, the total cobalt extracted from digested food samples such rice, spinach, broccoli and onion before determined by the AT-FAAS. The mechanism of extraction is based on the interaction of nitrogen(--NH) and thiol (--SH) groups of the penicillamine with cobalt ions using dative/covalent bonding (Schema 1). The results showed that efficient extraction of cobalt ion in water/food samples was performed by the



Schema 1. The mechanism of extraction between nitrogen and thiol of the penicillamine with cobalt ions

penicillamine ligand under optimized conditions such as the amount of the penicillamine ligand, pH, ionic liquids content, sample volume, and interfering ions

3.1. Amount of ligand

In the presented procedure, the amount of penicillamine as a ligand was optimized for separation/extraction of cobalt from the water and digested food samples. Thus, the amounts of penicillamine on cobalt extraction were studied in the range of 0.02-0.3 g in the presence of cobalt concentration ($1.5\text{-}62\ \mu\text{g L}^{-1}$) for 50 mL of liquid samples. The results showed that the quantitative extraction was obtained at 0.10 g of penicillamine. So, 0.12 g of penicillamine was used as a final amount of ligand which was added to IL /acetone as an extraction phase for water and food samples. Also, the effects of ILs on the extraction of cobalt were examined without any ligand and the recovery of ILs for cobalt was achieved less than 5%. Due

to Figure 2, the cobalt was efficient extracted by complexation of penicillamine more than 95%.

3.2. Amount of ionic liquids/acetone

By the USA-DLLME procedure, the effects of different ionic liquids, [OMIM][PF₆], [BMIM][PF₆], [HMIM][PF₆] and [EMIM][PF₆] were studied as trapping agents for cobalt extraction. So, the amounts of the hydrophobic ILs on the cobalt extraction were evaluated in the range of 20-250 mg of ILs containing $1.5\text{-}62\ \mu\text{g L}^{-1}$ of cobalt for 50 mL of water and digested food samples at pH=6. The quantitative recovery was achieved for cobalt with 160 mg [OMIM][PF₆]. So, 180 mg of [OMIM][PF₆] was used as an optimal IL for water and food samples. In addition, the effects of [OMIM][PF₆] for cobalt extraction were evaluated without any ligand and the maximum recovery was obtained less than 5%. Therefore, the [OMIM][PF₆] as a trapper green solvent with highly efficient recovery can be collecting cobalt –ligand from the liquid phase (Fig. 3).

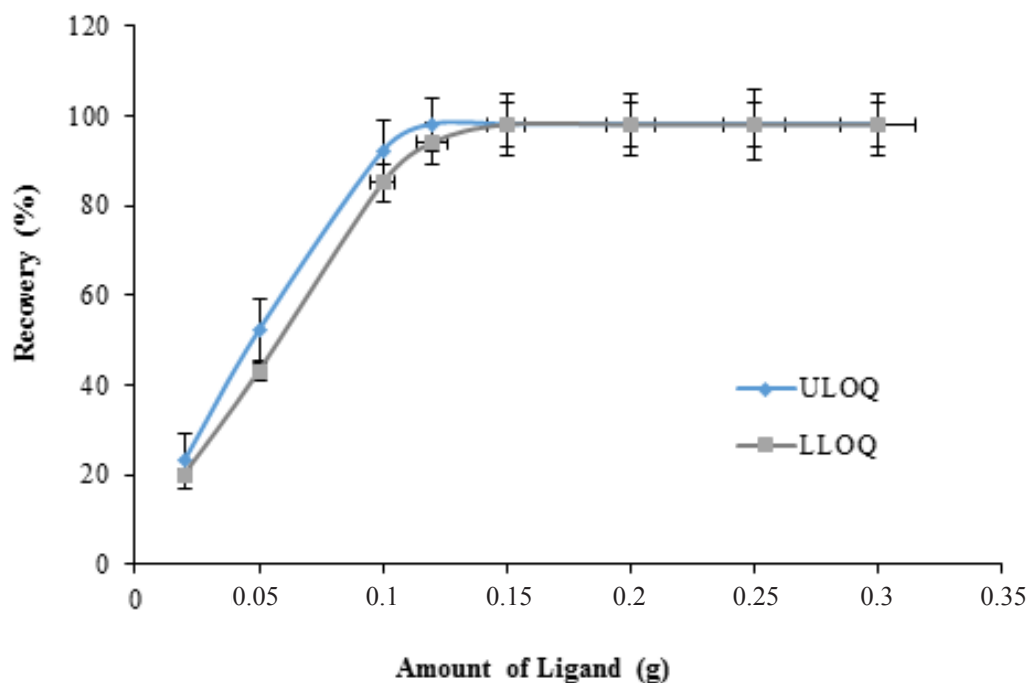


Fig.2. The effect of amount of penicillamine ligand on cobalt extraction by the USA-DLLME procedure (ULOQ: Upper Limit of Quantification, LLOQ: Lower Limit of Quantification)

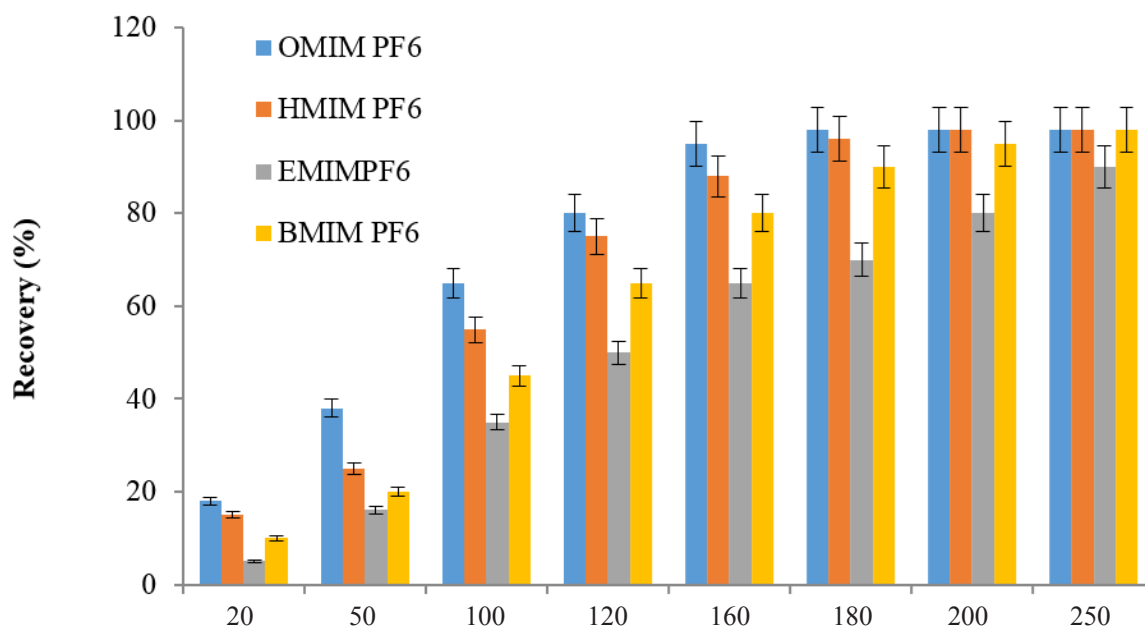


Fig.3. The effect of amount of IL on cobalt extraction by the USA-DLLME procedure

3.3. Sample volume

Sample volume is the main parameters for cobalt extraction in water and foods samples which must be optimized. Therefore, the different sample volumes for cobalt extraction/separation/preconcentration in water and foods samples between 5-100 mL based

on penicillamine ligand were studied containing $1.5\text{--}62 \mu\text{g L}^{-1}$ of cobalt. According to Figure 4, the efficient extraction was obtained for 5-60 mL of water and food samples at pH=6. So, 50 mL of water or digested food samples were selected as an optimal volume by the USA-DLLME procedure (Fig. 4).

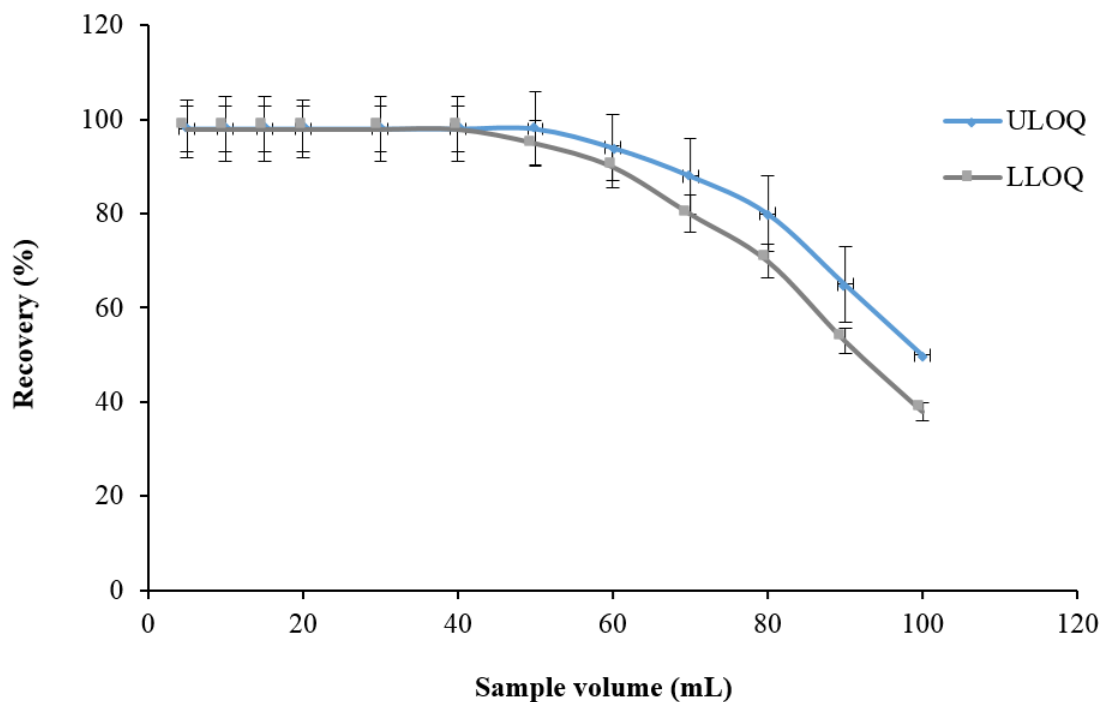


Fig.4. The effect of sample volume on cobalt extraction by the USA-DLLME procedure

3.4. pH Effect

pH is one of the most important parameters for cobalt extraction in water and digested food samples. Therefore, the pH ranges from 2 to 10 was prepared and adjusted by buffer solution for cobalt extraction in aqueous samples. Efficient recovery based on penicillamine ligand /IL was observed for cobalt concentrations ($1.5\text{--}62\ \mu\text{g L}^{-1}$) at pH of 5.5–6.5 in water samples. So, pH 6.0 was used for extraction of cobalt in water and digested food samples by the USA-DLLME procedure (Fig. 5). The proposed mechanism of cobalt extraction has been shown in the Schema 1 based on dative/covalent bond of thiol (HS) and amine (NH_2) functional groups of penicillamine with the positive charge of cobalt (Co^{2+}) at pH 6.0. Due to results, the isoelectric pH of penicillamine is 4.85, it can be concluded that above this pH, the

amine and thiol groups of penicillamine are free and they have nucleophilic ability to attack to orbitals of cobalt ion, and they easily participate in the complex formation process to extract cobalt ion. So in acidic pH, the (NH_2) group of penicillamine ligand has positive charged (NH_3^+) and the complexation wasn't occurred due to electrostatic repulsion between Co^{2+} and NH_3^+ , if some complexation is formed, it is due to the participation of the thiol group in this process. Also, the observed decline in the Figure 5 at pH above of 6.5 may be due to the competition of hydroxyl ions with the penicillamine ligand for complex formation resulting in the formation of stable cobalt hydroxide. So, the complexation of penicillamine ligand with Co^{2+} ions decreased at more than pH=6.5 as participated cobalt ions by hydroxide form ($\text{Co}(\text{OH})_2$).

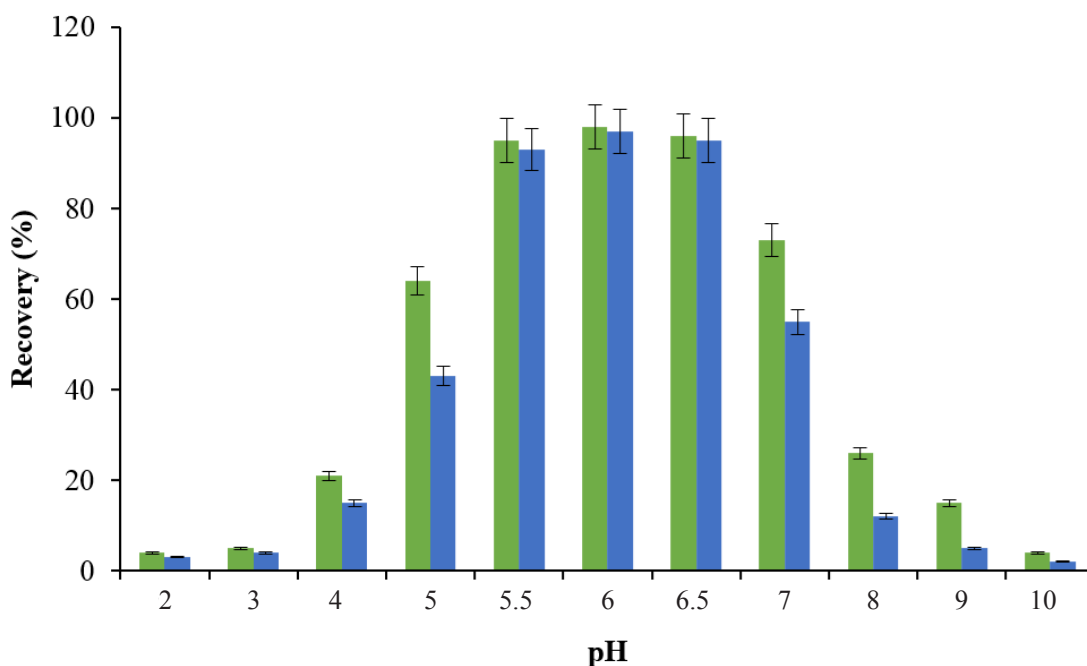


Fig.5. The effect of pH on cobalt extraction at LLOQ (Blue) and ULOQ (green) by the USA-DLLME procedure

3.5. Effect of interference of ions

The effect of interference ions on cobalt extraction based on penicillamine ligand in water/food samples was evaluated by the USA-DLLME procedure. So, the main concomitant ions were studied in water and food samples with different concentrations between 0.5-3 mgL⁻¹ for 50 mL of samples at pH=6. The results showed that the interfering ions had not affected for the cobalt extraction in water/food samples by the proposed procedure (Table 1). Also, the concentration ratio of interfering ions/cobalt ions (C_M/C_{Co}) for water ranged between 100-1800. The mean ratios for mercury, nickel and lead were seen at about 100-200, 700-850, 600-800 in water and digested food samples, respectively. So, the penicillamine ligand/ionic liquid phase can be extracted cobalt ions in the presence of the main interfering ions.

3.6. Eluent concentration and volume

The various eluents such as HNO₃, HCl and H₂SO₄ were used for back extraction of cobalt ions from the penicillamine ligand/IL/acetone. At acidic pH, the complexation of Co...SH-P was broken down and cobalt ions released into acid solution. Therefore, the various acid solutions based on different volumes and concentrations (0.2-1 mol L⁻¹, 0.1-1 mL were used for cobalt back extraction from IL phase. The Co(II) ions were quantitatively back-extracted from the penicillamine ligand/IL by HNO₃ with concentration more than 0.4 M. So, the 0.5 mol L⁻¹ of HNO₃ solution was selected as an eluent. Moreover, the various volumes of eluents between 0.1-1 mL were used for back-extraction of cobalt ions in water/food samples. Due to Figure 6, the 0.25 mL of HNO₃ (0.5 M) had the efficient back-extraction of Co(II) ions from IL phase. Finally, the remained solution was diluted with DW up to 0.5 mL before determining by AT-FAAS.

Table 1. The effect of interfering ions on extraction of Co(II) in water and digested food samples by the USA-DLLME procedure

Interfering Ions in blood (M)	Mean ratio ($C_M/C_{Co(II)}$)	Recovery (%)
	Co(II)	Co(II)
Cr ³⁺ , Al ³⁺ , Fe ³⁺	750	97.0
Mn ²⁺ , Cd ²⁺ , Mo ²⁺	800	96.6
Pb ²⁺	700	99.4
Zn ²⁺ , Cu ²⁺	600	97.8
I ⁻ , Br ⁻ , F ⁻ , Cl ⁻	1200	97.4
Na ⁺ , K ⁺ , Ca ²⁺ , Mg ²⁺	1400	98.1
CO ₃ ²⁻ , PO ₄ ³⁻ , HCO ₃ ⁻ , SO ₄ ²⁻	1000	99.2
Ni ²⁺	800	97.9
NH ₄ ⁺ , SCN ⁻ , NO ₃ ⁻	900	98.3
Hg ²⁺	150	97.2

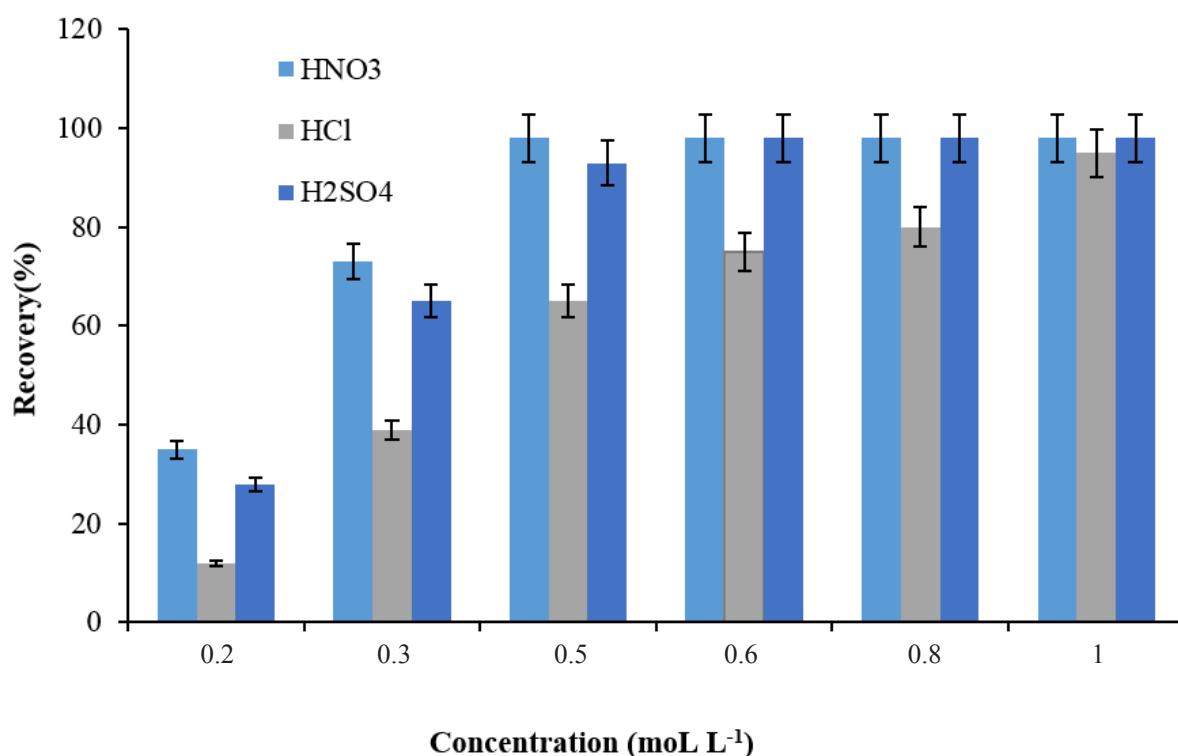


Fig.6. The effect of eluents on cobalt extraction by the USA-DLLME procedure

3.7. Real sample analysis

The extraction of cobalt (II) ions with the penicillamine ligand in water/food samples were developed by the USA-DLLME procedure at pH 6. Also, the total Co(II) in rice, spinach, broccoli and onion was determined after the digestion process by proposed procedure. The total Co(II) determined in digested foods samples after extraction by the penicillamine ligand/[OMIM][PF₆] at pH 6.0. Moreover, the real water and food samples were validated by spiking of standard solutions of cobalt in optimized conditions (Table 2). Therefore, the various concentrations of Co(II) were spiked to real samples. The results showed us that the high recovery for Co(II) ions in water/food samples was created by 1.2 g of the penicillamine ligand and 150 mg of [OMIM][PF₆].

Based on Table 2, the efficiency extraction and the satisfactory results was demonstrated the penicillamine ligand/[OMIM][PF₆] can be obtained the accurate and precision results for cobalt in liquid samples. Also, the method

validation was achieved based on the ET-AAS and the ICP –MS analyzer by microwave digestion process (Table 3).

4. Conclusions

A simple and sensitive method based on the penicillamine ligand/[OMIM][PF₆] was obtained for the Co (II) ions determination in water and digested food samples at pH=6. The concentrations of cobalt ions were determined by the AT-FAAS detection method after sample preparation by the USA-DLLME procedure. Recovery was achieved between 95.2–103.6 and relative standard deviation (RSD%) between 1.9–4.5 under optimized conditions. In this procedure, the shaking and centrifuging time were 4.5 and 3.0 minutes, respectively. The working range of 1.5–153 $\mu\text{g L}^{-1}$ were achieved by the presented method. Therefore, cobalt ions were extracted and determined effectively using penicillamine ligand/[OMIM][PF₆] in water/food samples with the USA-DLLME coupled to AT-FAAS.

Table 2. Validation of methodology for Co(II) determination with penicillamine ligand/[OMIM][PF₆] based on spiking standard samples by the USA-DLLME procedure coupled to AT-FAAS

Sample*	Added ($\mu\text{g L}^{-1}$)	*Found W ($\mu\text{g L}^{-1}$)/F ($\mu\text{g g}^{-1}$)	Recovery (%)
Well water A	---	12.1 \pm 0.4	---
	10	21.9 \pm 0.9	98.0
Wastewater B	---	45.6 \pm 2.3	---
	50	95.2 \pm 4.5	99.2
Wastewater C	---	34.5 \pm 1.7	---
	50	85.2 \pm 3.9	101.4
Rice	---	21.2 \pm 0.8	---
	20	40.9 \pm 1.6	98.5
Spinach	---	24.6 \pm 1.1	---
	25	49.2 \pm 2.3	98.4
Broccoli	---	30.2 \pm 1.2	---
	30	60.8 \pm 2.4	102
Onion	---	27.8 \pm 1.3	---
	30	57.3 \pm 2.7	98.3

*Mean of three determinations of samples \pm confidence interval ($P = 0.95$, $n = 10$)

Food samples digested by Microwave and determined by proposed procedure

All food samples prepared from supermarket Tehran

Well water A: 25 mL of water prepared from Shahre Ray, Tehran

Wastewater B: 25 mL of water prepared from petrochemical industry, Tehran, Iran

Wastewater C: 25 mL of water prepared from paint factory, Arak, Iran

The linear range for 25 mL of water samples is 3-124 $\mu\text{g L}^{-1}$

Water: W ($\mu\text{g L}^{-1}$) and Food: F ($\mu\text{g g}^{-1}$)

Table 3. The comparing of USA-DLLME /AT-FAAS method with ET-AAS and ICP –MS for cobalt determination in water and digested food samples (Mean, water ($\mu\text{g L}^{-1}$)/ Food ($\mu\text{g g}^{-1}$), $n=20$)

Sample	Ψ ICP-MS	ET-AAS Ψ	Ψ USA-DLLME	r^*	r^{\otimes}
Wastewater A	11.9 \pm 0.1	12.6 \pm 0.3	12.3 \pm 0.4	0.77	0.70
Wastewater B	46.1 \pm 0.9	44.9 \pm 2.3	45.5 \pm 2.4	0.81	0.73
Rice	21.6 \pm 0.5	20.6 \pm 1.0	21.3 \pm 0.8	0.65	0.78
Spinach	24.1 \pm 0.8	25.3 \pm 1.3	24.6 \pm 1.1	0.62	0.81
Onion	26.9 \pm 0.7	29.1 \pm 1.5	27.6 \pm 1.3	0.59	0.74

* r : Correlation of ET-AAS with USA-DLLME /AT-FAAS method for cobalt determination ($n=20$)

$\otimes r$: Correlation of ICP-MS with USA-DLLME /AT-FAAS method for cobalt determination ($n=20$)

*Mean of three determinations of samples \pm confidence interval ($P = 0.95$, $n = 20$)

5. Acknowledgments

The authors wish to thank from Department of Medicinal Chemistry, Faculty of Pharmacy, Kerman University of Medical Sciences, Kerman, Iran and Environmental Health Engineering Research Center, Kerman University of Medical Sciences, Kerman, Iran.

6. References

- [1] D. J. Paustenbach, B. E. Tvermoes, K. M. Unice, B. L. Finley, B. D. Kerger, A review of the health hazards posed by cobalt, *Crit. Rev. Toxicol.*, 43 (2013) 316–362.
- [2] J. E. Gray, R. G. Eppinger, Distribution of Cu, Co, As, and Fe in mine waste, sediment, soil, and water in and around mineral deposits and mines of the Idaho Cobalt Belt, USA, *Appl. Geochemistry*, 27 (2012) 1053–1062.
- [3] H. P. Hutter, P. Wallner, H. Moshhammer, G. Marsh, Dust and cobalt levels in the austrian tungsten industry: workplace and human biomonitoring data, *Int. J. Environ. Res. Public Health*, 13 (2016) 931–938.
- [4] M. Klasson, I. Bryngelsson, C. Pettersson, B. Husby, H. Arvidsson, H. Westberg, Occupational exposure to cobalt and tungsten in the swedish hard metal industry: air concentrations of particle mass, number, and surface area, *Ann. Occup. Hyg.*, 60 (2016) 684–699.
- [5] World Health Organization (WHO), Guidelines for drinking water quality, 3rd edn. World Health Organization, Geneva, 2011. <https://www.who.int/publications-detail-redirect/9789241549950>.
- [6] S. Feng, X. Wang, G. Wei, P. Peng, Y. Yang, Z. Cao, Leachates of municipal solid waste incineration bottom ash from Macao: Heavy metal concentrations and genotoxicity, *Chemosphere*, 67 (2007) 1133–1137.
- [7] S. R. Lim, J. Schoenung, Human health and ecological toxicity potentials due to heavy metal content in waste electronic devices with flat panel displays, *J. Hazard. Mater.*, 177 (2010) 251–259.
- [8] M. Moghadam, S. Jahromi, A. Darehkordi, Simultaneous spectrophotometric determination of copper, cobalt, nickel and iron in foodstuffs and vegetables with a new bis thiosemicarbazone ligand using chemometric approaches, *Food Chem.*, 192 (2016) 424–431.
- [9] Z. Tekin, S. Erarpat, A. Şahin, D. Selali Chormey, S. Bakirdere, Determination of vitamin B12 and cobalt in egg yolk using vortex assisted switchable solvent based liquid phase microextraction prior to slotted quartz tube flame atomic absorption spectrometry, *Food Chem.*, 286 (2019) 500–505.
- [10] K. A. Fox, T. M. Phillips, J. H. Yanta, M. G. Abesamis, Fatal cobalt toxicity after total hip arthroplasty revision for fractured ceramic components, *Clin. Toxicol.*, 54 (2016) 874–877.
- [11] A. Cheung, Systemic cobalt toxicity from total hip arthroplasties: review of a rare condition Part 1 - history, mechanism, measurements, and pathophysiology, *Bone Joint J.*, 98 (2016) 6–13.
- [12] B. Tvermoes, B. Finley, K. Unice, J. Otani, D. Paustenbach, D. Galbraith, Cobalt whole blood concentrations in healthy adult male volunteers following two-weeks of ingesting a cobalt supplement., *Food Chem. Toxicol.*, 53 (2012) 432–439.
- [13] A. Hart, P. Buddhdev, P. Winship, N. Faria, J. J. Powell, J. Skinner, Cup inclination angle of greater than 50 degrees increases whole blood concentrations of cobalt and chromium ions after metal-on-metal hip resurfacing, *HIP Int.*, 18 (2008) 212–219.
- [14] X. Zhang, D-penicillamine modified copper nanoparticles for fluorometric determination of histamine based on aggregation-induced emission, *Microchim. Acta*, 18 (2020) 7329.
- [15] Y. Hong, S. Jo, J. Park, J. Park, J. Yang, High sensitive detection of copper II ions using D-penicillamine coated gold nanorods based on localized surface plasmon resonance, *Nanotechnol.*, 29 (2018) 215501.

- [16] Z. Tekin, T. Unutkan, F. Erulaş, E. G. Bakirdere, S. Bakirdere, A green, accurate and sensitive analytical method based on vortex assisted deep eutectic solvent-liquid phase microextraction for the determination of cobalt by slotted quartz tube flame atomic absorption spectrometry, *Food Chem.*, 310 (2020) 125825.
- [17] M. Shirani, F. Salari, S. Habibollahi, A. Akbari, Needle hub in-syringe solid phase extraction based a novel functionalized biopolyamide for simultaneous green separation/preconcentration and determination of cobalt, nickel, and chromium (III) in food and environmental samples with micro sampling flame atomic absorption spectrometry, *Microchem. J.*, 152 (2019) 104340.
- [18] M. Asli, M. Azizzadeh, A. Moghaddamjafari, M. Mohsenzadeh, Copper, iron, manganese, zinc, cobalt, arsenic, cadmium, chrome, and lead concentrations in liver and muscle in Iranian Camel (*Camelus dromedarius*), *Biol. Trace Elem. Res.*, 194 (2020) 390–400.
- [19] S. G. Elci, Determination of cobalt in food by magnetic solid-phase extraction (MSPE) preconcentration by polyaniline (PANI) and polythiophene (PTH) coated magnetic nanoparticles (MNPs) and microsample injection system– flame atomic absorption spectrometry (MIS-FAAS), *Instrum. Sci. Technol.*, 49 (2021) 258–275.
- [20] F. Salimi, M. Shamsipur, E. Koosha, M. Ramezani, A new dispersive micro-solid phase extraction based on rejection property method combined with FAAS for the simultaneous determination of cobalt and copper after optimisation by Box-Behnken design, *Int. J. Environ. Anal. Chem.*, (2020) 1–13.
- [21] Q. Han, Y. Huo, X. Yang, Y. He, J. Wu, Dispersive liquid–liquid microextraction coupled with graphite furnace atomic absorption spectrometry for determination of trace cobalt in environmental water samples, *Int. J. Environ. Anal. Chem.*, 100 (2020) 945–956.
- [22] H. Kang, J. Li, C. Zhang, J. Lu, Q. Wang, Y. Wang, Study of the electrochemical recovery of cobalt from spent cemented carbide, *RSC Adv.*, 10 (2020) 22036–22042.
- [23] R. Kakitha, S. Pulipaka, D. Puranam, Simultaneous determination of iron and cobalt using spectrophotometry after cationic mixed micellar cloud point extraction procedure, *Orient. J. Chem.*, 36 (2020) 1168–1172.
- [24] K. Kafumbila, Cobalt precipitation with MgO: material balance from kinetic samples cobalt precipitation with MgO: Material balance from kinetic samples. Independent Metallurgical Operations Pty Ltd (IMO), 2020.
- [25] A. Ghasemi, M. R. Jamali, Z. Es’haghi, Ultrasound assisted ferrofluid dispersive liquid phase microextraction coupled with flame atomic absorption spectroscopy for the determination of cobalt in environmental samples, *Anal. Lett.*, 54 (2021) 378–393.
- [26] S. Keshipour, K. Adak, Magnetic d-penicillamine-functionalized cellulose as a new heterogeneous support for cobalt (II) in green oxidation of ethylbenzene to acetophenone. *Appl. Org. Chem.*, 31(2017) e 3774. <https://doi.org/10.1002/aoc.3774>



Developing a magnetic nanocomposite adsorbent based on carbon quantum dots prepared from Pomegranate peel for the removal of Pb(II) and Cd(II) ions from aqueous solution

Hamideh Asadollahzadeh^{a,*}, Mahdijeh Ghazizadeh^a and Mohammad Manzari^a

^aDepartment of Chemistry, Faculty of Science, Kerman branch,
Islamic Azad University, Kerman, Iran, P. O. Box 7635131167, Kerman, Iran

ARTICLE INFO:

Received 2 Jun 2021

Revised form 5 Aug 2021

Accepted 27 Aug 2021

Available online 29 Sep 2021

Keywords:

Carbon quantum dots,
Iron oxide nanoparticles,
Adsorption,
Lead and Cadmium,
Isotherms,
Flame atomic absorption spectrometry

ABSTRACT

Agriculture waste is a good choice for the production of carbon dots owing to its abundance, wide availability, eco-friendly nature. In this study a novel magnetic bioadsorbent based on carbon quantum dots (Fe₃O₄-PPCQDs) from Pomegranate peel (PP) was used as adsorbent to remove lead (Pb) and cadmium (Cd) from 50 mL of water and wastewater samples by magnetic solid phase extraction (MSPE). After adsorption ions with Fe₃O₄-PPCQDs at pH=6, the concentration of Pb(II) and Cd (II) ions were determined by flame atomic absorption spectrometry (F-AAS). The manufactured of Fe₃O₄-PPCQDs and GO nanostructures were structurally characterized by scanning electron microscopy (SEM), transmission electron microscopy (TEM), X-ray diffraction (XRD) and Fourier transform infrared spectroscopy (FT-IR). The quantum dots were optically characterized by UV-Vis spectroscopy. Batch adsorption experiment was conducted to examine the effects of pH, contact time, temperature and initial concentration of Pb(II) and Cd(II) from the water. The preconcentration factor and LOD for Cd and Pb were obtained 50 and (1.3 µg L⁻¹; 15.5 µg L⁻¹), respectively. The equilibrium data of ions sorption were well described by Langmuir and Freundlich model. The R² values obtained by Langmuir model were higher. The absorption capacity of Fe₃O₄-PPCQDs for cadmium and lead were obtained 17.92 and 23.75 mg g⁻¹, respectively.

1. Introduction

Environmental pollution based on the organic chemical compounds (VOCs) and heavy metals (M) have needed a serious threat due to the rapid development of the chemical industry and the toxic effect in environment. The contamination of heavy metals in water through the industrial wastewater is the global environmental problems [1]. The heavy metals compounds cannot be decomposed naturally

and cause the various health problems in the living organism and human. Recently, the elimination of heavy metals is becoming a significant concern as a result of their persistence into the atmosphere [2]. Among of heavy metals, cadmium and lead (Cd and Pb) can be discharged from the several industrial effluents. Cadmium is liberated into the environment from the steel production, the cement manufacture, the Ni-Cd battery manufacture, cadmium electroplating, the phosphate fertilizers etc. [3]. Bivalent cadmium causes a number of deformities and diseases in humans, such as the muscle cramps, the lung problems, the

*Corresponding Author: [Hamideh Asadollahzadeh](mailto:Hamideh.Asadollahzadeh@iaukerman.ac.ir)

Email: asadollahzadeh90@yahoo.com

<https://doi.org/10.24200/amecj.v4.i03.149>

kidney degradation, the proteinuria, the skeletal deformation [4]. On the other hand, common anthropogenic causes of lead contamination in groundwater include the smelting, the mining, the consumption of fossil fuels and the incinerating solid waste [5]. Lead can cause a cognitive dysfunction in children, high blood pressure, the illnesses of the immune system and the reproductive system [6]. Numerous techniques have been used to reduce the harmful effects of cadmium and lead on water source, including the chemical oxidation and the reduction, the chemical precipitation, the ion exchange, the electrochemical processes, and the membrane filtration [7]. The performance and perform of above processes are difficult without any selectivity. However, among these methods, the adsorption technique is flexible, low cost and has a high efficient recovery [8]. Adsorption is a mass transfer process where a substance is transferred from the liquid phase to the surface of the solid through physical or chemical interaction. Many kinds of adsorbents, including the activated carbon [9], the inorganic minerals [10], the biomass adsorbents [11-13], and polymer [14-17] are used to remove the metal ions from the liquid phased such as water and wastewater. By-products from agriculture feed have always considered due to its availability and the cost features. Moreover, the other important characteristics are biocompatibility, biodegradability and the renewable [18]. Thus there is an interest in use of agricultural wastes as a source for preparation of carbon based nanomaterial. Carbon based quantum dots are new class of carbon nanomaterials that have been explored due to their excellent properties [19]. However, the separation of adsorbents, obtained from agricultural waste, required a high-speed centrifugation or filter due to they are too small [20]. Iron oxide has excellent magnetic properties, the high biocompatibility, easy separation through external magnetic field, reusability and comparatively low cost. The magnetic iron oxide was fixed inside the polymer adsorbent matrix with the highest adsorption rates [21]. The surface modification of the activated carbon-based iron

oxide using the coating technique improves their sorption capacity because, the surface coating phenomenon helps to converting the closely - packed cubic geometry of magnetic nanoparticles into compact [22].

Pomegranate peel (PP), as a by-product of the pomegranate juice industry is an inexpensive material. It is composed of several constituents, including polyphenols, ellagic tannin and ellagic acids [23]. So far, no study has been done on surface modification of iron oxide by using carbon quantum dots prepared from pomegranate peel for developing magnetic nanocomposite (Fe_3O_4 -PPCQDs). The PPCQDs adsorbent has generated from the pomegranate peel and functionalized with Fe_3O_4 as magnetic nanostructure which was used for removing toxic ions from wastewater. Another advantage is that the loaded adsorbents could be easily separated from the aqueous solution using magnet instead of centrifugation thus conserving energy. In this study, the material preparation, the characterization and the batch-type removal experiments were carried out wherein the feasibility of the above described composite for the removal of heavy metals Cd(II) and Pb(II) from aqueous solution which were investigated by varying the process conditions.

2. Material and Methods

2.1. Apparatus

The concentration of heavy metals (Pb and Cd) in the aqueous solution was measured using flame atomic absorption spectrometry (F-AAS, Model AAnalyst 800, Air acetylene, Perkin Elmer, USA). The wavelength of 217.0 nm (Slit :1, Current lamp: 5mA) and 228.8 nm (Slit: 0.5, Current lamp: 3 mA) was used for lead and cadmium determination, respectively. The working ranges for lead and cadmium were achieved 2.5-20 mg L⁻¹ and 0.2-1.8 mg L⁻¹, respectively by sensitivity of 0.06 mg L⁻¹. The LOD of F-AAS for lead and cadmium was achieved 0.1 mg L⁻¹ and 0.05 mg L⁻¹, respectively. The auto-sampler from 0.5 to 5 mL was used for sample introduction to F-AAS. The pH was measured by electronic pH meter (Benchtop meter inoLab pH 7110 model, WTW company, Germany).

2.2. Chemicals

Pomegranate peel were obtained from Mahan, Kerman, Iran. Sodium hydroxide (NaOH), cadmium nitrate tetrahydrate (Cd(NO₃)₂·4H₂O), lead nitrate (Pb(NO₃)₂), the ferric chloride hexahydrate (FeCl₃·6H₂O), the ferric sulfate heptahydrate (FeSO₄·7H₂O) hydrochloric acid (HCl) with a purity of 37%, nitric acid (HNO₃) with purity 63% was purchased from Merck and all the chemical reagents were analytical grade. All the aqueous solutions were prepared by using double distilled water. The pH of the solution was adjusted and measured using electronic pH meter. The pH of the solution was adjusted by adding 0.1M HCl or 0.1M NaOH and measured using electronic pH meter (Benchtop meter inoLab pH 7110 model, WTW company, Germany).

2.3. Synthesis of Magnetic Carbon Quantum Dots (Fe₃O₄-CQDs)

The pomegranate peel (PP) has carbon structure which was ground after washed/ dried in the oven 100°C. The ground powder is sifted by small mesh to obtained for used for synthesis of CQDs. First of all, 100 grams of ground powder of the pomegranate peel (PP) mixed with 8 Liters of DW in the 500 mL closed container. The closed container adjusted on temperature between 200-230°C for two days and then the temperature decreased (cooling) up to room temperature for one day. The sediments were separated in by Watman filter paper based on the vacuum pump and the black brown product is created. After UV irradiation (400 nm), the color of product change into blue photoluminescence which was showed that a quantum dot particles synthesized correctly. The CQDs cab be absorbed the UV irradiation at 220 nm spectrophotometer. The final liquid product filtered / dried completely at temperature of 100 °C and finally converted into powder. The powder put in the oven based on quartz type, N₂ gas and 700 °C (1 hour). Then the product powder was carbonized and impurities get out of oven. After synthesis PPCQDs, the absorption of UV was obtained at 210 nm which was confirmed by UV peak by spectrophotometer (Fig.1a). the

magnetic Fe₃O₄-PPCQDs were prepared by co-precipitation of FeCl₂·4H₂O and FeCl₃·6H₂O, in the presence of PPCQDs [24]. To prepare the nano magnetic PPCQDs, 10 mg of PPCQDs in 10 mL of DW was ultra-sonicated for 1 h. To the resulting mixture was added 12.5 mL solution of FeCl₂·4H₂O (125 mg) and FeCl₃·6H₂O (200 mg) in deionized water (10 mL) at room temperature. Then, 30% ammonia solution was added for the pH = 11 and the temperature was increased to 60 °C. After being stirred for 1 h, the product was cooled at 25°C. finally, the black powder of Fe₃O₄-PPCQDs centrifuged at 4000 rpm for 20 min, washed and dried at 75°C (Fig.1 b).

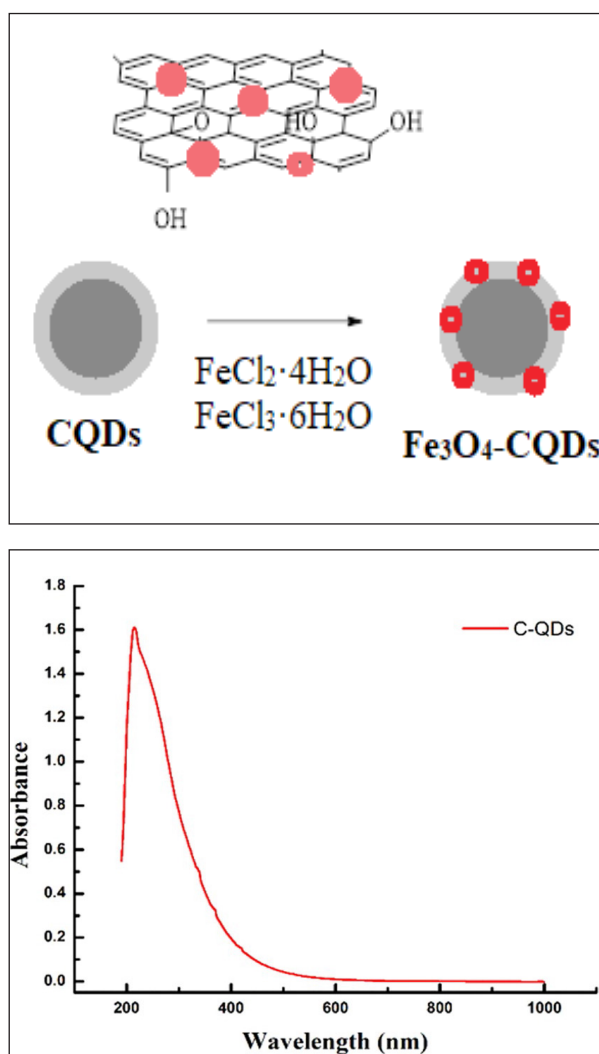


Fig.1. a) UV absorption by CQDs product **b)** The mechanism of synthesis of Fe₃O₄-PPCQDs

2.4. Batch mode adsorption and analytical procedure

Adsorption of Pb(II) and Cd(II) based on Fe₃O₄-PPCQDs adsorbent was achieved in optimized experimental conditions such as pH, the contact time, the amount of adsorbent and temperature. The experiments were carried out in 50 ml Erlenmeyer flasks. Experiment parameters were achieved from pH 2 to 8, the sample volume of 50 mL, the contact time between 2 - 60 minute, the amount of biosorbent from 0.01 to 0.2 g, the temperature between 5-45°C and the concentration of ions 5-150 mg L⁻¹. To adjust required The pH of aqueous solution was adjusted with HCl (0.1 M) and NaOH (0.1 M). Finally, the thermodynamic parameters and isotherms were studied. The Fe₃O₄-PPCQDs were separated with a magnet using its magnetic field, and the filtrate was kept for the further determination of remaining Pb(II) and Cd(II) in water by F-AAS after back extraction solid phase by 1 mL mixture of HNO₃ 0.1 M/DW. Moreover, the linear ranges of MSPE procedure for cadmium and lead based on Fe₃O₄-PPCQDs were achieved 4-20 µg L⁻¹ and 50-140 µg L⁻¹, respectively (RSD%<2.4). So, the trace analysis of lead and cadmium (sub-ppb) can be created by the Fe₃O₄-PPCQDs adsorbent. The quantity of adsorbed ion per unit mass of biosorbent was calculated from Equation 1:

$$q_e = (C_0 - C_e) \times V/m \quad (1)$$

where C₀ and C_e are the concentrations of Pb(II)

and Cd(II) at the beginning and at the end of the adsorption process.

3. Result and discussion

3.1. Characterization

X-ray diffraction (XRD) patterns were recorded on a Seifert TT 3000 diffractometer (Ahrensburg, Germany). The specific surface areas and pore volume of the sorbents were calculated by the Brunauer-Emmett-Teller (BET) and Barrett-Joyner-Halenda (BJH) methods, respectively. Scanning electron microscopy (SEM, Phillips, Netherland) was used for surface image of the CQDs. The morphology of sorbent was examined by transmission electron microscopy (TEM, Philips, Netherland). The Fourier transform infrared spectrophotometer (FTIR, Bruker GmbH, Germany) using KBr pelleting method was used in the 4000–200 cm⁻¹.

3.2. Fourier-transform infrared spectroscopy (FTIR)

The FTIR spectra of Fe₃O₄-PPCQDs adsorbent are shown in Figure 2. The prime spectrum of FTIR of CQDs is shown in black line as nonactivated form (Fig. 2a) and red line (activated/HNO₃) which has different wavenumbers but both of them is similar. In these figures, the peak of 1020 cm⁻¹, 1200 cm⁻¹, 1250 cm⁻¹ belong to C-O bond and the peak of 1381 cm⁻¹ shows the formation of C-H bond. Additionally a peak of 1585 cm⁻¹ is observed for C=C bond and the another peak appeared in

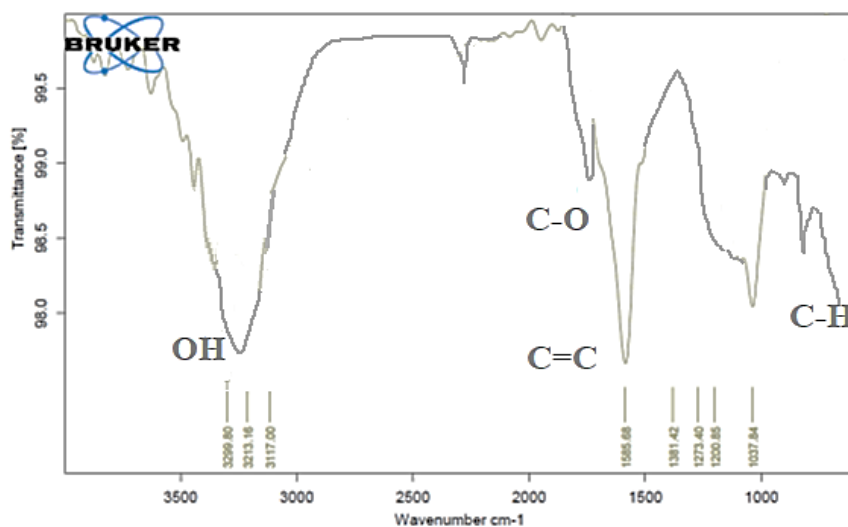


Fig.2(a). The spectrum of FTIR of CQDs

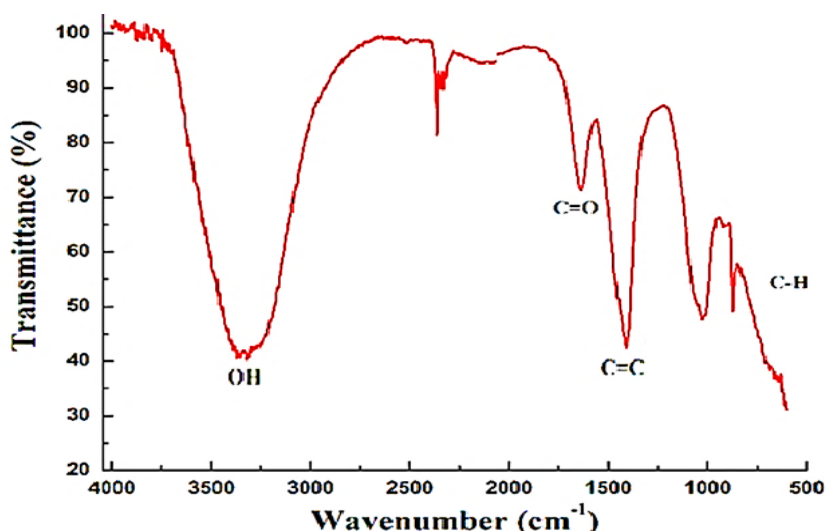


Fig.2(b). The spectrum of FTIR of HNO₃-CQDs

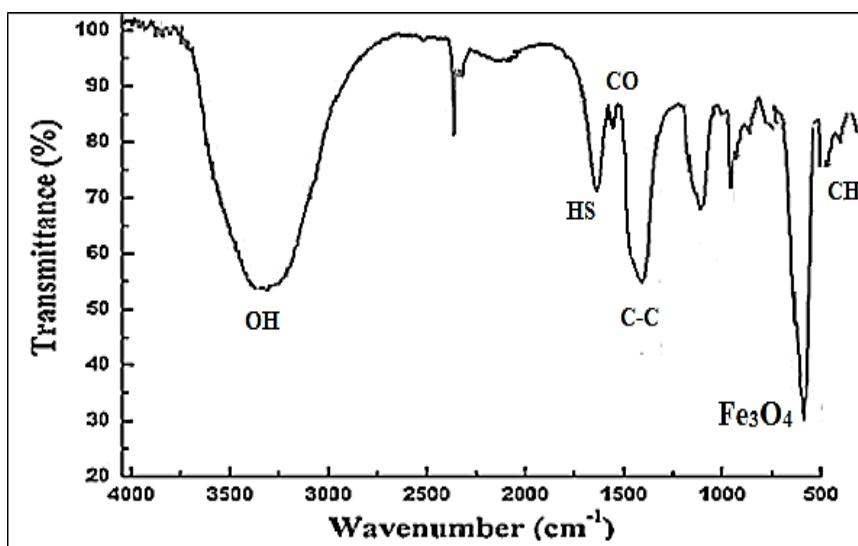


Fig.2(c). The spectrum of FTIR of Fe₃O₄-PPCQDs

3300 cm⁻¹ shows the O-H bond. In Figure 2 (b), the red graph is the sample activated with nitric acid vapour. Meanwhile similar peaks of 3340 cm⁻¹ (O-H bond) were observed in Figure 2(a,b). In addition FTIR of Fe₃O₄-PPCQDs was shown in Figure 2 C which has a peak in 582 cm⁻¹ belong to Fe₃O₄.

3.3. XRD spectra of CQD

In Figure 3, the X-ray diagram was shown for carbon quantum dots(CQDs) and magnetic carbon quantum dots (Fe₃O₄-PPCQDs). The XRD curve of Fe₃O₄-PPCQDs is similar to simple

form of CQDs. In this pattern two main Peaks in 2θ is equal to 22-24 degrees and 45 degrees were observed. The observed wide peak is in the intensity of 24 degrees in page (002) relates to the graphite. The width peak can have related to small size of carbon quantum dots. The observed Fe₃O₄-PPCQDs peak in 45 degree angle relate to (101) which indicates similar to graphene formed by quantum dot particles. The XRD pattern for CQDs is similar to Fe₃O₄-PPCQDs which was indicated that carbon quantum dots modified with PP and Fe₃O₄ did not changed on the structural order of CQDs.

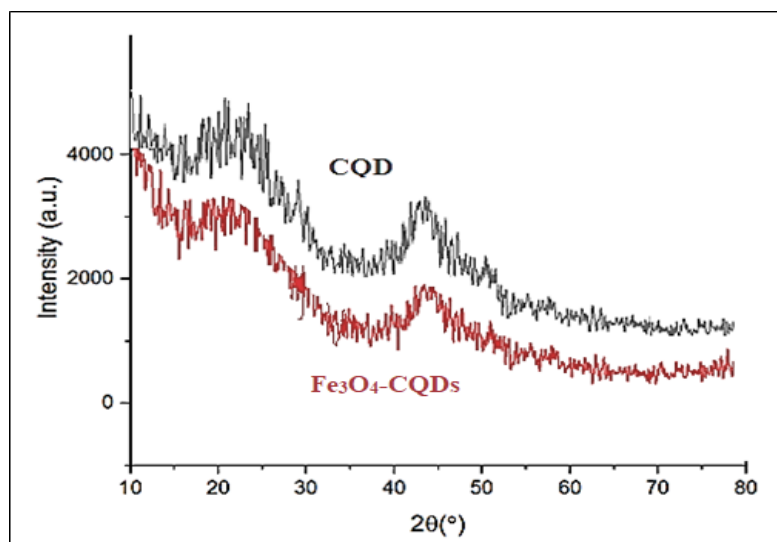


Fig.3. The XRD diagram of CQDs and Fe_3O_4 -PPCQDs

3.4. Field emission scanning electron microscope (FE-SEM)

The surface morphology of the CQDs was reported a field emission scanning electron microscope (FE-SEM). The FE-SEM of CQDs have been shown in [Figure 4\(a\)](#). The CQDs primary samples were formed as blocks of nano particles carbon. The blocks are as a colony and forms big volume of CQDs. The smallest size the structure was between 10 to 30 nanometer which consists of very small particles of CQDs. The FE-SEM of the Fe_3O_4 -PPCQDs was shown in [Figure 4\(b\)](#) with size of 10-25 nm.



Fig.4a. The FESEM of CQDs

3.5. Transmission electron microscopy (TEM)

Transmission electron microscopy (TEM) was used to study of the nanostructure size. The microscopic pictures of the CQDs have been shown in [Figure 5a](#). These pictures are shown clearly a magnified picture which the carbon particles are so small. Moreover, the formation of Fe_3O_4 -PPCQDs has very small particles which is clearly visible by TEM ([Fig.5b](#)).

3.6. Batch adsorption studies

3.6.1. pH dependent studies

The effect of pH ([Fig. 6a and b](#)) on the adsorption of Pb(II) and Cd(II) ions was studied by Fe_3O_4 -PPCQDs.

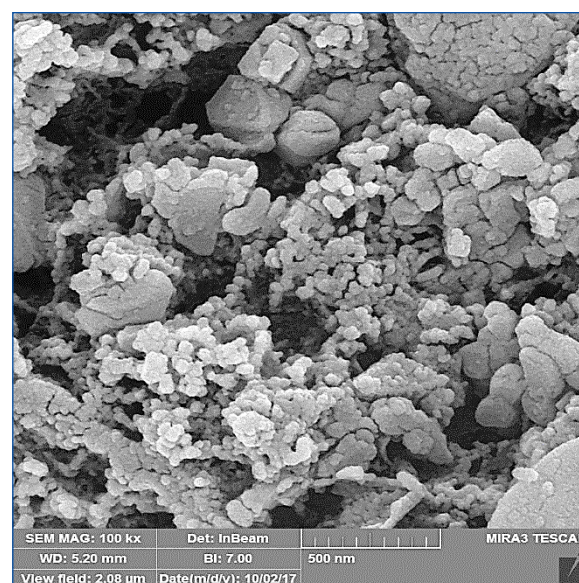


Fig.4b. The FESEM of Fe_3O_4 -CQDs

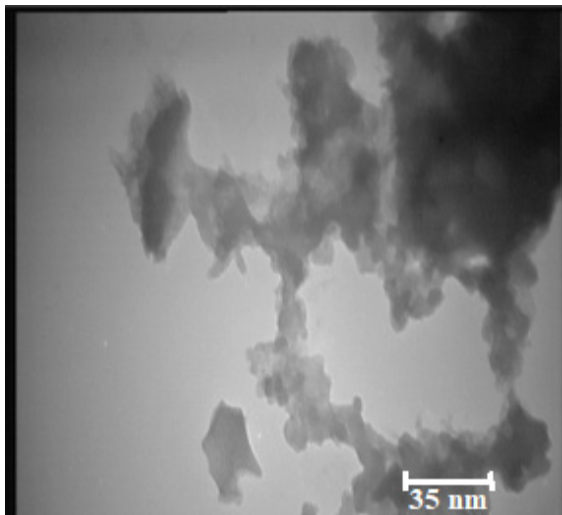


Fig.5a. The TEM of CQDs

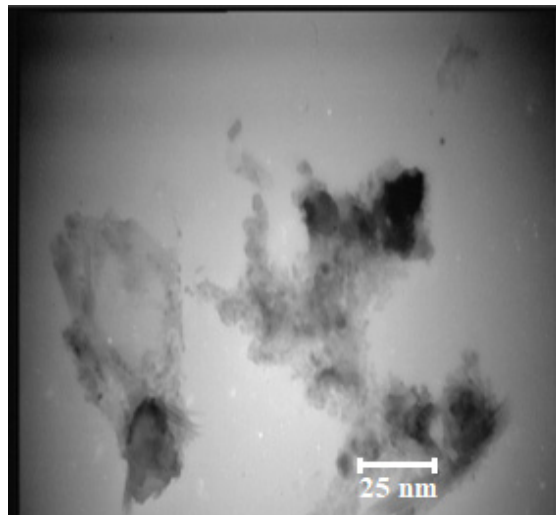


Fig.5b. The TEM of Fe₃O₄-PPCQDs

In order to determine the optimum pH, the pH range between 2.0–11.0 was evaluated for Pb(II) and Cd(II) ions. While screening the pH values, all the other process variables were kept constant. A control experiment was also run (in the absence of Fe₃O₄-PPCQDs) for the removal Pb(II) and Cd(II) to explore the effect of chemical precipitation (Fig. 6a). The control experiment revealed that there was no removal of Pb(II) and Cd(II) up to pH 7.0 but when the pH was more than 7.0 both ions precipitated as hydroxides [Pb(OH)₂ and Cd(OH)₂] in the solution thus, leading to their complete removal without Fe₃O₄-PPCQDs. Also, the adsorption of Fe₃O₄-PPCQDs was shown in Figure 6b. Due to interaction of ions with adsorbent, the maximum removal for Pb(II) and Cd(II) was achieved at

pH 6.0. The adsorption of Pb(II) and Cd(II) was decreased at lower and upper pH of 6 (5.5 > pH > 6.5). This behavior may be due to the reason that: lower pH leads to an abundance of hydronium ions (H₃O⁺) in the solution that causes competition between hydronium ions and Pb(II) and Cd(II) ions for adsorption onto Fe₃O₄-PPCQDs. Thereby lowering the overall adsorption efficiency of these metal ions occurred at lower pH [25]. On the other hand, by increasing pH, the adsorption also increased, which can be showed that in this range (neutral and weakly acidic) most metals are available as soluble and free cations for adsorption. One of the important factors related to the chemical structure of the adsorbent is the point – zero charge pH (pH_{pzc}). At this pH, there is no charge on the surface.

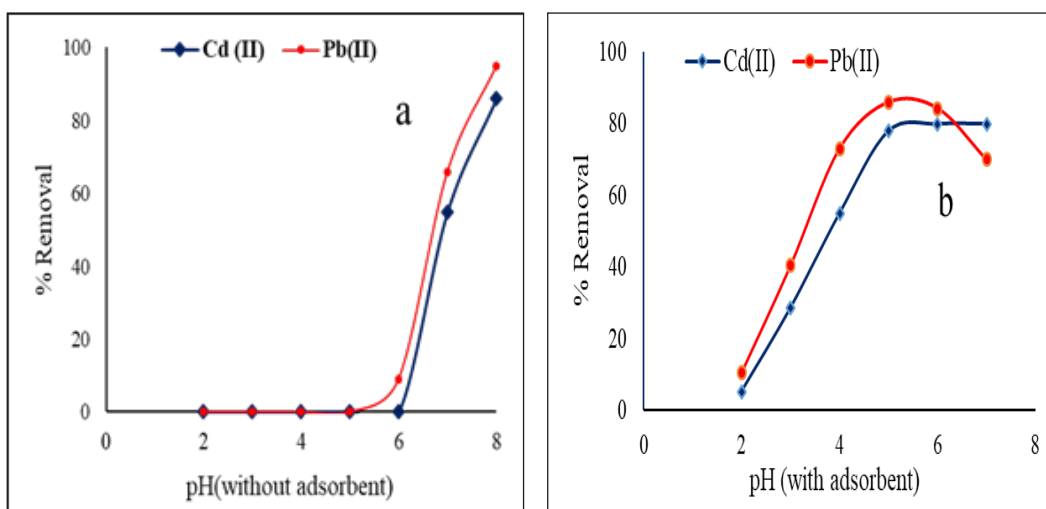


Fig.6. a) Effect of pH on Pb(II) and Cd(II) removal without Fe₃O₄-PPCQDs, b) with Fe₃O₄-PPCQDs adsorbent

3.6.2. Effect of time

The effect of contact time on the removal of Pb(II) and Cd(II) by Fe₃O₄-PPCQDs was investigated to determine the optimum time taken to attain the equilibrium. The adsorption experiments were carried out by varying the contact time between 2 and 60 min, keeping all other process variables constant. Figure 7 depicts that the removal percentage was increased by increasing of the contact time. The equilibrium was achieved for 20 min and after this time, the further removal for Pb(II) and Cd(II) ions was not observed (constant). It was observed that, the rate of adsorption of ions was faster at initial stages, that this may be attributed to the quick uptake of ions onto the large surface area of Fe₃O₄-PPCQDs up to 20 min and after it the adsorption progress was slowly followed and remained constant.

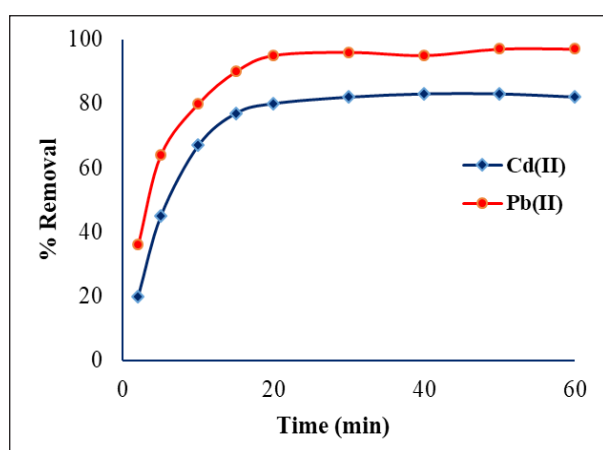


Fig. 7. Effect of contact time on Pb(II) and Cd(II) removal by Fe₃O₄-PPCQDs

3.6.3. Effect of amount of adsorbent

The effect of amount of Fe₃O₄-PPCQDs was investigated under optimized conditions (pH=6 and contact time: 20 min.). As shown in Figure 8, the adsorption increased with the Fe₃O₄-PPCQDs amount up to 0.1 g. Also, the adsorbent surface has saturated with the extra value of Pb(II) and Cd(II) ions in optimized mass. At higher amount of adsorbent, the adsorption yield is almost unchanged, because the most of Pb(II) and Cd(II) ions interact with Fe₃O₄-PPCQDs surface.

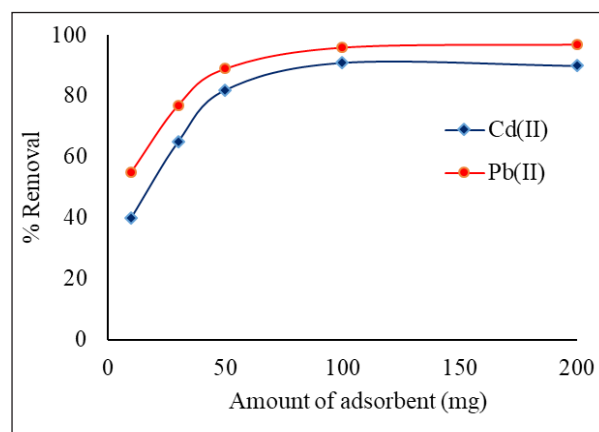


Fig. 8. The effect of adsorbent amount on Pb(II) and Cd(II) removal Fe₃O₄-PPCQDs

3.6.4. Effect of temperature

The effect of the temperature on adsorption of Pb(II) and Cd(II) ions was examined. As shown in Figure 9, the adsorption was reduced as the temperature rising (5 °C–45 °C). The desorption of metal ions on Fe₃O₄-PPCQDs was exothermic process and by increasing temperature the removal efficiency decreased. So, the high adsorption of Pb(II) and Cd(II) ions on Fe₃O₄-PPCQDs adsorbent depended on the low temperature.

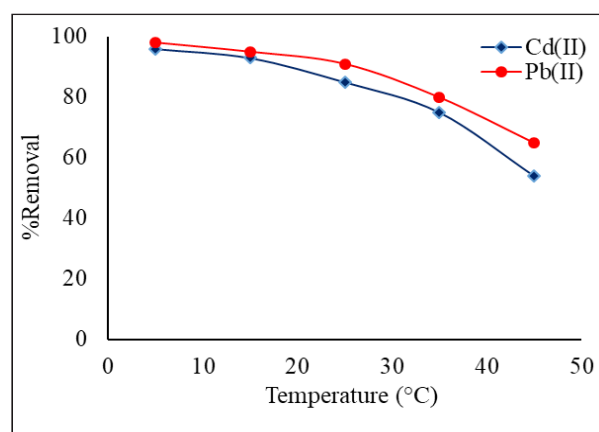


Fig. 9. The effect of temperature on Pb(II) and Cd(II) removal by the Fe₃O₄-PPCQDs

3.6.5. Effect of initial concentration of Cd(II) and Pb(II)

The effect of initial concentrations of Pb(II) and Cd(II) on adsorption process based on Fe₃O₄-PPCQDs were evaluated at various concentration from 10 to 150 mg L⁻¹. In addition, the all of other parameters are

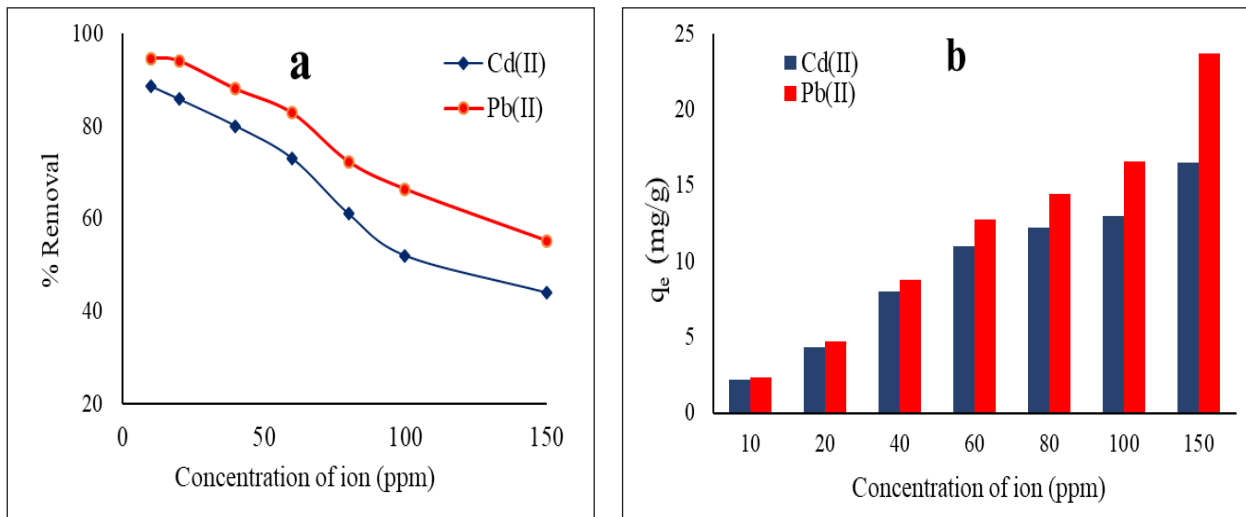


Fig. 10. a). Effect of initial metal ion concentration on Pb(II) and Cd(II) removal by Fe₃O₄-PPCQDs, **b)** adsorption capacity against metal ion concentration.

constant which is shown in Figure 10a. The Figure 10a revealed that the metal removal was reduced by the Fe₃O₄-PPCQDs when the metal concentration increased from 10 to 150 mg L⁻¹ in the solution. The results showed, the removal efficiencies (%) were decreased for Cd(II) and Pb(II) from 88.60 to 44 and 94.61 to 55.22, respectively. The reduce of removal efficiency (%) by increasing the metal concentration may be due to covering /coating of the most surface sites of Fe₃O₄-PPCQDs with high concentration of Pb(II) and Cd(II) and the adsorption capacity of the adsorbent get exhausted due to non-availability of free binding sites [25]. Also, at low concentration ranges, the percentage of adsorption is high because of the availability of more active sites on the surface of adsorbent. Figure 10b showed that the adsorption capacity against ion concentrations. The increase in adsorption capacity depended on initial metal concentration which was led to increase the diffusion of Pb(II) and Cd(II) ions from the liquid phase to the surface of the solid phase. So, the driving force of the metal ions cause to lead to the collisions between metal ions and the nanoparticles surface. Therefore, the adsorption capacity was increased [23].

3.7. Adsorption thermodynamic

The adsorption process was analyzed by thermodynamic theory. The thermodynamic

parameters viz. standard Gibb's free energy (ΔG°), standard enthalpy (ΔH°) and standard entropy (ΔS°) for the removal of Pb(II) and Cd(II) by the Fe₃O₄-PPCQDs were calculated by Equations 2-5 [26]:

$$\Delta G^\circ = -RT \ln K \quad (\text{Eq. 2})$$

$$\Delta H^\circ = \left[\frac{RT_1 T_2}{(T_2 - T_1)} \right] \ln \left(\frac{K_2}{K_1} \right) \quad (\text{Eq. 3})$$

$$\Delta S^\circ = \left(\frac{\Delta H^\circ - \Delta G^\circ}{T} \right) \quad (\text{Eq. 4})$$

$$K = \left(\frac{qe}{Ce} \right) \quad (\text{Eq. 5})$$

where R (8.314 J mol⁻¹ K⁻¹) is the universal gas constant, K is the equilibrium constant at temperature T, T is the absolute temperature (K), Ce (mg L⁻¹) is the equilibrium concentration and qe is the amount of Cd(II) and Pb(II) adsorbed on the surface of the Fe₃O₄-PPCQDs. Figure 11 shows the relationship between ΔG° and temperature. Table 1 gives the thermodynamic parameters for adsorption of Cd(II) and Pb(II) adsorbed on the surface of the Fe₃O₄-PPCQDs adsorbent at different temperatures. As can be seen from the Table 1 the negative value of ΔG° signifies that the adsorption process is feasible and spontaneous in nature. With the increase in temperature, ΔG° shifts to more positive values indicating that the increase in temperature

was not favorable for the adsorption process [27]. The negative value of ΔH° signifies that the adsorption process is exothermic. That was also the reason equilibrium adsorption of Cd(II) and Pb(II) decreased as the rising of solution temperature (Effect of temperature). The value of ΔS were -20.31 and $-6.38 \text{ J mol}^{-1} \text{ K}^{-1}$ for adsorption of Cd(II) and Pb(II) ions, which reflected that the randomness at the interface of the Fe_3O_4 -PPCQDs and solution was reduced during the adsorption process.

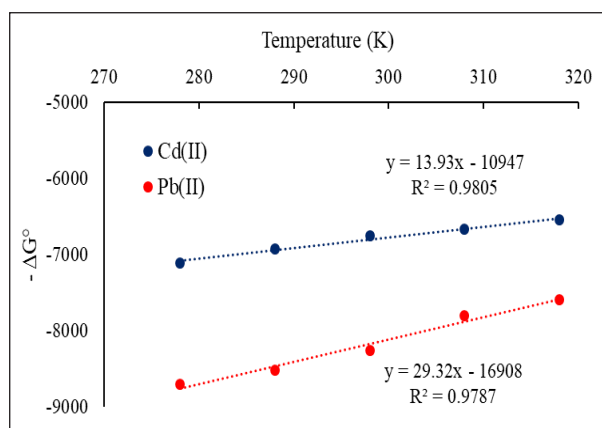


Fig.11. Relationship between ΔG° and temperature

3.8. Adsorption isotherms

The most popular isotherms are Langmuir and Freundlich [28] models. The Langmuir model describes monolayer adsorption, however Freundlich model show heterogeneous surface. The linear form of Langmuir model is given by following Equation 6:

$$\frac{C_e}{q_e} = \frac{1}{(K_L q_m)} + \frac{C_e}{q_m} \quad (\text{Eq. 6})$$

where C_e (mg L^{-1}) is the equilibrium concentration of the solution, q_e (mg g^{-1}) is the amount of metal adsorbed per specific amount of adsorbent, q_m (mg g^{-1}) is the maximum amount of metal ions required to form monolayer, K (L mg^{-1}) is the adsorption equilibrium constant (Fig. 12). Freundlich adsorption model demonstrate that adsorbents have a heterogeneous surface having site with different adsorption potential. It moreover expects that stronger binding sites are occupied first and the binding strength decreases with the increasing degree of occupation. The Freundlich adsorption model in its linear form is given in Equation 7:

$$\log_{10} q_e = \log_{10}(K_f) + \left(\frac{1}{n}\right) \log_{10}(C_e) \quad (\text{Eq. 7})$$

where K_f (mg g^{-1}) is the Freundlich constant indicating adsorption capacity, n (L mg^{-1}) is the adsorption intensity that is the measure of the change in affinity of the adsorbate with the change in adsorption density. The Freundlich constants K_f and n were calculated from the slope and intercept of the plot of C_e versus $\log_{10} q_e$ (Fig. 13) that shown in Table 2. The values of Langmuir R^2 for Cd(II) and Pb(II) by the Fe_3O_4 -PPCQDs were higher than Freundlich model thus, indicating that Langmuir model fitted the data in good congruence, thereby indicating monolayer adsorption.

Table 1. Thermodynamic parameters for adsorption of Pb(II) and Cd(II) by Fe_3O_4 -PPCQDs at different temperatures

Ion	T (K)	ΔG (J mol^{-1})	ΔH (J mol^{-1})	ΔS (J mol^{-1})	R^2
Pb (II)	278	-8700	-16908	-29.32	0.978
	288	-8510			
	298	-8256			
	308	-7800			
	318	-7589			
Cd (II)	278	-7105	-10947	-13.93	0.980
	288	-6923			
	298	-6748			
	308	-6664			
	318	-6538			

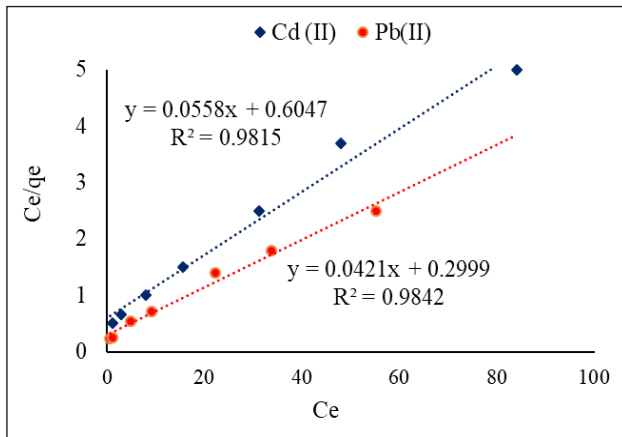


Fig. 12. Linear Langmuir isotherm for Pb(II) and Cd(II) removal by the Fe₃O₄-PPCQDs.

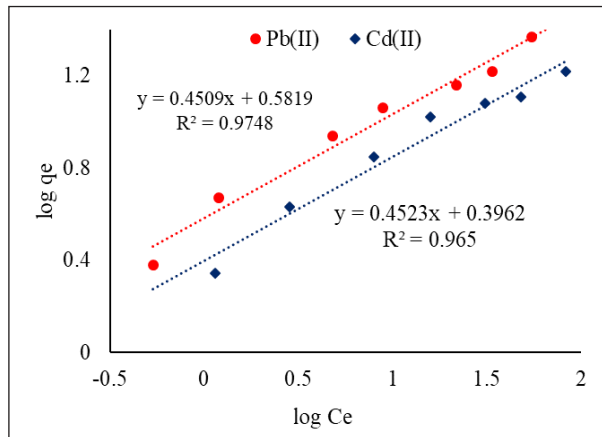


Fig. 13. Linear Freundlich isotherm for Pb(II) and Cd(II) removal by the Fe₃O₄-PPCQDs.

Table 2. Langmuir and Freundlich isotherm parameters for the removal of Pb(II) and Cd(II) by the Fe₃O₄-PPCQDs

Parameters	Pb(II)	Cd(II)
<i>Langmuir parameters</i>		
q_m (mg g ⁻¹)	23.75	17.92
b (L mg ⁻¹)	0.120	0.092
R^2	0.9842	0.9815
<i>Freundlich Parameters</i>		
K_f (mg g ⁻¹)	3.82	2.5
n (L mg ⁻¹)	2.22	2.21
R^2	0.9748	0.965

3.9. Comparison of adsorption capacity with other adsorbents

The maximum adsorption capacity of Fe₃O₄-PPCQDs nanocomposite for the removal of Pb(II) and Cd(II) was compared with other adsorbents reported in the

literature and the values are given in Table 3. It is clear from Table 3, that the adsorption capacity of Fe₃O₄-PPCQDs. is comparable with other nanomaterials suggesting that, it is effective in removing Pb(II) and Cd(II) from aqueous solutions [29-33].

Table 3. Comparison of adsorption capacity of the Fe₃O₄-PPCQDs with other adsorbents.

Adsorbents	Adsorption capacity (mg g ⁻¹)		pH	Adsorbent mass (mg).	Ref.
	Cd (II)	Pb (II)			
CFe ₃ O ₄	4.106	3.795	3	50	29
PMNPs	29.60	3.103	1 to 8	50	30
Kaniar Fe ₃ O ₄	2.20	1.35	5	200	31
MCANF	----	44	6	100	32
Sawdust (Fe ₃ O ₄ /SC)	63	----	6.5	400	33
This study	17.92	23.75	6	100	----

CFe₃O₄: Chitosan/iron oxide nanocomposite

PMNPs: Polymer-modified magnetic nanoparticles

Kaniar Fe₃O₄: Magnetic Bauhinia purpurea (Kaniar) powders

MCANF: Fe₃O₄ nanoparticles onto cellulose acetate nanofibers nanocomposite

4. Conclusions

In this article, the adsorption potential of the Fe₃O₄-PPCQDs nanocomposite was investigated for the removal of Pb(II) and Cd(II) ions. TEM analysis revealed that the synthesized nanoparticles have an average particle size of 10-25 nm for the Fe₃O₄-PPCQDs. The XRD analysis of Fe₃O₄-PPCQDs confirmed the presence of magnetite phase exhibiting average crystal size similar to that indicated by the TEM analysis. Batch adsorption experiments were led to study the effect of various parameters like agitation time, adsorbent dosage, initial concentration of the Pb(II) and Cd(II), temperature, and pH. The conditions for the highest removal efficiency of synthesized nanocomposite for the removal of Pb(II) and Cd(II) were achieved (pH=6.0, temperature=25 ±1°C, initial metal ion concentration=50 mg L⁻¹ contact time =20 min). Based on procedure, the maximum Langmuir adsorption capacity was obtained 17.92 mg g⁻¹ for Cd(II) and 23.75 mg g⁻¹ for Pb(II) at pH 6. In addition, the working ranges of cadmium and lead adsorption based on Fe₃O₄-PPCQDs nanocomposite in 50 mL of water samples were obtained 4-36 µg L⁻¹ and 50-400 µg L⁻¹, respectively by the MSPE procedure (PF=50, RSD%<2.4). Therefore, the ultra- trace analysis of Pb(II) and Cd(II) ions was done by Fe₃O₄-PPCQDs nanocomposite at pH=6.

5. Acknowledgments

The authors would like to thank from Department of Chemistry, Kerman Branch, Islamic Azad University, Kerman, Iran.

6. References

- [1] A. T. Jan, M. Azam, K. Siddiqui, A.A.I. Choi, Q.M.R. Haq, Heavy metals and human health: mechanistic insight into toxicity and counter defense system of antioxidants. *Int. J. Mol. Sci.*, 16 (2015) 29592–29630.
- [2] R. Singh, N. Gautam, A. Mishra, R. Gupta, Heavy metals and living systems: an overview. *Indian J. Pharmacol.*, 43 (2011) 246-253.
- [3] W. Shoty, G.L. Roux, A. Sigel, H. Sigel, R.K.O. Sigel, Metal ions in biological systems, Taylor and Francis, Boca Raton, Chapter 10, 2005.
- [4] M.A.A. Zaini, R. Okayama, M. Machida, Adsorption of aqueous metal ions on cattle-manure compost based activated carbons, *J. Hazard. Mater.*, 170 (2009) 1119-1124.
- [5] A. Vázquez-Guerrero, R. Cortés-Martínez, R. A. Cuevas-Villanueva, E. M. Rivera-Muñoz, R. Huirache-Acuña, Cd(II) and Pb(II) adsorption using a composite obtained from *Moringa oleifera* Lam, cellulose nanofibrils impregnated with iron nanoparticles, *Water*, 13 (2021) 89.
- [6] W. Zhang, X. Shi, Y. Zhang, W. Gu, B. Li, Synthesis of water-soluble magnetic graphene nanocomposites for recyclable removal of heavy metal ions, *J. Mater. Chem. A*, 1 (2013) 1745-1753.
- [7] H. Isawi, Using zeolite/polyvinyl alcohol/sodium alginate nanocomposite beads for removal of some heavy metals from wastewater, *Arab. J. Chem.*, 13 (2020) 5691-5716.
- [8] R. Ahmad, A. Mirza, Facile one pot green synthesis of chitosan-iron oxide (CS-Fe₂O₃) nanocomposite: removal of Pb(II) and Cd(II) from synthetic and industrial wastewater, *J. Clean. Prod.*, 186 (2018) 342-352.
- [9] H. C. Tao, H. R. Zhang, J. B. Li, W. Y. Ding, Biomass based activated carbon obtained from sludge and sugarcane bagasse for removing lead ion from wastewater, *Bioresour. Technol.*, 192 (2015) 611-617.
- [10] M. F. Gao, Q. L. Ma, Q.W. Lin, J. L. Chang, H. Z. Ma, A novel approach to extract SiO₂ from fly ash and its considerable adsorption properties, *Mater. Design.*, 116 (2017) 666–675.
- [11] Y. K. Tang, L. Chen, X. R. Wei, Q. Y. Yao, T. Li, Removal of lead ions from aqueous solution by the dried aquatic plant, *Lemna perpusilla* Torr, *J. Hazard. Mater.*, 244 (2013) 603-612.

- [12] J. G. Wang, J. Wei, J. Li, Rice straw modified by click reaction for selective extraction of noble metal ions, *Bioresour. Technol.*, 177 (2015) 182-187.
- [13] T. M. Abdel-Fattah, M. E. Mahmoud, S. B. Ahmed. Biochar from woody biomass for removing metal contaminants and carbon sequestration, *J. Ind. Eng. Chem.*, 22 (2015) 103-109.
- [14] S. Haider, F.A.A. Ali, A. Haider, W. A. Al-Masry, Y. Al-Zeghayer, Novel route for amine grafting to chitosan electrospun nanofibers membrane for the removal of copper and lead ions from aqueous medium, *Carbohydr. Polym.*, 199 (2018) 406-414.
- [15] Q. Feng, D. Wu, Y. Zhao, A. Wei, Q. Wei, H. Fong, Electrospun AOPAN/RC blend nanofiber membrane for efficient removal of heavy metal ions from water, *J. Hazard. Mater.*, 344 (2018) 819–828.
- [16] Q. Lv, X. Hu, X. Zhang, L. Huang, Z. Liu, G. Sun, Highly efficient removal of trace metal ions by using poly (acrylic acid) hydrogel adsorbent, *Mater. Design.*, 181 (2019) 107934.
- [17] F. Arshad, M. Selvaraj, J. Zain, F. Banat, M. Abu Haija, Polyethylenimine modified graphene oxide hydrogel composite as an efficient adsorbent for heavy metal ions, *Sep. Purif. Technol.*, 209 (2019) 870-880.
- [18] R. Song, M. Murphy, C. Li, K. Ting, C. Soo, Z. Zheng, Current development of biodegradable polymeric materials for biomedical applications, *Drug Des. Devel. Ther.*, 24 (2018) 3117-3145.
- [19] H. Baweja, K. Jeet, Economical and green synthesis of graphene and carbon quantum dots from agricultural waste, *Mater. Res. Express*, 6 (2019) 0850g8.
- [20] M. M. Rhaman, M. R. Karim, M. K. Mohammad Ziaul, Y. Ahmed, Removal of chromium (VI) from effluent by a magnetic bioadsorbent based on Jute Stick powder and its adsorption isotherm, kinetics and regeneration study, *Water Air Soil Pollut.*, 231 (2020) 1-18.
- [21] P.N. Dave, L.V. Chopda, Application of iron oxide nanomaterials for the removal of heavy metals, *J. Nanotechnol.*, 4 (2014) 1-14
- [22] M.O. Ojemaye, O.O. Okoh, A.I. Okoh, Surface modified magnetic nanoparticles as efficient adsorbents for heavy metal removal from wastewater, progress and prospects, *Mater. Express*, 7 (2017) 439-456.
- [23] B. R. Seeram, M. Lee, D. Heber, Rabid large scale purification of ellagitunnins from pomegranate husk, *Sep. Purif. Technol.*, 41 (2005) 49-55.
- [24] H. Wang, X. Xu, Z. Ren, B. Gao, Removal of phosphate and chromium(VI) from liquids by an aminocrosslinked nano-Fe₃O₄ biosorbent derived from corn straw, *RSC Adv.*, 6 (2016) 47237-47248.
- [25] M. Jain, M Yadav, T. Kohout, M. Lahtinen, V.K. Garg, Development of iron oxide/activated carbon nanoparticle composite for the removal of Cr(VI), Cu(II) and Cd(II) ions from aqueous solution, *Water Resour. Ind.*, 20 (2018) 54-74
- [26] M.I. Panayotova, Kinetics and thermodynamics of copper ions removal from wastewater by use of zeolite, *Waste Manag.*, 21 (2001) 671-676.
- [27] L. Xu, X. Zheng, H. Cui, Z. Zhu, J. Liang, J. Zhou, Equilibrium, kinetic, and thermodynamic studies on the adsorption of cadmium from aqueous solution by modified biomass ash, *Bioinorg. Chem. Appl.*, 2017 (2017) 1-9. <https://doi.org/10.1155/2017/3695604>
- [28] H. Zare, H. Heydarzadeh, M. Rahimnejad, A. Tardast, M. Seyfi, S.M. Peyghambarzade, Dried activated sludge as an appropriate biosorbent for removal of copper (II) ions, *Arab. J. Chem.*, 8 (2015) 858-864.
- [29] M. Keshvardoostchokami, L. Babaei, A. A. Zamani, A. H. Parizanganeh, F. Piri, Synthesized chitosan/iron oxide nanocomposite and shrimp shell in removal

- of nickel, cadmium and lead from aqueous solution, *Global J. Environ. Sci. Manag.*, 3 (2017) 267–278.
- [30] F. Ge, M. Li, H. Ye, B. Zhao, Effective removal of heavy metal ions Cd^{2+} , Zn^{2+} , Pb^{2+} , Cu^{2+} from aqueous solution by polymer-modified magnetic nanoparticles, *J. Hazard. Mater.*, 211 (2012) 366–372.
- [31] R. Sharma, A. Sarswat, C.U. Pittman, D. Mohan, Cadmium and lead remediation using magnetic and non-magnetic sustainable biosorbents derived from bauhinia *Purpurea* Pods, *RSC Adv.*, 7 (2017) 8606–8624.
- [32] T. I. Shalaby, M.F. El-Kady, A.E.H.M. Zaki, S. M. El-Kholy. Preparation and application of magnetite nanoparticles immobilized on cellulose acetate nanofibers for lead removal from polluted water, *Water Supply*, 17 (2017) 176–187.
- [33] N. Kataria, V. K. Garg, Green synthesis of Fe_3O_4 nanoparticles loaded sawdust carbon for cadmium (II) removal from water: regeneration and mechanism, *Chemosphere*, 208 (2018) 818–828.



A novel modified fenton-like process for efficient remediation of anthracene-contaminated soils before analysis by ultraviolet–visible spectroscopy

Mahdia Hamidinasab^{a,b,*}, Mohammad Ali Bodaghifard^{a,b}, Sepideh Ahmadi^b, Ali Seif^a
and Zahra Najahi Mohammadizadeh^a

^a Department of Chemistry, Faculty of Science, Arak University, Arak 88138-38156, Iran.

^b Institute of Nanosciences and Nanotechnology, Arak University, Arak 88138-38156, Iran.

ARTICLE INFO:

Received 20 May 2021

Revised form 30 Jul 2021

Accepted 17 Aug 2021

Available online 30 Sep 2021

Keywords:

Polycyclic aromatic hydrocarbon (PAH),
Remediation, Modified Fenton's
reaction,
Magnetite nanoparticle,
Urea-hydrogen peroxide (UHP)

ABSTRACT

Due to the persistence of polycyclic aromatic hydrocarbons (PAHs) in soil and sediments, and their toxic, mutagenic, and carcinogenic effects, the remediation of PAH-contaminated sites is an important role for environment pollution. In this study, the chemical oxidative remediation of anthracene-contaminated soils was investigated by magnetite nanoparticles (Fe_3O_4) catalyzed Fenton-like oxidation in the presence of hydrogen peroxide 30% (H_2O_2) and urea-hydrogen peroxide (UHP) at neutral pH. Urea-hydrogen peroxide (UHP), as a safer oxidizing agent, is used for the first time in the Fenton process. The magnetite nanoparticles improved the production of hydroxyl radicals, and the removal of polycyclic aromatic hydrocarbons (anthracene as a model compound) from the soil samples. The structure of Fe_3O_4 nanoparticles was characterized by Fourier-transform infrared spectroscopy (FT-IR), X-ray powder diffraction (XRD), scanning electron microscopy (SEM), and vibrating sample magnetometer (VSM). The removal efficiency of anthracene at an initial concentration $2500 \text{ (mg kg}^{-1}\text{)}$ was 95% for 2.5 mmol by using hydrogen peroxide and 93% for 0.1 mmol of UHP at the optimum oxidation condition. The anthracene reaction was analyzed by ultraviolet-visible spectroscopy (UV-Vis). The UHP safety and efficiency, neutral pH condition, the limited iron leaching and its easy magnetic separation makes magnetite nanoparticles-UHP a promising catalytic system in remediation of polycyclic aromatic hydrocarbons in contaminated soils.

1. Introduction

The sixteen polycyclic aromatic hydrocarbons (PAHs) in the United States environmental protection agency and European community (US, EPA) are considered as priority pollutants [1, 2] The PAHs are toxic organic contaminants with great environmental and health concern, which consist of

two or more fused aromatic rings. PAHs containing up to two fused benzene rings such as anthracene and phenanthrene are known as light PAHs and those containing more than four benzene rings such as ovalene and corannulene are called heavy PAHs[3]. The main source of PAHs contamination is incomplete combustion and pyrolysis of wood or fossil fuels, the motor oil and petroleum spill which are disposed of improperly each year into soil[4]. Owing to the persistence of PAHs in soil

*Corresponding Author: [Mahdia Hamidinasab](mailto:Mahdia.Hamidinasab@arak.ac.ir)

Email: mahdiahamidinasab@yahoo.com

<https://doi.org/10.24200/amecj.v4.i03.140>

and sediments, and their toxic, mutagenic, and carcinogenic effects, the remediation of PAH-contaminated sites is an important environmental issue. Various remediation techniques including incineration, thermal conduction, solvent extraction/soil washing, chemical oxidation, bio-augmentation, bio-stimulation, phytoremediation, composting/bio-piles and bioreactors have been explored and studied for the removal of persistent PAHs from complex matrices like soil or sediments. Integrating physico-chemical and biological technologies is also widely practiced for better clean-up of PAH contaminated soils. Electrokinetic remediation, vermiremediation and biocatalyst assisted remediation are at the development stage[5] In situ chemical oxidation (ISCO) has emerged as a cost-effective and viable remediation technology for the treatment of several pollutants in ground waters, soils and sediments[6–8]. Remediation by chemical oxidation involves the injection of strong oxidants such as hydrogen peroxide[9], ozone gas[10], potassium permanganate[11], etc. In last two decades a lot of researches have been addressed to this aim and pointed out the prominent role of a special class of oxidation techniques defined as advanced oxidation processes (AOPs), which usually operated at or near ambient temperature and pressure[12, 13]. Advanced oxidation processes (AOPs) are attracting significant attention because of their effective and rapid degradation performance, including photocatalysis [4, 14, 15], ozonisation[16], electrochemical reactions[17] and Fenton method[18, 19]. Among chemical oxidation processes, special attention has been paid to the use of Fenton's reagent, which release the hydroxyl radicals with high oxidation potential ($E^\circ=2.73$ V), from the catalytic decomposition of H_2O_2 in the presence of Fe (II) or Fe (III) ions. The Fenton method has the ability to oxidize a wide range of organic pollutants and convert them to CO_2 , H_2O and inorganic compounds or, at least, transform them into harmless or biodegradable products[20–23]. This conventional Fenton's process is limited by the optimum pH (~3), such as at low pH results in negative impacts on soil

properties and is incompatible with subsequent biodegradation. In the novel process as known as Fenton-like oxidation, the iron minerals or organic chelating agents can be applied to extend its range of applicability at circumneutral soil pH. The degradation of PAHs has been reported by Fenton-like reaction catalyzed by various Fe (III) oxides like ferrihydrite, hematite or goethite[24–26]. Recently, Fe(II) bearing minerals such as magnetite (Fe_3O_4) were found to be the most effective nanocatalyst as compared to the only Fe(III) oxides for heterogeneous catalytic oxidation of organic pollutants[26-29]. The researchers must be very careful when dispensing oxidizers from storage containers, avoid spilling material and contaminating their skin or clothing which can cause serious accidents. Urea-hydrogen peroxide (UHP) contains solid and water-free hydrogen peroxide, which offers a higher stability and better controllability than liquid hydrogen peroxide when used as an oxidizing agent. Urea-hydrogen peroxide adducts (UHP) is stable, inexpensive and an easily handled reagent. So, the UHP is used as a solid state agent for efficient oxidation of different organic molecules.

In this study, the anthracene as a model polycyclic aromatic hydrocarbon was removed from contaminated soil by a modified Fenton's reaction, using hydrogen peroxide and urea-hydrogen peroxide separately in the presence of bare magnetite nanoparticles (Fe_3O_4) as a nanocatalyst at circumneutral soil pH.

2. Experimental

2.1. Materials and apparatus

Anthracene 96% (CAS 120-12-7) and H_2O_2 30% (CAS 7722-84-1) were used as a contaminant and oxidant respectively. Ethanol 99.7% (CAS 64-17-5), Iron (II) chloride tetra hydrate 99% (CAS 13478-10-9) and Iron (III) chloride hexahydrate 98% (CAS 10025-77-1) were purchased from Merck Company. All reagents were used without further purification. The FT-IR spectra were recorded on Bruker Alpha spectrophotometer in the region $400-4000\text{ cm}^{-1}$ using pressed KBr discs. The

field emission-scanning electron microscopy (FE-SEM) was carried out by a MIRA III TESCAN-XMU. The hysteresis loop was measured at room temperature using a vibrating sample magnetometer (Model 7300 VSM system, Lake Shore Cryotronic, Inc., Westerville, OH, USA). The UV-Vis spectrophotometer (Agilent 8453) was used to determine the oxidation process.

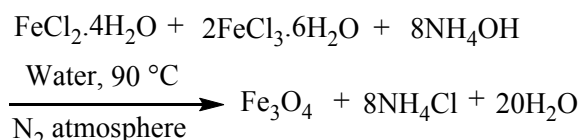
2.2. Soil Samples

Crushing and preparing of the samples was performed at geology department of Kharazmi University (Iran, Tehran) and powdering was done at the Iranian mineral processing research center (IMPRC). The analysis of whole-rock major and trace elements was conducted at ETH, Zurich. The major elements are summarized in Table 1.

2.3. Preparation of Fe₃O₄ nanoparticles

Magnetite nanoparticles (MNPs) was synthesized by co-precipitation method [31]. Aqueous solutions of FeCl₃.6H₂O (56 mmol) and FeCl₂.4H₂O (28

mmol) were prepared in de-ionized water (25 mL) and NaOH (3 M) solution was added to it slowly and stirred continuously using a magnetic stirrer to reach the pH=12. This solution was heated under N₂ atmosphere at 90 °C for 4 hours. The mixture was filtered and washed 3 times with deionized water DW/ ethanol before dried at 60 °C (Equation 1).



(Eq. 1)

2.4. Calibration curve

Figure 1 shows the UV-Vis absorption spectra and calibration curve of anthracene for different concentration. The absorption coefficient (ϵ) obtained by using the Lambert-Beer's law (Equation 2) [32].

$$A = \epsilon cd \quad (\text{Eq. 2})$$

Table 1. Total elemental analyses of soil sample.

Compound	SiO ₂	TiO ₂	Al ₂ O ₃	Fe ₂ O ₃	FeO	MnO	MgO	CaO	Na ₂ O	K ₂ O	P ₂ O ₅
Wt.%	56.84	0.69	16.84	0.90	5.98	0.11	2.15	6.20	4.38	1.93	0.19

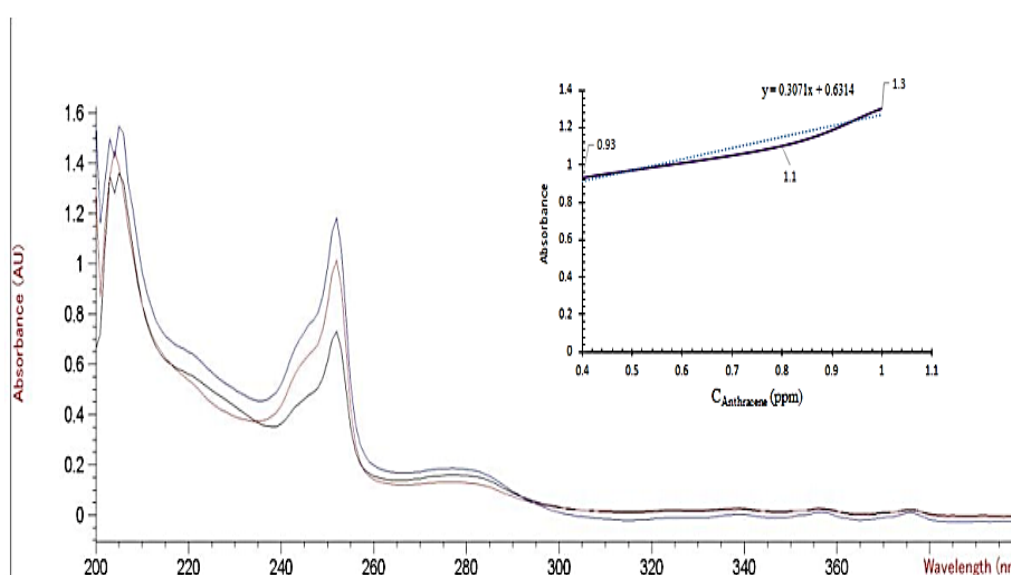


Fig. 1. UV-Vis absorption spectra and calibration curve of anthracene in the wavelength range 200-400 nm

2.5. Preparation of anthracene-contaminated soil

Soil samples was prepared as detailed in the literature,[33] where an ethanol solution with approximately 500 mg of anthracene was distributed and mixed manually onto 20 g of clean soil with a spatula which was homogenized.

2.6. Procedure od anthracene extraction

All experiments were carried out without pH adjustment and the experiments were done on a laboratory scale. All experimental runs were performed at room temperature. For all experiments, 1 gr (dry mass) of contaminated soil sample was placed in the tube, 2 mL of deionized water (DW) was added, followed by the required quantities of oxidants (H_2O_2 and urea- H_2O_2) and magnetite as a nanocatalyst (Table 2). The samples were shaken for 30 minutes. The residual anthracene in the soil sample was extracted in 8 mL of ethanol during 10 minutes and controlled the tube centrifugation for 15 min at 3000 rpm. The presence of anthracene in the solutions was analyzed by UV-Vis spectrophotometer ($\lambda_{\text{max}}=250$ nm). Figure 2 illustrates the oxidation process of anthracene in modified Fenton's reaction. The quantify decomposition of anthracene in soil was

shown in Equation 3 as follows,

$$X_{\text{Anthracene}} = \frac{C_0^{\text{Anthracene}} - C_t^{\text{Anthracene}}}{C_0^{\text{Anthracene}}} \times 100 \quad (\text{Eq. 3})$$

Where $X_{\text{Anthracene}}$ is the percentage of anthracene decomposed in soil, C_0 and C_t are the initial and final concentration of anthracene at a given time.

3. Result and discussions

3.1. Characterizations

The Fe_3O_4 nanoparticles were carefully prepared[34] and characterized by Furrier-transform infrared spectroscopy (FT-IR), X-ray powder diffraction (XRD), scanning electron microscopy (SEM), and vibrating sample magnetometer (VSM). The X-ray diffraction analysis (XRD) of Fe_3O_4 nanoparticles shows several diffraction peaks at $2\theta = 30.54, 35.89, 43.9, 54.28, 57.55, 63.3$ and 74.33 that attributed to the miller planes 220, 311, 400, 422, 511, 440 and 533 respectively (Fig. 3a). These results are in accordance with the standard patterns (JCPDS CardNo. 85-1436)[34] The FT-IR spectra of Fe_3O_4 MNPs is shown in Figure 3b. The appeared vibrational frequencies in the $584\text{-}631\text{ cm}^{-1}$ region are attributed to the Fe-O bonds.

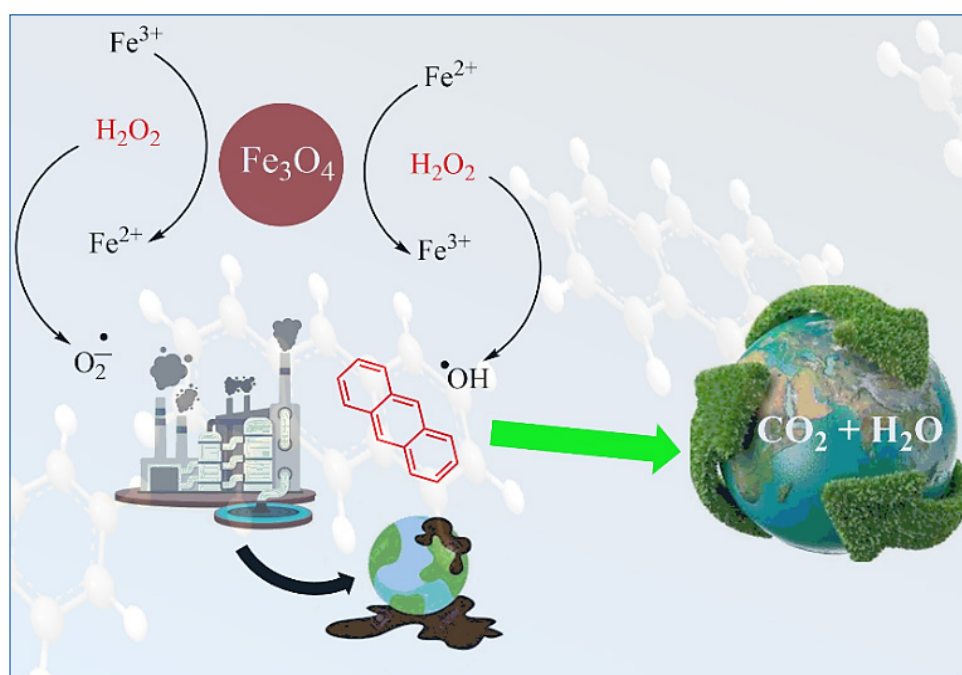


Fig. 2. The oxidation process of anthracene in modified Fenton's reaction

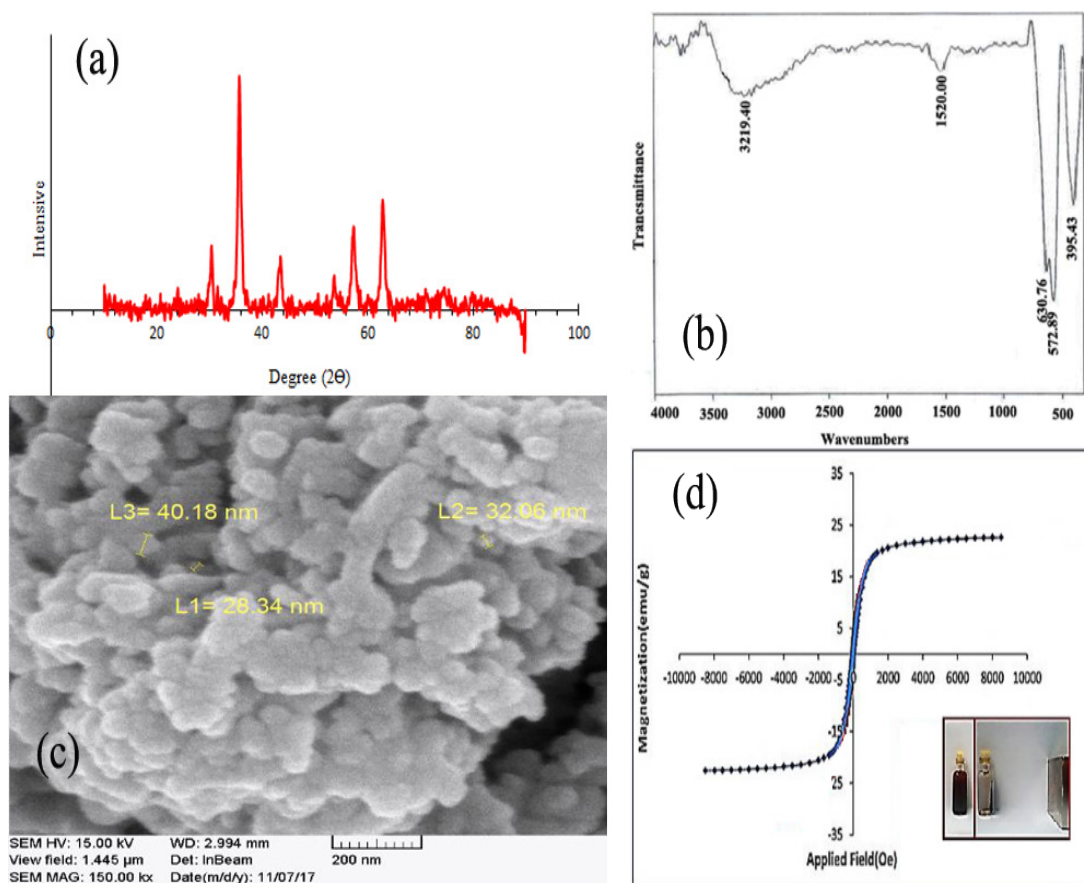


Fig. 3. The XRD spectra (a), The FT-IR spectra (b), The FE-SEM image (c) and The VSM (d) of Fe₃O₄ nanoparticles

The stretching frequencies of hydroxyl groups, on the surface of the nanoparticles, appeared at 3420 cm⁻¹ and the peak in the 1625 cm⁻¹ are related to the bending vibrations of OH groups. The morphology and particle size distribution of Fe₃O₄ nanoparticles was performed by FE-SEM technique. The average size of nanoparticle is 32 nm and confirm the spherical and regular shape of nanoparticles (Fig. 3c). The magnetic properties of the synthesized nanoparticles were determined by VSM at room temperature, which contains the magnetization curve (M) in terms of the applied magnetic field (H) (hysteresis curve) of Fe₃O₄ MNPs particles which shows the great paramagnetic properties (Fig. 3d).

3.2. The optimization of H₂O₂, urea-hydrogen peroxide and magnetite values

A different combination of magnetite and hydrogen peroxide was selected for optimization (Table 2).

First, the effect of varying H₂O₂ and urea-hydrogen peroxide concentrations on anthracene removal efficiency was investigated while the amount of magnetite was kept constant (Fig. 4). As H₂O₂ and UHP concentration rises, the removal of anthracene is increased and finally leveled off. The maximum removal efficiency of 95% at 0.2 mL H₂O₂ concentration and 93% at 6 mg UHP content was observed, respectively. Therefore, the H₂O₂ and UHP concentrations was optimized for further experiments. In the next stage, the effect of various amounts of magnetite on the Fenton oxidation of anthracene was investigated at optimum H₂O₂ concentration of 0.2 mL (2.5 mmol) and 6 mg UHP. The removal efficiency was increased with an increase in magnetite dosage up to 8 mg, and then was remained constant at higher concentrations (Fig. 5). The anthracene removal reached 93% at the optimum concentration levels of H₂O₂, UHP, and magnetite.

Table 2. Optimization of combination of magnetite and hydrogen peroxide

Entry	Samples	Magnetite (mg)	H ₂ O ₂ (ml)	Samples	Magnetite (mg)	Urea-H ₂ O ₂ (mg)
1	M ₁₀ ^a -H _{0.1} ^b	10	0.1	M ₁₀ -UHP ₃ ^c	10	3
2	M ₈ -H _{0.1}	8	0.1	M ₈ -UHP ₃	8	3
3	M ₆ -H _{0.1}	6	0.1	M ₆ -UHP ₃	6	3
4	M ₁₀ -H _{0.2}	10	0.2	M ₁₀ -UHP ₆	10	6
5	M ₈ -H _{0.2}	8	0.2	M ₈ -UHP ₆	8	6
6	M ₆ -H _{0.2}	6	0.2	M ₆ -UHP ₆	6	6
7	M ₁₀ -H _{0.3}	10	0.3	M ₁₀ -UHP ₁₀	10	10
8	M ₈ -H _{0.3}	8	0.3	M ₈ -UHP ₁₀	8	10
9	M ₆ -H _{0.3}	6	0.3	M ₆ -UHP ₁₀	6	10
10	M ₁₀ -H _{0.4}	10	0.4	M ₁₀ -UHP ₁₅	10	15
11	M ₈ -H _{0.4}	8	0.4	M ₈ -UHP ₁₅	8	15
12	M ₆ -H _{0.4}	6	0.4	M ₆ -UHP ₁₅	6	15
13	-	-	-	M ₁₀ -UHP ₂₀	10	20
14	-	-	-	M ₈ -UHP ₂₀	8	20
15	-	-	-	M ₆ -UHP ₂₀	6	20

^aMagnetite, ^bH₂O₂ 30%, ^cUrea-H₂O₂ (UHP)

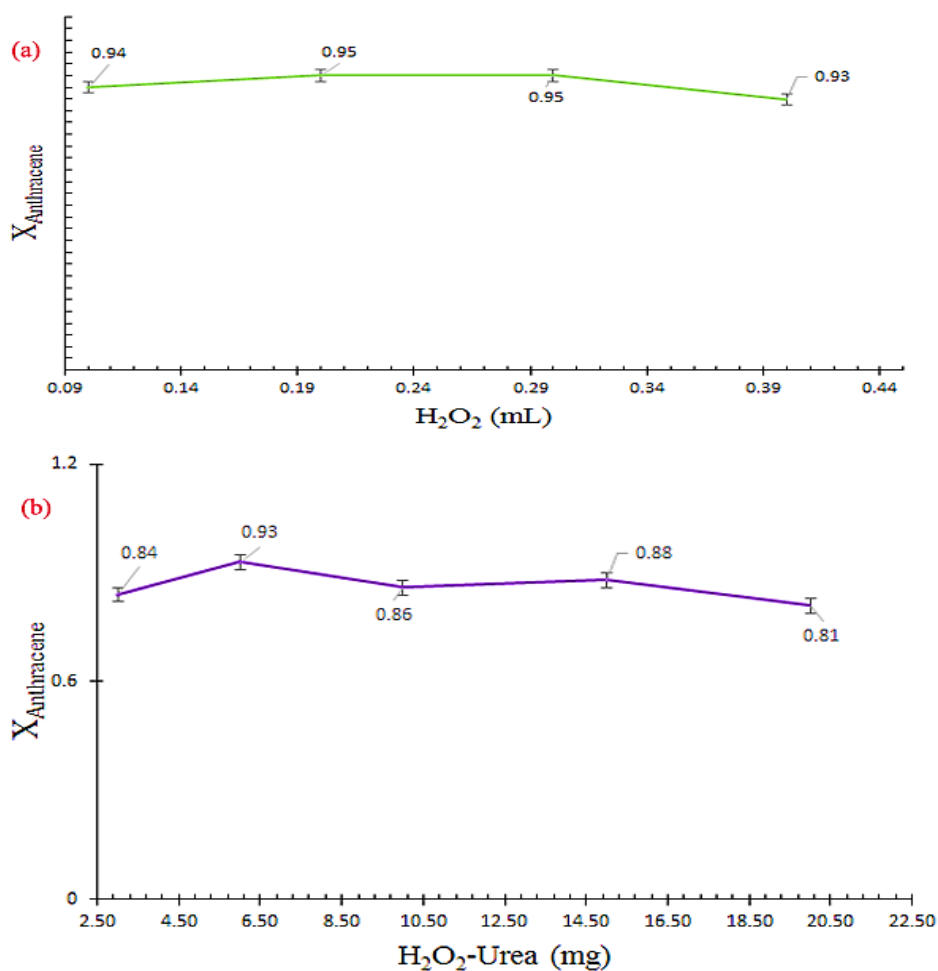


Fig. 4. The anthracene removal efficiency in varying (a) H₂O₂ concentrations of 0.1-0.4 mL (b) UHP 0.1-0.4 mg (reaction time of 30 min, pH=7 and magnetite concentration of 8 mg)

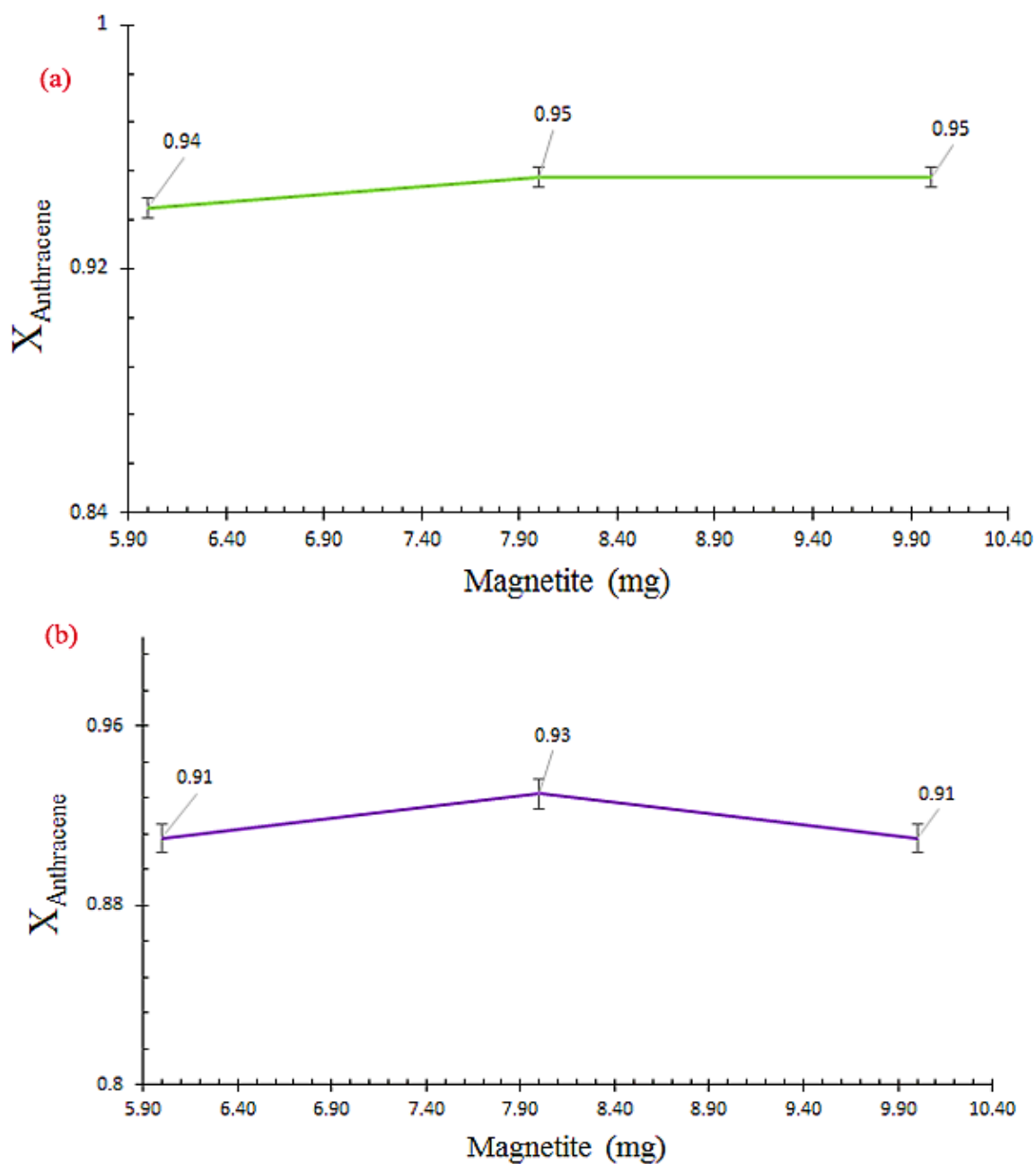


Fig. 5. The anthracene removal efficiency varying Fe₃O₄ content in optimized (a) H₂O₂ and (b) UHP concentration (reaction time of 30 min and pH=7)

3.3. The effect of contact time on anthracene removal

The effect of reaction time on anthracene removal at optimum H₂O₂ or UHP and magnetite concentration was investigated (Fig. 6).

The reaction time positively affected the removal efficiency and the anthracene removal of 98% was achieved after 30 min of contact time. After 24 h, about 99% conversion was achieved for all contaminants.

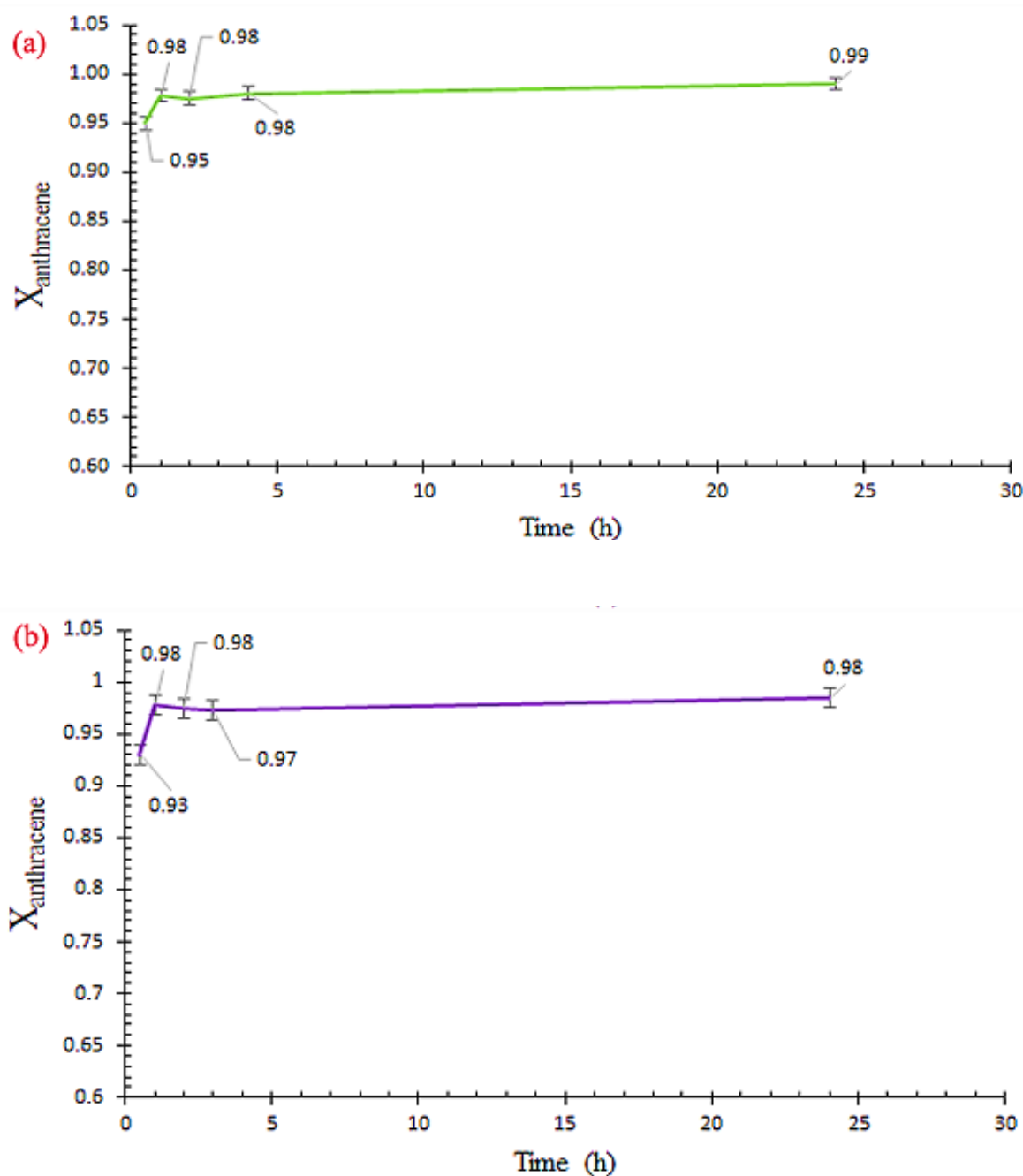


Fig. 6. The effect of contact time on anthracene removal in optimum H_2O_2 , UHP and magnetite concentrations at pH=7

3.4. The blank experiments

After the remediation experiments, two blank tests were performed. In a sample experiment, 2 ml of deionized water was used without adding the magnetite and hydrogen peroxide (blank 1) to contaminated soil. In other sample, only 0.2 mL H_2O_2 without magnetite was added (blank 2) to

contaminated soil. The evolution of the conversion of anthracene in blank 1 and blank 2 is shown in Figure 7. In the blank 1, the degradation is attributed to the natural attenuation during the reaction period (45 days). It is shown the low anthracene content (20%) in the soil was remediated during 45 days, which is attributed to biodegradation of anthracene.

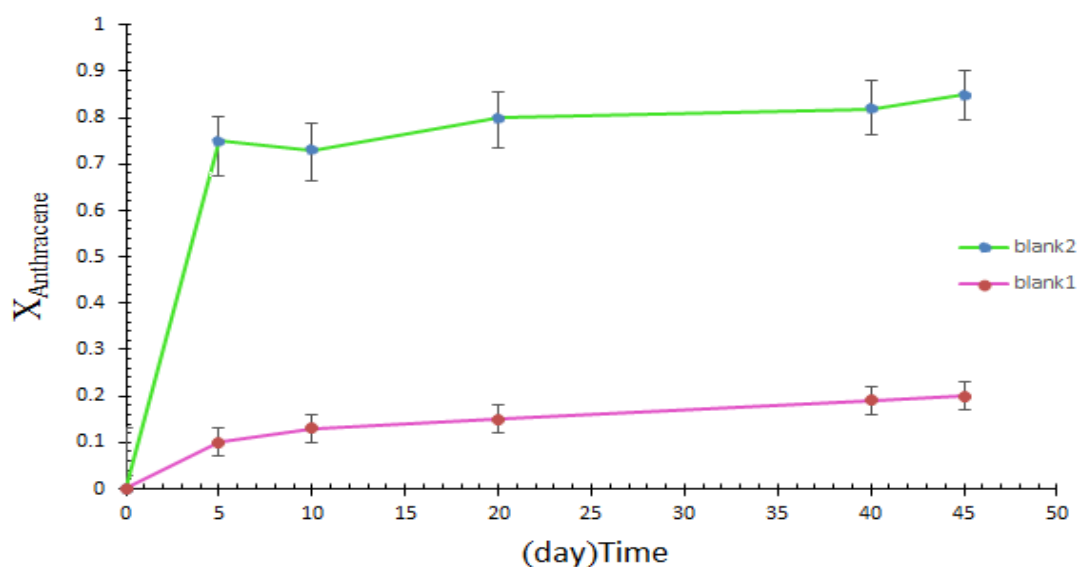


Fig. 7. The blank experiments in optimum oxidation condition

The comparative study confirmed the Fenton-like oxidative capability of the magnetic nanoparticles for efficient degradation of anthracene using 8 mg of the nanocatalyst, 0.2 mL H₂O₂ 30 % (2.5 mmol) and 6 mg urea-H₂O₂ (0.1 mmol) at neutral pH as optimum operational

parameters under mild reaction conditions. The solid urea-H₂O₂ is safer than liquid H₂O₂ (Fig. 8a). The magnetite (Fe₃O₄) is an efficient nanocatalyst for the degradation of anthracene and the urea-H₂O₂ with lower content has a better oxidizing effect than H₂O₂ (Fig. 8b).

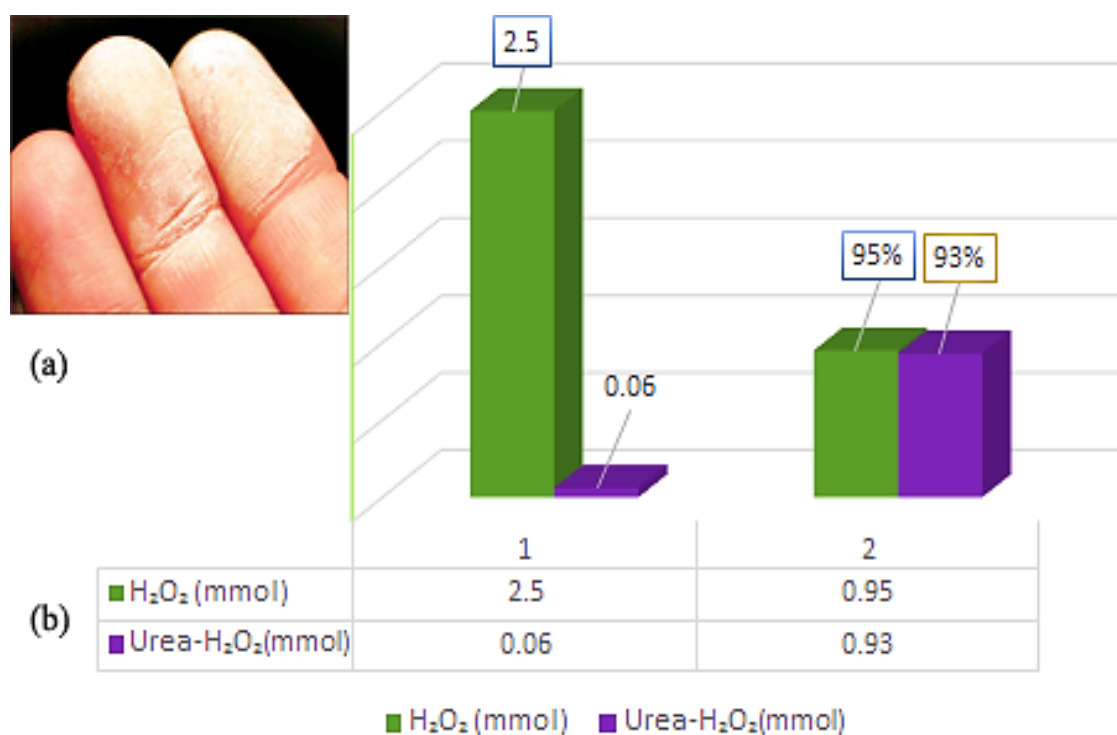


Fig. 8. (a) The sign of acute exposure of skin to hydrogen peroxide (H₂O₂ 30%)
 (b) The comparison of H₂O₂ and urea-H₂O₂ as oxidants in Fenton's method

4. Conclusions

In the present study, the Fenton-like oxidation capability of the magnetite nanoparticles for the efficient degradation of anthracene at neutral pH under mild reaction conditions, was confirmed. The urea-H₂O₂ with lower content has a better oxidizing effect than H₂O₂. Furthermore, the solid urea-H₂O₂ is safer than liquid H₂O₂. The natural concentration attenuation during the treatment time (45 days) was less than 20% of the anthracene in soil. It was stated that the magnetite nanocatalyst could activate molecular oxygen via single-electron reduction pathway to produce reactive oxygen species, including hydroxyl radical (^oOH), which are capable of oxidizing contaminants. The generated hydroxyl radicals oxidized the polycyclic aromatic hydrocarbon contaminants by breaking them down into non-toxic products. Therefore, the magnetite/UHP system is a promising and environmentally benign catalytic process for the remediation of PAH-contaminated soils.

5. Acknowledgements

The Authors gratefully acknowledge the research council of Arak University and department of chemistry for providing the chemicals and apparatus.

6. Declaration of funding

The Authors gratefully acknowledge the partial support from the research council of Arak University.

7. References

- [1] L. Wu, R. Sun, Y. Li, C. Sun, Sample preparation and analytical methods for polycyclic aromatic hydrocarbons in sediment, *Trends Environ. Anal. Chem.*, 24 (2019) e00074.
- [2] Y. Sun, S. Wu, G. Gong, Trends of research on polycyclic aromatic hydrocarbons in food: A 20-year perspective from 1997 to 2017, *Trends food sci. technol.*, 83 (2019) 86-98.
- [3] H.K. Bojes, P.G. Pope, Characterization of EPA's 16 priority pollutant polycyclic aromatic hydrocarbons (PAHs) in tank bottom solids and associated contaminated soils at oil exploration and production sites in Texas, *Regul. Toxicol. Pharmacol.*, 47 (2007) 288–295.
- [4] X.P. Yang, L.X. Xie, J. Tang, J. Lin, Removal and degradation of phenanthrene and pyrene from soil by coupling surfactant washing with photocatalysis, *Appl. Mech. Mater.*, 446 (2014) 1485–1489.
- [5] S. Kuppusamy, P. Thavamani, K. Venkateswarlu, Y.B. Lee, R. Naidu, M. Megharaj, Remediation approaches for polycyclic aromatic hydrocarbons (PAHs) contaminated soils: Technological constraints, *Emerg. Trends Future Directions*, 168 (2017) 944-968.
- [6] M. Usman, P. Faure, K. Hanna, M. Abdelmoula, C. Ruby, Application of magnetite catalyzed chemical oxidation (Fenton-like and persulfate) for the remediation of oil hydrocarbon contamination, *Fuel*, 96 (2012) 270–276.
- [7] R. Andreatti, V. Caprio, A. Insola, R. Marotta, Advanced oxidation processes (AOP) for water purification and recovery, *Catal. Today*, 53 (1999) 51–59.
- [8] Q. Zhou, Y. Wang, J. Xiao, H. Fan, C. Chen, Preparation and characterization of magnetic nanomaterial and its application for removal of polycyclic aromatic hydrocarbons, *J. Hazard. Mater.*, 371 (2019) 323–331.
- [9] A. Romero, A. Santos, F. Vicente, S. Rodriguez, A.L. Lafuente, In situ oxidation remediation technologies: Kinetic of hydrogen peroxide decomposition on soil organic matter, *J. Hazard. Mater.*, 170 (2009) 627–632.
- [10] J. Shao, F. Lin, Z. Wang, P. Liu, H. Tang, Y. He, K. Cen, Low temperature catalytic ozonation of toluene in flue gas over Mn-based catalysts: Effect of support property and SO₂/water vapor addition, *Appl. Catal. B: Environ.*, 266 (2020) 118662.
- [11] C.M. Kao, K.D. Huang, J.Y. Wang, T.Y. Chen, H.Y. Chien, Application of potassium

- permanganate as an oxidant for in situ oxidation of trichloroethylene-contaminated groundwater: A laboratory and kinetics study, *J. Hazard. Mater.*, 153 (2008) 919–927.
- [12] J.A. Khan, X. He, H.M. Khan, N.S. Shah, D.D. Dionysiou, Oxidative degradation of atrazine in aqueous solution by UV/H₂O₂/Fe²⁺, UV/S₂O₈²⁻/Fe²⁺ and UV/HSO₅⁻/Fe²⁺ processes: A comparative study, *Chem. Eng. J.*, 218 (2013) 376–383.
- [13] K. Ayoub, E.D. van Hullebusch, M. Cassir, A. Bermond, Application of advanced oxidation processes for TNT removal: A review, *J. Hazard. Mater.*, 178 (2010) 10–28.
- [14] M. Bellardita, V. Loddo, A. Mele, W. Panzeri, F. Parrino, I. Pibiri, L. Palmisano, Photocatalysis in dimethyl carbonate green solvent: Degradation and partial oxidation of phenanthrene on supported TiO₂, *RSC Adv.*, 4 (2014) 40859–40864.
- [15] M. Ruokolainen, T. Gul, H. Permentier, T. Sikanen, R. Kostianen, T. Kotiaho, Comparison of TiO₂ photocatalysis, electrochemically assisted Fenton reaction and direct electrochemistry for simulation of phase metabolism reactions of drugs, *Eur. J. Pharm. Sci.*, 83 (2016) 36–44.
- [16] S.N. Malik, P.C. Ghosh, A.N. Vaidya, S.N. Mudliar, Hybrid ozonation process for industrial wastewater treatment: Principles and applications: A review, *J. Water Process Eng.*, 35 (2020) 101193.
- [17] K. Ayoub, E.D. Van Hullebusch, M. Cassir, A. Bermond, Application of advanced oxidation processes for TNT removal: A review, *J. Hazard. Mater.*, 178 (2010) 10–28.
- [18] M.D. Nicodemos Ramos, L.A. Sousa, A. Aguiar, Effect of cysteine using Fenton processes on decolorizing different dyes: a kinetic study, *Environ. Technol.*, 57 (2020) 1–132.
- [19] C.M. Dominguez, A. Romero, A. Santos, Selective removal of chlorinated organic compounds from lindane wastes by combination of nonionic surfactant soil flushing and Fenton oxidation, *Chem. Eng. J.*, 376 (2019) 120009.
- [20] C.G.S. Lima, N.M. Moreira, M.W. Paixão, A.G. Corrêa, Heterogenous green catalysis: Application of zeolites on multicomponent reactions, *Curr. Opin. Green Sustain. Chem.*, 15 (2019) 1–7.
- [21] P.T. Silva, V.L. da Silva, B. de B. Neto, M.O. Simonnot, Phenanthrene and pyrene oxidation in contaminated soils using Fenton's reagent, *J. Hazard. Mater.*, 161 (2009) 967–973.
- [22] F. Pardo, M. Peluffo, A. Santos, A. Romero, Optimization of the application of the Fenton chemistry for the remediation of a contaminated soil with polycyclic aromatic hydrocarbons, *J. Chem. Technol. Biotechnol.*, 91 (2016) 1763–1772.
- [23] G. Vilardi, D. Sebastiani, S. Miliziano, N. Verdone, L. Di Palma, Heterogeneous nZVI-induced Fenton oxidation process to enhance biodegradability of excavation by-products, *Chem. Eng. J.*, 335 (2018) 309–320.
- [24] E.G. Garrido-Ramírez, B.K.G. Theng, M.L. Mora, Clays and oxide minerals as catalysts and nanocatalysts in Fenton-like reactions - A review, *Appl. Clay Sci.*, 47 (2010) 182–192.
- [25] Y. Wang, Y. Gao, L. Chen, H. Zhang, Goethite as an efficient heterogeneous Fenton catalyst for the degradation of methyl orange, *Catal. Today*, 252 (2015) 107–112.
- [26] M. Lu, Z. Zhang, W. Qiao, Y. Guan, M. Xiao, C. Peng, Removal of residual contaminants in petroleum-contaminated soil by Fenton-like oxidation, *J. Hazard. Mater.*, 179 (2010) 604–611.
- [27] M. Munoz, Z.M. de Pedro, J.A. Casas, J.J. Rodriguez, Preparation of magnetite-based catalysts and their application in heterogeneous Fenton oxidation - A review, *Appl. Catal. B: Environ.*, 176 (2015) 249–265.
- [28] S. Rostamnia, B. Gholipour, X. Liu, Y. Wang, H. Arandiyan, NH₂-coordinately immobilized tris(8-quinolinolato)iron onto the silica coated magnetite nanoparticle:

- $\text{Fe}_3\text{O}_4@\text{SiO}_2\text{-FeQ}_3$ as a selective Fenton-like catalyst for clean oxidation of sulfides, *J. Colloid Interface Sci.*, 511 (2018) 447–455.
- [29] H.Y. Xu, B. Li, T.N. Shi, Y. Wang, S. Komarneni, Nanoparticles of magnetite anchored onto few-layer graphene: A highly efficient Fenton-like nanocomposite catalyst, *J. Colloid Interface Sci.*, 532 (2018) 161–170.
- [30] C.H. Han, H.D. Park, S.B. Kim, V. Yargeau, J.W. Choi, S.H. Lee, J.A. Park, Oxidation of tetracycline and oxytetracycline for the photo-Fenton process: Their transformation products and toxicity assessment, *Water Res.*, 172 (2020) 115514.
- [31] S.S. Li, Z. Tian, D.Z. Tian, L. Fang, Y.W. Huang, J. Xu, Preparation and Surface Modification of Magnetic Fe_3O_4 Nanoparticles, *Adv. Sci. Eng. Med.*, 12 (2020) 131–136.
- [32] W. Măntele, E. Deniz, UV–VIS absorption spectroscopy: Lambert-Beer reloaded, *Spectrochim. Acta Part A: Mol. Biomol. Spec.*, 173 (2017) 965–968.
- [33] V.C. Mora, L. Madueño, M. Peluffo, J.A. Rosso, M.T. Del Panno, L.S. Morelli, Remediation of phenanthrene-contaminated soil by simultaneous persulfate chemical oxidation and biodegradation processes, *Environ. Sci. Pollut. Res.*, 21 (2014) 7548–7556.
- [34] Z. Najahi Mohammadizadeh, M. Hamidinasab, N. Ahadi, M.A. Bodaghifard, A novel hybrid organic-inorganic nanomaterial: preparation, characterization and application in synthesis of diverse heterocycles, *Polycycl. Aromat. Compd.*, (2020). <https://doi.org/10.1080/10406638.2020.1776346>



A fast, low-cost and eco-friendly method for routine determination of Bisphenol-A in landfill leachate employing vortex assisted liquid-liquid extraction

Gustavo Waltzer Fehrenbach^a, Daniel Ricardo Arsand^{a,*}, Sergiane Caldas Barbosa^b, Katia R L Castagno^a,

Pedro Jose Sanches Filho^a and Ednei Gilberto Primel^b

^aChemistry Department, Sul-rio-grandense Federal Institute of Education, Science and Technology, 360-96015, Praça 20 de Setembro – 455, Pelotas, RS, Brazil.

^bSchool of Chemistry and Food, Federal University of Rio Grande, 900-96203, Av. Itália - Km 8, Rio Grande, RS, Brazil.

ARTICLE INFO:

Received 5 Jun 2021

Revised form 9 Aug 2021

Accepted 30 Aug 2021

Available online 29 Sep 2021

Keywords:

Sanitary landfill,
Endocrine disruptors,
VALLME,
Bisphenol-A,
Contaminant

ABSTRACT

Landfills are sites designed to receive and final disposal of a broad variety of urban solid wastes (USW). The decomposition and biodegradation processes generate a leachate of high complexity and toxicity, containing persistent and recalcitrant contaminants that are not usually monitored. Bisphenol-A (BPA) is a synthetic compound applied mostly on the production of polycarbonate plastics, epoxy resins, and is an endocrine disruptor. BPA negatively affects biological receptors, resulting in harmful effects to nervous and reproductive system as well metabolic and immune function. The presence of BPA in USW urges the development of feasible analytical methods to support the effluent treatment plants and reduce the risks of contamination. The main goal of this work was to develop an efficient, eco-friendly, fast and simple method for routine analysis of BPA in the leachate from landfill. A vortex assisted liquid-liquid extraction (VALLME) using 1-octanol as solvent was performed. BPA recoveries at spiking levels of 2.5, 6.5 and 12.5 $\mu\text{g L}^{-1}$ were between 60 to 104% with relative standard deviation (RSD) lower than 26%. The linearity of the method was evaluated and the correlation coefficient was (r) 0.9985. The limit of quantification (LOQ) was 2.5 $\mu\text{g L}^{-1}$ with a pre-concentration factor of 20. The method has advantages such as low consumption of extraction solvent (150 μL), low cost, easy and fast determination.

1. Introduction

Bisphenol-A (BPA) is a synthetic compound of wide applicability used in the synthesis of materials as detergents, polycarbonates, thermal paper, epoxy resin, and food packaging [1]. It is classified as endocrine disrupter for having a structure similar to the steroid hormone

17- β -estradiol, what confers ability to imitate the estrogen activity [1-3]. BPA effects were discussed in neurochemistry alterations, prostate cancer, breast cancer, hormonal alterations, infertility, and ovaries problems [1, 4, 5]. The usage of BPA in packs of plastic, thermal papers, coating of food cans, pharmaceuticals, and general industry represents a direct source for human and environment contamination [6,7]. In countries where the classification and recycling

*Corresponding Author: [Daniel Ricardo Arsand](mailto:danielarsand@pelotas.ifsul.edu.br)

Email: danielarsand@pelotas.ifsul.edu.br

<https://doi.org/10.24200/amecj.v4.i03.146>

of urban solid wastes (USW) is not efficient, the final disposal of USW occurs mainly in landfill sites. These sites are projected to work in a long and slowly process of degradation. Although, degradation processes as photolysis, hydrolysis and biological still occurs and generates a leachate of high complexity and toxicity, where the presence of BPA threatens the environment safety [8, 9]. A reliable and efficient method is necessary to evaluate the trace levels of BPA in the complex matrix of leachate. For that, a pre-concentration and/or clean-up step have been used to prepare the sample prior to extraction and analytical determination of BPA, allowing the quantification of BPA at trace levels in water and plastic materials as toys. [10, 11]. In general, the sample preparation has been performed by methods based on liquid or solid phase extraction. In the solid phase extraction (SPE), the analyte is extracted from the sample by passing the sample through a column/cartridge packed with polar (e.g. alumina) or nonpolar sorbent (e.g. C18). Modifications as solid phase microextraction (SPME) have also been observed for BPA extraction. On the other hand, liquid-liquid extraction (LLE) methods are based on the usage of solvents to extract and separate the analyte from the matrix, usually in an aqueous and organic phase [7, 11, 13, 14]. SPE and LLE have been used and adapted for years and their application is well dependent to the matrix composition, sample properties and concentration. However, there is a need for non-tedious and environmentally friendly methods, employing lower volumes of non-toxic solvents and significant recoveries. Vortex-assisted liquid-liquid microextraction (VALLME) is a technique based on emulsification procedure where the extraction applies reduced volumes of a low-density solvent into water associated with high energy of vortex mixing [15]. The fine droplets can rapidly extract target analytes from water due to shorter diffusion distance and larger interfacial area. After centrifugation, the floating extractant phase restores its initial single-drop shape for the following instrumental analysis. This technique

has showed to be eco-friendly for BPA extraction in water samples [16]. Gas chromatography (GC) and high-pressure liquid chromatography (HPLC) are the main analytical instruments used for BPA detection. Either are based on the difference of interaction between the sample in mobile phase (liquid for HPLC, and gas for GC) and stationary phase (packed column). Then, the analyte interacts with the detector that generates an electronic signal, translated into a peak. Different GC and HPLC setups have already been described. The mass spectrometry (MS), ultraviolet (UV) and fluorescence are detectors frequently used in HPLC, while in GC the MS have been more applied for the detection of BPA [3, 5, 10-15]. In this work, the usage of HPLC with diode-array detector has been chosen due advantages as the simultaneous acquisition in different wavelengths, improving the separation of peaks, an important factor to be considered when working with complex matrices as leachate [11, 14, 15]. The challenges of controlling the destiny of USW to landfills and aware society of a responsible waste discard is aggravated by the analytical limitations of detection and quantification methods for BPA in complex matrices. On this way, a feasible and low-cost method could collaborate with better health policies and increase the alert to BPA exposure. The aim of this study was to develop a fast, robust, low-cost and accuracy method for routine analysis of BPA in the complex matrix of landfill leachate, employing VALLME and HPLC-DAD.

2. Material and Methods

2.1. Chemical and samples

The bisphenol A (BPA) standard and analytical grade acetonitrile (J.T Baker, Mallinckrodt, NJ, USA) were purchased from Sigma-Aldrich (São Paulo, Brazil). BPA standard solutions were prepared in methanol and stored at 4 °C until use. Ultrapure water was prepared in a Direct-Q UV3 (Millipore, France), and used as mobile phase as well as acetonitrile.

The leachate used in this study was collected according to standard methods (SM:2005) from a

landfill located in the city of Camaquã, located at the south of Brazil (30° 49' 41.9''S 51° 47' 39.3''W). The samples were stabilized with H₂SO₄ (1 mol L⁻¹) and kept in the dark at 4 °C until the analytical procedures. Then, leachate samples were filtered out with a Micropore system using cellulose acetate membranes of 0.45 μm (Sartorius Biolab Products, Goettingen, Germany), assisted with vacuum from a vacuum-pump Tecnal TE-0581 (Tecnal, São Paulo, Brazil), and kept in a pre-washed amber bottle with acetone aqueous solution 1 mol L⁻¹.

2.2. Apparatus

The BPA determination was carried out in a Waters high performance liquid chromatography coupled to a diode array detector 2996 (Waters, Milford, MA, USA), equipped with a quaternary pump model 600, Empower PDA software was employed on the data acquisition. The separation was realised in a silica-based, reversed-phased analytical column C18 5 μm ODS2 150 mm x 4.6 (Waters, Milford, MA, USA). The analytes were eluted with a mixture of ultrapure 60% H₂O and 40% analytical grade ACN as mobile phase in isocratic mode and at a flow-rate of 1 mL min⁻¹. The injection was made manually using a syringe with 20 μL of VALLME extracted sample.

2.3. Vortex-assisted liquid-liquid microextraction procedure

VALLME extractions were carried out in 10 mL glass tubes with conical bottom with 10 mL of filtered leachate and 150 μL of 1-octanol in quadruplicate (Sigma-Aldrich, São Paulo, Brazil). The tubes were vortexed (Certomat MV, B. Braun Biotech International) at 4500 rpm for 5 min, and centrifuged at 2000 rpm for 5 min (Quimis, São Paulo, Brazil). The supernatant was taken out after phase separation with a 250 μL syringe and transferred to 2 mL tube (Eppendorf 5804 R, Eppendorf, São Paulo, Brazil). The 2 mL tube was centrifuged once more at 2000 rpm for 2 min and the supernatant was collected with a syringe, transferred to a new tube and the volume filled up to 0.5 mL with methanol. The parameters related to VALLME and HPLC-DAD were adjusted before the validation process. The lowest volume of solvent and sample that resulted in a detectable and reliable signal of BPA were chosen. Vortex and centrifugation were based on the visual formation and stability of the organic layer. Then, a second centrifugation was realised to remove possible contaminants carried by the pipetting. Five hundred microliters of methanol were used to ensure the complete resuspension of organic phase (Fig.1).

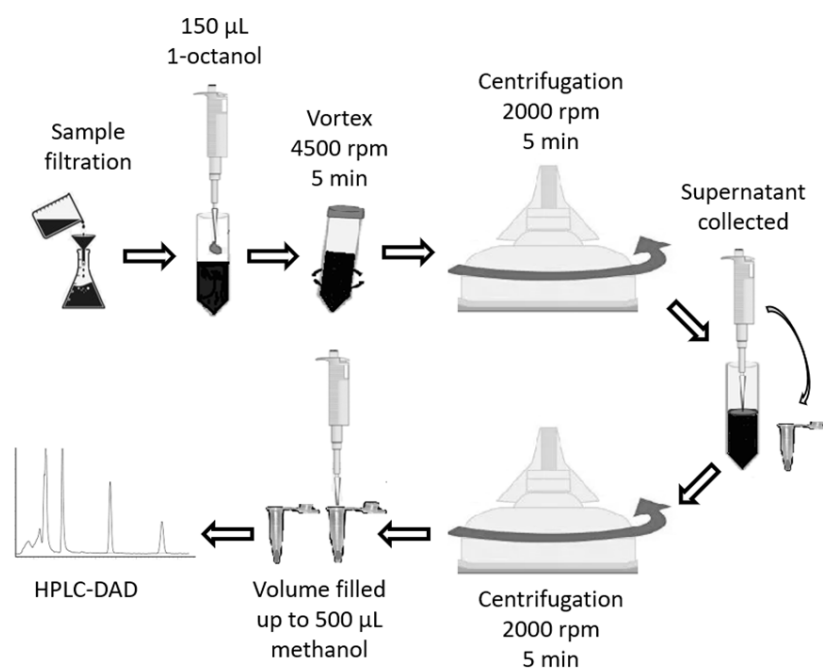


Fig. 1. Vortex-assisted liquid-liquid microextraction (VALLME) procedure.

2.4. Analytical performance

The proposed method was validated by analysing parameters as analytical curve, linearity, limit of detection (LOD), limit of quantification (LOQ), recovery and precision (intermediate precision and repeatability), according to Brazilian legislation (INMETRO - DOQ-CGCRE - 008, 2011) which establish the procedures and standards for analytical determinations. Accuracy was evaluated using recovery experiments with extraction of 3 different BPA standard concentrations: 2.5, 6.25 and 12.5 $\mu\text{g L}^{-1}$. The precision in terms of repeatability was obtained by carrying out the extraction and analysis of fortified samples. Each spike level was extracted in three replicates and each extract injected three times in the HPLC-DAD equipment. Different days were used for the same spike levels of repeatability to evaluate the intermediate precision of the method. Limit of detection (LOD) and the limit of quantification (LOQ) were obtained using the ratio signal/noise 3:1 and 10:1, respectively.

3. Results and discussion

3.1. Preliminary analysis

Landfill sites receives a broad variety of solid waste from different sources. The wide application of BPA and indiscriminate holding of plastic materials at these sites represents a direct source for BPA to contaminate soil, water, and environment, posteriorly reaching human by direct contact or indirect through contaminated food. Due to the matrix complexity and low concentrations, a method to identify and quantify estrogens need to be specific and selective [17]. A standard solution of BPA was diluted in methanol (mobile phase) and added to leachate sample to verify the presence of interferences in the absorption spectrum of BPA, required to avoid false positive results. The retention time for BPA standard in methanol was at 5.8 min of run and detection wavelength at 227 nm. BPA fortification was detected in leachate sample at same retention time as in methanol. The chromatogram of landfill leachate with no fortification is presented in Figure 2, and it can be observed the absence of interference at BPA retention time (5.8 min) and 227 nm, confirming the method selectivity.

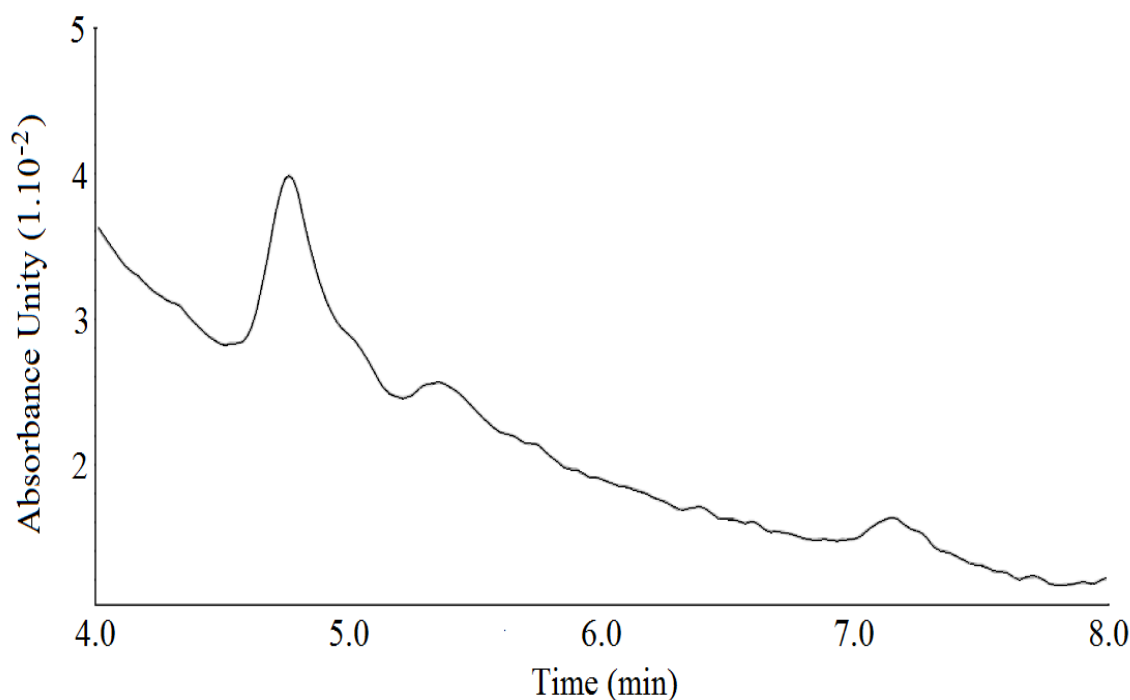


Fig. 2. Chromatogram of landfill leachate without BPA fortification. No interference was detected at retention time for BPA (5.8 min)

3.2. Validation of analytical procedure

The determination of analyte concentration in different matrices is usually made by a calibration curve, preparing concentrations of stock standard solution and relating to absorbance units obtained for each concentration, generating an equation used to quantify the analyte in real samples. Furthermore, this procedure is also applied to measure the correlation between 2 factors, a necessary factor in the process of validation. The maximum value for correlation coefficient (r) is 1, ensuring the relation between absorbance and concentration. The calibration curve was prepared with 5 concentrations of standard BPA in methanol, ranging from 0.05 to 2.5 mg L⁻¹ ($n=3$). The curve showed a high linear correlation (r) of 0.9985, overcoming the requirements established by the Brazilian legislation (ANVISA: 0.99 and INMETRO:

0.90) and allowing the use to determine BPA in leachate sample.

LOD and LOQ represents the limits of detection and quantification of a method. LOD is defined as the smaller concentration of analyte that can be detected without guarantee or reliability. LOQ is the lowest concentration where the analyte can be determined with precision. Applying the ratio signal-noise to obtain the LOD (3:1) and LOQ (10:1), the values found were 0.8 and 2.5 $\mu\text{g L}^{-1}$, respectively. These values are in agreement with other microextraction techniques proposed for BPA detection as showed in Table 1. Recoveries were determined in 2.5, 6.25 and 12.5 $\mu\text{g L}^{-1}$ levels (Fig. 3), obtaining an RSD from 60 to 104% and RSD from 11 to 26%. Intermediate precision was determined in different days of analyses and the recoveries obtained were between 81% and 97% with RSD lower than 16%.

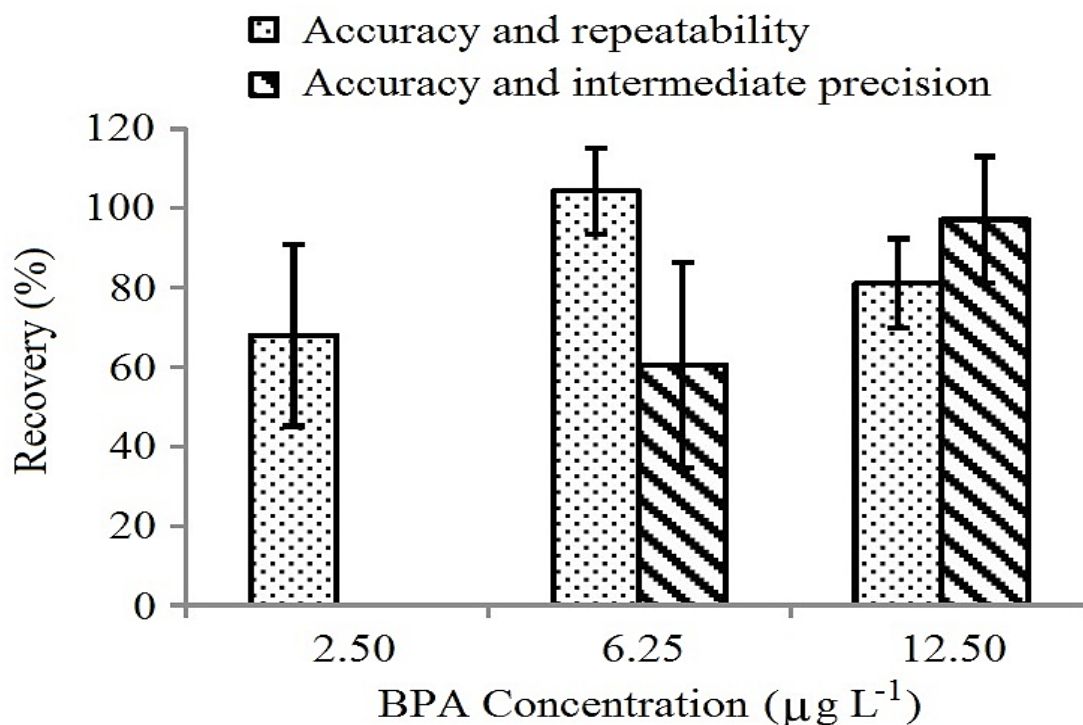


Fig. 3. Evaluation of method accuracy, repeatability, and intermediate precision by recoveries (%) of different BPA fortifications ($\mu\text{g L}^{-1}$)

Table 1. Recoveries (%) in landfill leachate fortified with 2.5, 6.25, and 12.5 $\mu\text{g L}^{-1}$ of BPA stock. Results are based on the recoveries obtained for the respective stock in methanol.

Stock ($\mu\text{g L}^{-1}$)	Samples (%recovery)				
	1	2	3	4	5
2.5	69.89	73.87	38.87	75.93	40.28
6.25	103.46	110.89	105.49	95.13	95.73
12.5	97.00	93.24	114.55	117.02	80.66

The highest recoveries and consequently accuracy, repeatability and intermediate precision were obtained with 12.5 $\mu\text{g L}^{-1}$ of BPA. These results can also be observed in Table 1, where are presented the corresponding recoveries of 2.5, 6.25, and 12.5 $\mu\text{g L}^{-1}$ BPA fortifications in landfill leachate.

The specificity of the method is also observed in the chromatograms (Fig. 4) of BPA in methanol (4a) and landfill fortified leachate (4b).

In the Table 2 are presented the results of BPA determination in diverse matrices less complex than landfill leachate. Therefore, the obtained results

in our research agree with the literature for BPA extraction from liquid samples: SPE [7] with serial processes of homogenization-vortex-sonication-centrifugation-evaporation-resuspension of sample [18], Micro-QuEChERS-GC/MS [19], and DLLME [20]. Correia-Sá et al [19] obtained recoveries of BPA from 70 to 120% and RSD from 3 to 11% applying Micro-QuEChERS-GC/MS in human urine, a simpler matrix than landfill leachate. Laganà et al [17] obtained 99-103% of recovery for BPA fortifications in river and sewage treatment (influent and effluent) samples.

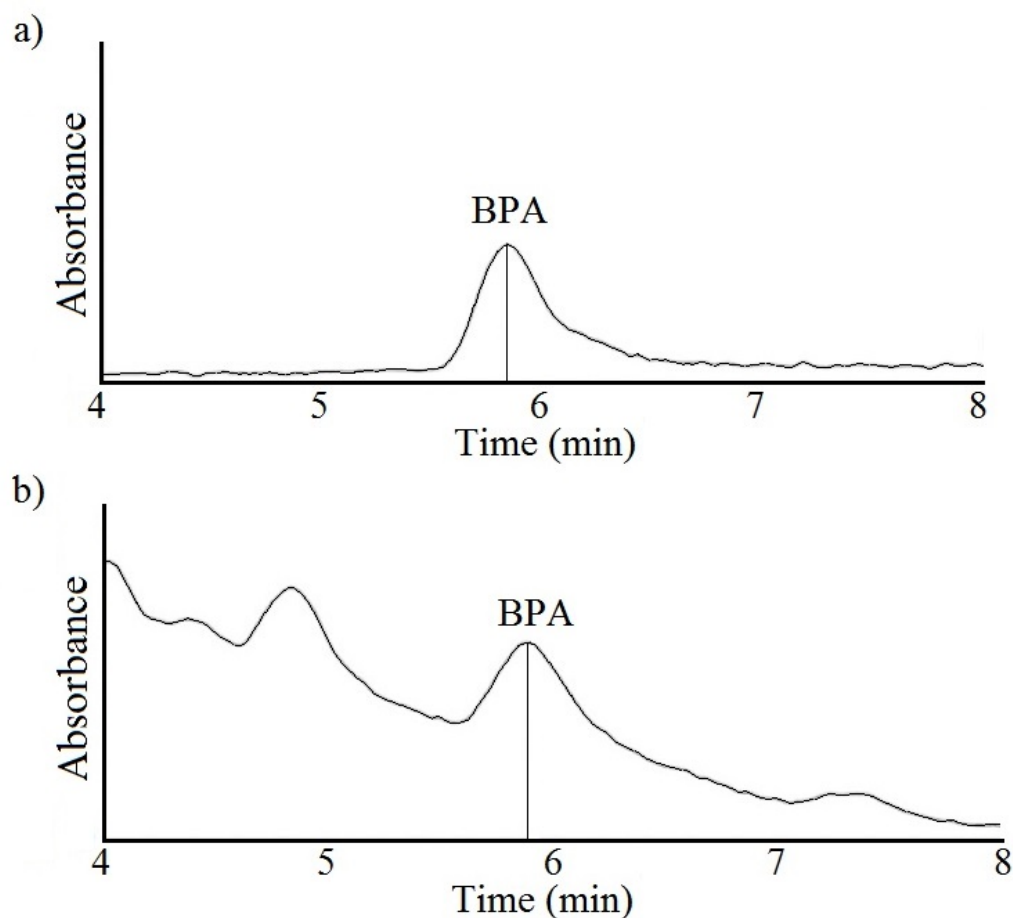


Fig. 4. Chromatogram of BPA standard solution (a) and fortified sample (b).

The signals were generated with 12.5 $\mu\text{g L}^{-1}$ of BPA

Table 2. Recovery (%), limit of quantification (LOQ), limit of detection (LOD) and relative standard deviation (RSD%) of BPA determination methods obtained by different authors in diverse matrices and complexities.

Matrix	Recoveries (%)	LOQ	LOD	RSD (%)	References
Landfill leachate	60-104	2.5 $\mu\text{g L}^{-1}$	0.8 $\mu\text{g L}^{-1}$	11-26	**
Urine	0-120	0.43 $\mu\text{g L}^{-1}$	0.13 $\mu\text{g L}^{-1}$	3-11	[19]
Sewage effluent/ influent	88.6-96.2	Effluent: 0.98 ng L^{-1} Influent: 3.84 ng L^{-1}	*	1.5-15	[21]
Blood serum	101-106	0.028 ng mL^{-1}	0.009 ng mL^{-1}	3.9-5.8	[22]
River water	84.7-95.7	0.01 ng mL^{-1}	0.003 ng mL^{-1}	5.3-9.6	[23]
Effluent wastewater, bottled and surface water	89-113	6; 24 and 7 ng L^{-1}	20; 7; 22 ng L^{-1}	<17	[24]
Wastewater effluent and estuarine water	89-94	11-20 ng L^{-1}	*	2-13	[25]

As showed in Figure 4, BPA can be determined in landfill leachate with no significant matrix interference and reliable results, followed by easily detection. The method is also eco-friendly, requiring less than 1 mL of solvent per analysis and not time demanding.

The protocol in this method is ideal for routine and quick analysis, versatile and can be used in a broad spectrum of matrix with high extraction rates, easy cleanup step, low RSD, feasibility, low consumption of solvents, and non-expensive.

4. Conclusions

On this article we developed an analytical procedure for BPA determination in landfill leachate. A low volume of 1-octanol (150 μL) was used as extraction solvent in the vortex-assisted liquid-liquid microextraction (VALLME) in a simple procedure that takes around 20 min to be executed. The proposed method was validated by adding standard concentrations of BPA in leachate and quantifying the recoveries, with a full analysis of standard deviation, accuracy, repeatability, intermediate precision, LOD, and LOQ. BPA recoveries were between 60 to 104% with relative standard deviation (RSD) lower than 26%, and linearity of 0.9985. The limit of quantification (LOQ) was 2.5 $\mu\text{g L}^{-1}$ with a pre-concentration factor of 20. Thereby, the proposed

methodology is eco-friendly, requiring a low volume of sample and extraction solvent. The method present technical features that adequate for BPA routine analysis and also the potential to be applied in BPA quantification in simpler matrices.

5. Declaration of interest

The authors declare no conflict of interest.

6. Acknowledgements

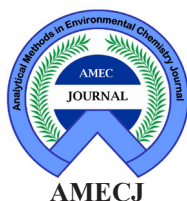
The authors are grateful to the Brazilian National Council for Scientific and Technological Development (CNPq) for providing grants for this study, to Sul-rio-grandense Federal Institute for Education, Science and Technology (IFSul) and to University of Rio Grande (FURG) for its financial support.

7. References

- [1] Y. Ma, H. Liu, J. Wu, L. Yuan, Y. Wang, X. Du, R. Wang, P.W. Marwa, P. Petlulu, X. Chen, H. Zhang, The adverse health effects of bisphenol A and related toxicity mechanisms, *Environ. Res.*, 176 (2019) 108575.
- [2] R. B. Gear, S. M. Belcher, Impacts of Bisphenol A and ethinyl estradiol on male and female CD-1 mouse spleen, *Sci. Rep.*, 7 (2017) 856.

- [3] S. M. Zimmers, E. P. Browne, P. W. O'Keefe, D. L. Anderton, L. Kramer, D. A. Reckhow, K. F. Arcaro, Determination of free Bisphenol A (BPA) concentrations in breast milk of U.S. women using a sensitive LC/MS/MS method, *Chemospher*, 104 (2014) 237-243.
- [4] Y-K. Leung, V. Govindarajah, A. Cheong, J. Veevers, D. Song, R. Gear, X. Zhu, J. Ying, A. Kendler, M. Medvedovic, S. Belcher, S-M. Ho, Gestational high-fat diet & bisphenol A exposure heightens mammary cancer risk, *Endocr. Relat. Cancer*, 24 (2017) 365-378.
- [5] N. Dorival-García, A. Zafra-Gómez, A. Navalón, J.L. Vilchez, Improved sample treatment for the determination of bisphenol A and its chlorinated derivatives in sewage sludge samples by pressurized liquid extraction and liquid chromatography-tandem mass spectrometry, *Talanta*, 101 (2012) 01-10.
- [6] S. Almeida, A. Raposo, M. Almeida-González, C. Carrascosa, Bisphenol A: Food Exposure and Impact on Human Health, *Compr. Rev. Food Sci. Food Saf.*, 17 (2018) 1503-1517.
- [7] X. Hu, X. Wu, F. Yang, Q. Wang, C. He, S. Liu, Novel surface dummy molecularly imprinted silica as sorbent for solid-phase extraction of bisphenol A from water samples, *Talanta*, 148 (2016) 29-36.
- [8] A. C. Narevski, M. I. Novaković, M. Z. Petrović, I. J. Mihajlović, N. B. Maoduš, G.V. Vujić, Occurrence of bisphenol A and microplastics in landfill leachate: lessons from South East Europe, *Environ. Sci. Pollut. Res.*, 28 (2021) 42196-42203.
- [9] H. Wang, H. Yan, C. Wang, F. Chen, M. Ma, W. Wang, X. J. Wang, Analysis of phenolic pollutants in human samples by high performance capillary electrophoresis based on pretreatment of ultrasound-assisted emulsification microextraction and solidification of floating organic droplet, *Chromatogr. A*, 1253 (2012) 16-21.
- [10] Y. Vicente-Martinez, M. Caravaca, A. Soto-Meca, Determination of very low concentration of bisphenol A in toys and baby pacifiers using dispersive liquid-liquid microextraction by In situ ionic liquid formation and high-performance liquid chromatography, *Pharmaceuticals*, 13 (2020) 301.
- [11] P-P, Hao, Determination of bisphenol A in barreled drinking water by a SPE-LC-MS method, *J. Environ. Sci. Health A Tox. Hazard. Subst. Environ. Eng.*, 55 (2020) 697-703.
- [12] M. Caban, O. Stepnowski, The Quantification of bisphenols and their analogues in wastewaters and surface water by an improved solid-phase extraction gas chromatography/mass spectrometry method, *Environ. Sci. Pollut. Res.*, 27 (2020) 28829-28839.
- [13] S. Cho, Y. S. Choi, H. M. D. Luu, J. Guo, Determination of total leachable bisphenol A from polysulfone membranes based on multiple consecutive extractions, *Talanta*, 101 (2012) 537-540.
- [14] M. Sadeghi, Z. Nematifar, N. Fattahi, M. Pirsaeheb, M. Shamsipur, Determination of bisphenol A in food and environmental samples using combined solid-phase extraction-dispersive liquid-liquid microextraction with solidification of floating organic drop followed by HPLC, *Food Anal. Methods*, 9 (2016) 1814-1824.
- [15] R. Amini, J. Khandaghi, M. R. A. Mogaddam, Combination of vortex-assisted liquid-liquid extraction and air-assisted liquid-liquid microextraction for the extraction of bisphenol A and bisphenol B in canned dough samples, *Food Anal. Methods*, 11 (2018) 3267-3275.
- [16] C. Bosch Ojeda, F. Sánchez Rojas, Vortex-assisted liquid-liquid microextraction (VALLME): applications, *Chromatographia*, 77 (2014) 745-754.
- [17] A. Laganà, A. Bacaloni, I. De Leva, A. Faberi,

- G. Fago, A. Marino, Analytical methodologies for determining the occurrence of endocrine disrupting chemicals in sewage treatment plants and natural waters, *Anal. Chim. Acta*, 501 (2004) 79-88.
- [18] A. Cariot, A. Dupuis, M. Albouy-Llaty, B. Legube, S. Rabouan, V. Migeot, Reliable quantification of bisphenol A and its chlorinated derivatives in human breast milk using UPLC-MS/MS method, *Talanta*, 100 (2012) 175-182.
- [19] L. Correia-Sá, S. Norberto, C. Delerue-Matos, C. Calhau, V. F. J. Domingues, Micro-QuEChERS extraction coupled to GC-MS for a fast determination of Bisphenol A in human urine, *Chromatogr. B*, 1072 (2017) 9-16.
- [20] J. López-Darias, V. Pino, J. H. Ayala, A. M. Afonso, 'In-situ ionic liquid-dispersive liquid-liquid microextraction method to determine endocrine disrupting phenols in seawaters and industrial effluents, *Microchim. Acta*, 174 (2011) 213-222.
- [21] X. Sun, J. Peng, M. Wang, C. Tang, L. Yang, H. Lei, F. Li, X. Wang, J. J. Chen, Determination of nine bisphenols in sewage and sludge using dummy molecularly imprinted solid-phase extraction coupled with liquid chromatography tandem mass spectrometry, *Chromatogr. A*, 1552 (2018) 10-16.
- [22] K. Owczarek, P. Kubica, B. Kudlak, A. Rutkowska, A. Konieczna, D. Rachoń, J. Namieśnik, A. Wasik, Determination of trace levels of bisphenol A analogues in human blood serum by high performance liquid chromatography-tandem mass spectrometry, *Sci. Total Environ.*, 628-629 (2018) 1362-1368.
- [23] Z. Wang, J. Yu, L. Wu, H. Xiao, J. Wang, R. J. Gao, Simultaneous identification and quantification of bisphenol A and 12 bisphenol analogues in environmental samples using precolumn derivatization and ultra high performance liquid chromatography with tandem mass spectrometry, *Separation Sci.*, 41 (2018) 2269-2278.
- [24] N. Fabregat-Cabello, J. Pitarch-Motellón, J. V. Sancho, M. Ibáñez, A. F. Roig-Navarro, Method development and validation for the determination of selected endocrine disrupting compounds by liquid chromatography mass spectrometry and isotope pattern deconvolution in water samples: comparison of two extraction techniques, *Anal. Methods*, 8 (2016) 2895-2903.
- [25] O. Ros, A. Vallejo, L. Blanco-Zubiaguirre, M. Olivares, A. Delgado, N. Etxebarria, A. Prieto, Microextraction with polyethersulfone for bisphenol-A alkyphenols and hormones determination in water samples by means of gas chromatography-mass spectrophotometry and liquid chromatography-tandem mass spectrometry analysis, *Talanta*, 134 (2015) 247-255.



Thallium extraction in urine and water samples by nanomagnetic 4-Aminothieno[2,3-d] pyrimidine-2-thiol functionalized on graphene oxide

Seyed Jamilaldin Fatemi ^{a,*}, Mohammad Reza Akhgar ^b and Masoud Khaleghi Abbasabadi ^c

^a Department of Chemistry, Shahid Bahonar University of Kerman, 133 -76169, Kerman, Iran

^b Department of Chemistry, Faculty of Science, Kerman Branch, Islamic Azad University, Kerman, Iran

^c Researcher in Nano Technology Center, Research Institute of Petroleum Industry (RIPI), P.O. Box 1998-14665, Tehran, Iran

ARTICLE INFO:

Received 20 May 2021

Revised form 18 Jul 2021

Accepted 13 Aug 2021

Available online 28 Sep 2021

Keywords:

Thallium,
Water and urine,
Nanomagnetic 4-Aminothieno[2,3-d] pyrimidine-2-thiol functionalized on graphene oxide,
Dispersive magnetic micro solid-phase extraction

ABSTRACT

Thallium is a water-soluble metal and extra dosage has toxicological effect in human body. Thallium is readily absorbed by inhalation, ingestion and skin contact. The symptomatology of thallium toxicity was seen in patients with hemorrhage, bone/gastrointestinal problems, delirium, convulsions and coma. So, accurate determination of thallium in water and human urine is necessary. In this research, a novel and applied method based on 25 mg of nanomagnetic 4-Aminothieno[2,3-d] pyrimidine-2-thiol functionalized on graphene oxide ($\text{Fe}_3\text{O}_4\text{-ATPyHS@GO}$) was used for thallium extraction in 50 mL of water, wastewater and urine samples by dispersive magnetic micro solid-phase extraction (DM- μ -SPE). After extraction and back-extraction of solid phase by 1 mL of nitric acid solution, the concentration of thallium ions determined by flame atomic absorption spectrometry (F-AAS). The working/linear range, the limit of detection (LOD), and preconcentration factor (PF) were achieved (4-1400 $\mu\text{g L}^{-1}$; 4-300 $\mu\text{g L}^{-1}$), 0.9 $\mu\text{g L}^{-1}$, and 50, respectively (Mean RSD%=1.8 water; 2.1 urine). The absorption capacity of GO and $\text{Fe}_3\text{O}_4\text{-ATPyHS@GO}$ adsorbent were achieved 7.2 mg g^{-1} and 137.5 mg g^{-1} for 5 mg L^{-1} of thallium, respectively. The procedure was validated by ICP-MS analyzer.

1. Introduction

The Thallium use as in semiconductor and optical industries. The concentration of thallium in rocks and soil (limestone, granite) ranges between 0.05-1.7 mg kg^{-1} and 1.7-55 mg kg^{-1} , respectively [1]. The organic slates and carbon source have 1000 mg kg^{-1} thallium [2], and high concentration of thallium exist sulfur salts of thallium [3]. Contamination with thallium is effected on the environmental and

human health. Thallium has toxic effect even at sub ppb concentration and accumulate in plant, vegetables, fruit, microorganisms, animals and human tissues due to water soluble [4,5]. The occupational exposure of thallium is 0.1 mg m^{-2} for skin and more than 15 mg m^{-2} is dangerous for human. Thallium can be absorbed from inhalation, ingestion and skin. So, the thallium toxicity must be evaluated in patients through determination in water, wastewater, urine, hair, nail and blood samples. The toxicity of this element is higher compared to mercury, cadmium and lead [6,7]. The mean daily diet contains 2 ng L^{-1} thallium

*Corresponding Author: Seyed Jamilaldin Fatemi

Email: fatemijam@uk.ac.ir

<https://doi.org/10.24200/amecj.v4.i03.150>

and the average content of thallium in the human body was 0.1 mg. The concentrations in blood is less than 3 μg L⁻¹ and due to reference values thallium has low concentration between 0.15–0.6 μg L⁻¹ in blood and 0.02– 0.3 μg L⁻¹ in serum [8,9]. Groesslova and Wojtkowiak showed that the toxicity of thallium is mainly related to the similarity between Tl (I) ions and K ions, which cause to the thallium interference with potassium and disorder of potassium associated metabolic processes. Also, thallium disrupts the disulfide bonds and cysteine cross-linking and cause to the keratin reduction [10,11]. The thallium-201, a radioactive isotope, was used for evaluating coronary artery disease. This type of thallium is more than 4000 times less potent. Thallium-201 is useful in distinguishing toxoplasmosis from Primary CNS lymphoma (PCNSL) in HIV patients. Also, the thallium-201 scintigraphy is useful to diagnose the Kaposi sarcoma, the thyroid imaging and various tumors of the lungs [12]. The acute thallium toxicity has been reported between 6-15% in humans by health organization and the dosage from 10 to 15 mg kg⁻¹ is a lethal dose for humans. Elimination phase for thallium starts about 24 hours' post-exposure and is mainly achieved through renal excretion and the elimination phase may take up to 30 days with long time. Symptoms of acute exposure of thallium are gastrointestinal, CNS problem, and skin [13,14]. The chronic exposure is gastrointestinal symptoms include, the abdominal pain, the vomiting and the diarrhea. Therefore, due to adverse effect of thallium in human health, the determination human urine, foods and waters must be considered [15]. Based on the thallium toxicity, the power technique must be used for determining of thallium in environmental (water) and human biological (urine) samples. Numerous papers showed that the measurement of this topic with different analytical methods in various matrixes such as, the laser excited atomic fluorescence spectrometry (LE-AFS) [16], the anodic stripping voltammetry (ASV) [17], the inductively coupled plasma optical

emission spectrometry (ICP-OES) [18], the flame atomic absorption spectrometry (FAAS) [19], the electrothermal atomic absorption spectrometry (ET-AAS) [19] and the high resolution inductively coupled plasma mass spectrometry (HR-ICP-MS) [20].

In this research, a novel method based on nanomagnetic 4-Aminothieno[2,3-d] pyrimidine-2-thiol functionalized on graphene oxide as a Fe₃O₄-ATPyHS@GO adsorbent was used for the extraction of thallium in the water, wastewater and the urine samples. The thallium concentration was determined based on dispersive magnetic micro solid-phase extraction by F-AAS.

2. Experimental

2.1. Apparatus and Characterization

The thallium value was determined by flame atomic absorption spectrometer coupled (F-AAS, Varian, USA). The Air-acetylene (C₂H₂) and the deuterium lamp was adjusted. The limit of detection (LOD) and sensitivity of F-AAS obtained 0.2 mg L⁻¹ and 0.15 mg L⁻¹. The HCL of Tl was adjusted based on catalog book with wavelength of 276.8 nm, slit of 0.5 nm and current of 10 mA. All samples injected to F-AAS by auto-injector (0.5-3 mL). The working range and linear range of AT-AAS were obtained 0.2-75 mg L⁻¹ and 0.2- 15 mg L⁻¹, respectively. The electrothermal atomic absorption spectrophotometer (ET-AAS, Varian, USA) was used for validation of thallium in urine and water samples. For suppress of ionization in F-AAS, the reagent of KNO₃ or KCl was used as a 2000 mg L⁻¹ of K in final solution. The pH was calculated by digital pH meter (Metrohm 744, Swiss). The different buffer of the acetate (PH 3–6) were used for adjusting pH. The ultra-sonication (Grant, U.K) and the Sigma 3K30 magnetic centrifuge (30.000 rpm, UK) was used. The natural flake graphite (325 mesh, 99.95%), were purchased from Merck chemical Company. The Perkin Elmer Spectrum spectrophotometer (65 FT-IR, USA) was used for FT-IR spectra. The PRO X-ray diffractometer was used for The XRD spectra. The images of field emission scanning electron microscope (FE-SEM) were prepared by SEM of Tescan Mira-3.

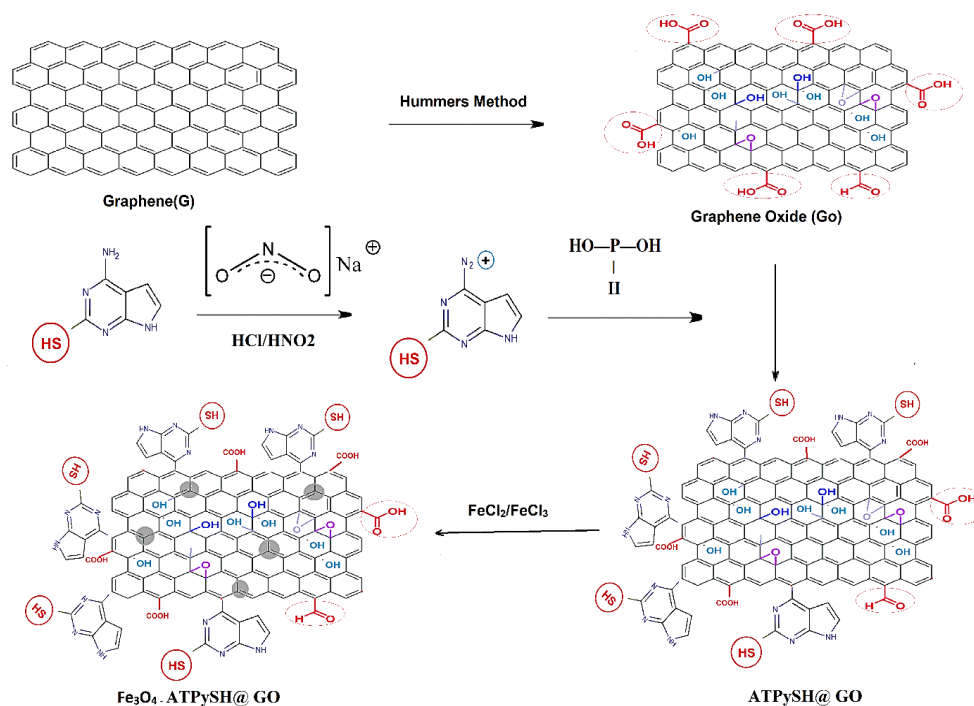


Fig.1. Synthesis of nanomagnetic ATPyHS@GO adsorbent by 4-aminothieno[2,3-d] pyrimidine-2-thioland and Fe₃O₄ on GO [22-24]

2.2. Materials

All reagents with analytical grade such as; the thallium solution (Tl NO₃), the acids and base solutions (HNO₃, HCl, NaOH) were purchased from sigma Aldrich (Germany). The standard solution of thallium nitrate (CAS N: 10102-45-1, Sigma, Germany) was prepared from stock of 1000 mg L⁻¹ solution in 1 % HNO₃ for further studies. The standard solutions for calibration were daily prepared by distilled water (DW) from Millipore (USA). The other reagents such as acetone and ethanol with analytical grade were purchased from Merck (Germany). The citric acid was used for phosphate citrate buffer for PH between 2.1–7.4 and the acetate buffer was used for pH from 2.8 to 6.2 which was purchased from Merck.

2.3. Synthesis of Fe₃O₄-ATPyHS@GO

The GO was prepared following the modified Hummers method. 5 g of graphite powder was mixed with 250 mL of H₂SO₄ and stirred for 24 h. Then, 30 g of KMnO₄ was gradually added to the mixture based on stirring at 50 °C [21]. Due to previous studies, 4-aminothieno[2,3-d] pyrimidine-

2-thiol (10 g) was added to 150 mL of ethanol and DW (1:1 v/v). Then, 180 mg of GO was added to the resulted solution at 35°C. The H₃PO₂ (50 mL, 50 wt%) was added to product and stirred for 90 min. The product of ATPyHS@GO was washed and dried by DW and oven, respectively. The magnetic nanostructure was prepared by co-precipitation of FeCl₂·4H₂O and FeCl₃·6H₂O, in the presence of 4-Aminothiopyridine-2-thiol graft on GO (ATPyHS@GO). First, the mixture of FeCl₂·4H₂O and FeCl₃·6H₂O was prepared with a molar ratio of 1:2. For synthesis nanomagnetic adsorbent, 10 mg of 4-aminothieno[2,3-d] pyrimidine-2-thiol grafted on graphene oxide (ATPyHS@GO) was solved to 10 mL of DW and sonicated for 40 min. Then 125 mg of FeCl₂·4H₂O and 200 mg of FeCl₃·6H₂O in 10 mL of deionized water were added to remain solution at 25°C. For adjusting of pH=11, the ammonia solution was added at 65°C. After 20 min stirring, the product was cooled at 25°C. Finally, the black Fe₃O₄-ATPyHS@GO was centrifuged at 4000 rpm for 50 min, washed for 10 times (DW) and dried at 70 °C based on vacuum accessory [22-24].

2.4. Extraction Procedure

By the DM-μ-SPE procedure, 50 mL of water and standard samples (4 - 300 μg L⁻¹) were used for separation and determination of thallium ions at pH 4-6. Firstly, 25 mg of Fe₃O₄-ATPyHS@GO added to water, urine and thallium standard solution and the sample sonicated for 3.0 min at pH=5. After sonication, the Tl ions was chemically absorbed on thiol groups (ATPyHS) of Fe₃O₄-ATPyHS@GO adsorbent (Tl⁺.....:SH-ATPy @ GO) and then, settled down in bottom of magnetic centrifuge conical tube. Then, the thallium ions were back-extracted from Fe₃O₄-ATPyHS@

GO at basic pH with NaOH solution (0.1 M, 0.5 mL) and was simply separated by the external magnetic accessory. Finally, the remain solution was determined by FAAS after dilution with DW up to 1 mL (Fig.2). The procedure was round for a blank solution without thallium ions for ten times. The analytical parameters showed in Table 1. The recovery of thallium extraction was calculated by the equation 1. The C_i and C_f are the primary and final concentration of thallium, which was determined by F-AAS (n=10).

$$\text{Recovery (\%)} = (C_i - C_f) / C_i \times 100 \quad (\text{Eq.1})$$

Table 1. The analytical parameters for determination thallium in water and urine samples based on Fe₃O₄-ATPyHS@GO adsorbent by the DM-μ-SPE procedure

Parameters	Values
Working pH	4-6
Amount of Fe ₃ O ₄ -ATPyHS@GO adsorbent (mg)	25
Sample volume of water (mL)	50
Volume of sample injection	1.0 mL
Linear range for water	4.0-300 μg L ⁻¹
working range for water	4.0-1400 μg L ⁻¹
Mean RSD %, n=10	1.8
LOD for water	0.9 μg L ⁻¹
Preconcentration factor	50
Volume and concentration of NaOH	0.5 mL, 0.4 M
Shaking time	3.0 min
Correlation coefficient	R ² = 0.9997

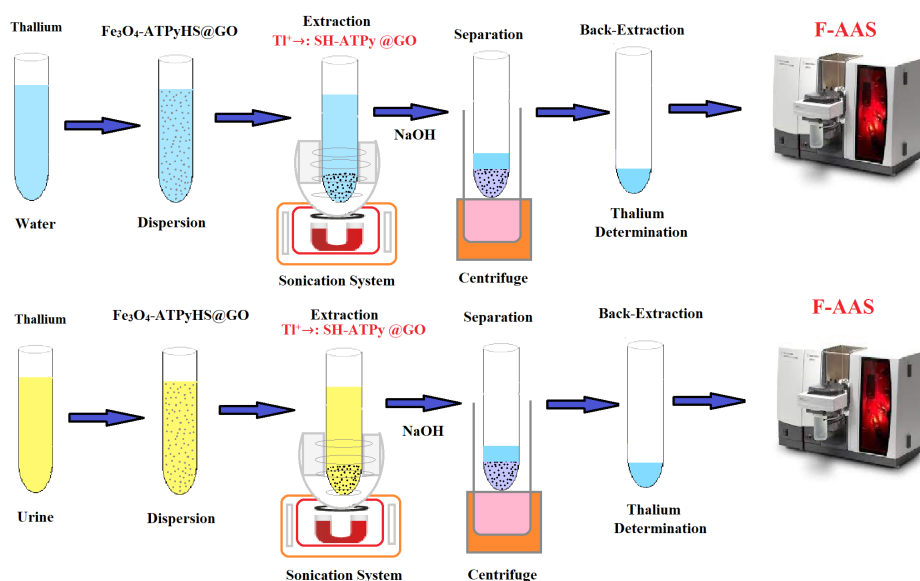


Fig.2. The extraction procedure of thallium in water and urine samples based on Fe₃O₄-ATPyHS@GO adsorbent by the DM-μ-SPE procedure

3. Results and Discussion

3.1. TEM Spectra

The TEM of Fe_3O_4 -ATPyHS@GO and GO adsorbent was prepared (Fig. 3a and 3b). Based on the TEM images, both of GO and Fe_3O_4 -ATPyHS@GO have the thin sheets about 30-80 nm. The Fe_3O_4 was seen as black point on surface of GO in TEM of Fe_3O_4 -ATPyHS@GO adsorbent (Fig. 3a).

3.2. FE-SEM Spectra

The morphology of Fe_3O_4 -ATPyHS@GO and GO adsorbent is prepared by the field emission scanning electron microscopy (FE-SEM) (Fig. 4a and 4b).

Based on the SEM images, both of GO and Fe_3O_4 -ATPyHS@GO have the thin sheets nearly related to each other. The SEM images of GO and Fe_3O_4 @4-PhMT-GO showed us, the HS and Fe_3O_4 had no effect on the morphology of the GO sheets. Also, the nanoparticles of Fe_3O_4 have a spherical morphology on HS-GO with a diameter of 40 nm.

3.3. FTIR diagram

The infrared spectra of pure GO and Fe_3O_4 -ATPyHS@GO are presented in Figure 5. The spectra of GO and Fe_3O_4 -ATPyHS@GO are showed to the stretching bands of (O-H;

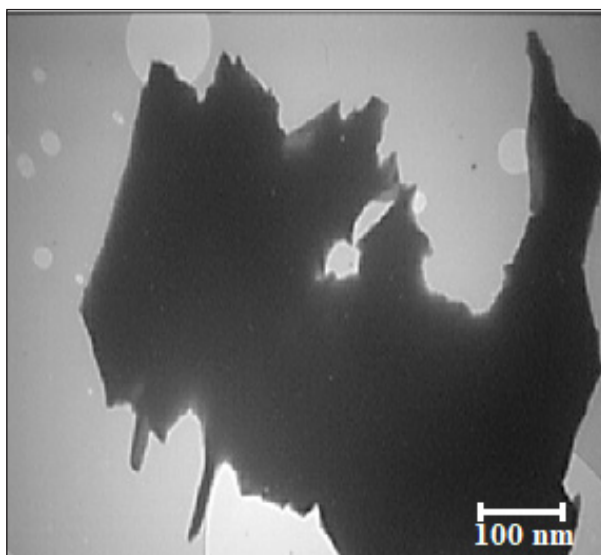


Fig. 3a. TEM of the Fe_3O_4 -ATPyHS@GO

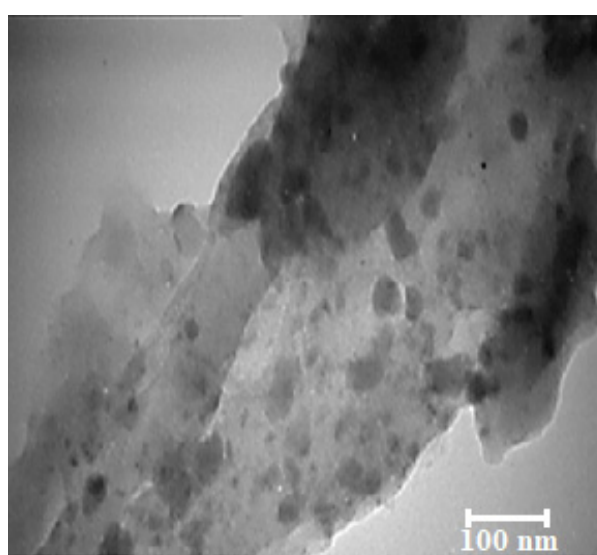


Fig. 3b. TEM of the GO adsorbent

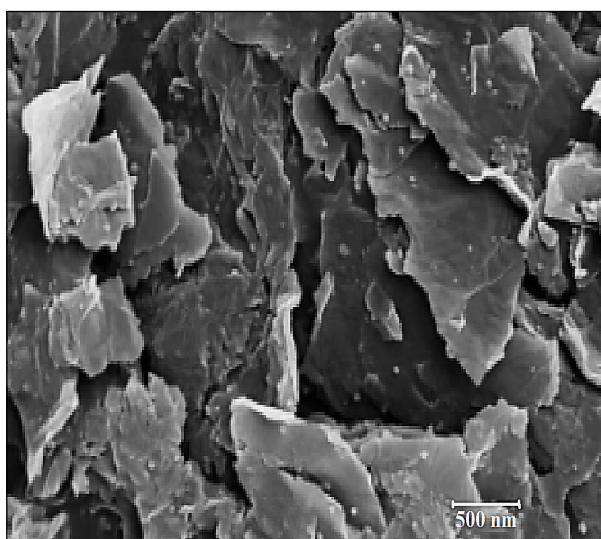


Fig. 4a. FE-SEM of the Fe_3O_4 -ATPyHS@GO

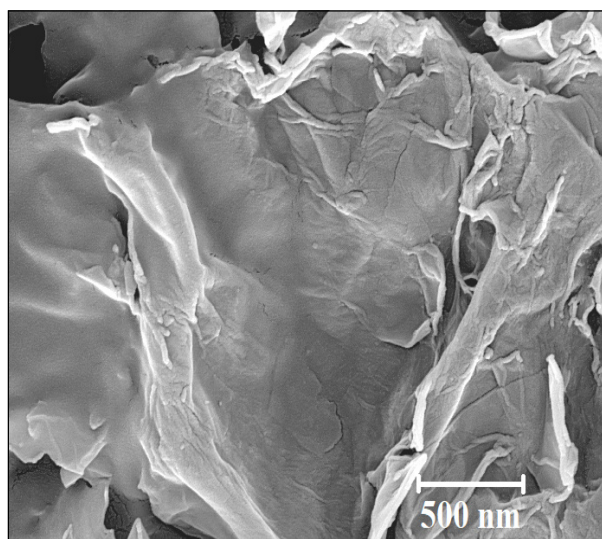


Fig. 4b. FE-SEM of the GO

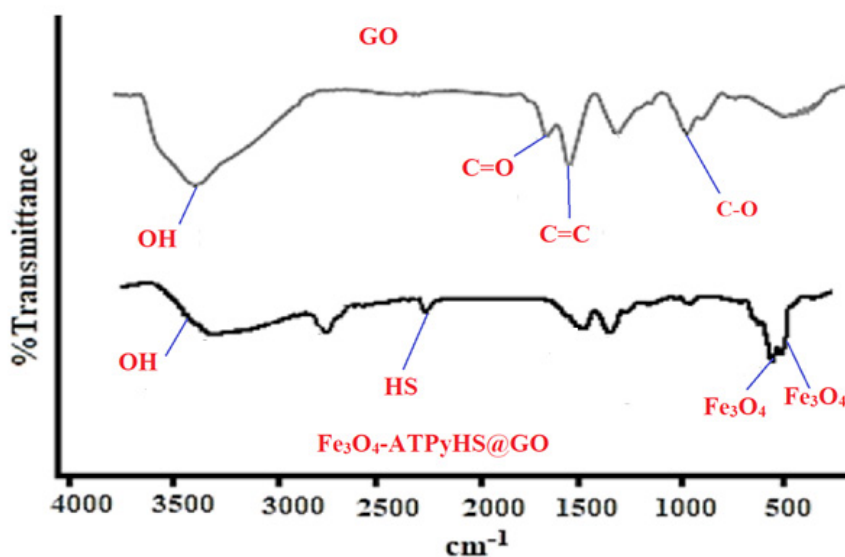


Fig. 5. The FTIR spectra of pure GO and Fe_3O_4 -ATPyHS@GO adsorbents

3415), (C=O; 1730), (C=C; 1624), and (C-O; 1061). Also, the peak of FTIR at range of 2600-3500 cm^{-1} belong to to the O-H and C=C(OH) function. Moreover, the peak of 1400 cm^{-1} and 2234 cm^{-1} related to tertiary hydroxyl groups(OH) and HS function on GO. In –addition the peaks at 628 cm^{-1} and 583 cm^{-1} belong to the Iron oxide [22-24].

3.4. X-ray diffraction (XRD) patterns

The X-ray diffraction patterns of Fe_3O_4 -ATPyHS@GO was shown in Figure 6. GO have a single original peak at $2\theta = 12^\circ$ which is related to the O_2 groups. In both of GO and Fe_3O_4 @4-PhMT-

GO adsorbent, the XRD peaks were observed at $2\theta = 12^\circ$ and 41.58° which are belonged to (002) and (100), respectively. Based on the XRD peak of Fe_3O_4 -ATPyHS@GO, the intensity of the peak at $2\theta = 12^\circ$ has decreased due to function on GO with HS and Fe_3O_4 . In addition, the peak at $2\theta = 12^\circ$ showed that the stability of O_2 functionalities even after the functionalization of GO with HS or Fe_3O_4 groups. The similar XRD peak of Fe_3O_4 can be seen for the Fe_3O_4 -ATPyHS@GO adsorbent which are confirmed to the cubic spinel crystal structure of Fe_3O_4 . So, the functionalities of HS and Fe_3O_4 were successfully done without changing in structure of GO.

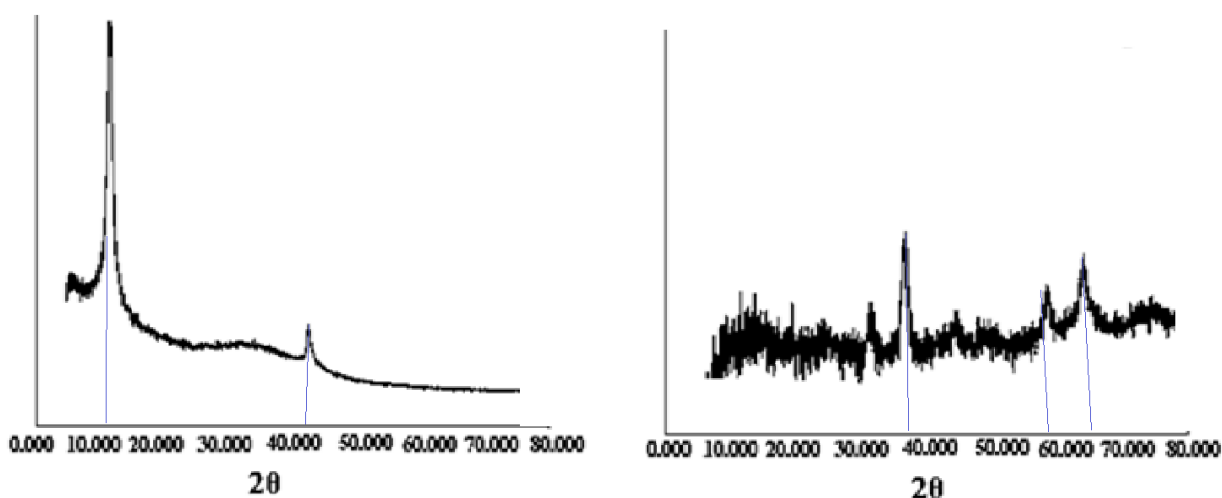


Fig. 6. XRD patterns of (a) GO adsorbent and (b) Fe_3O_4 -ATPyHS@GO adsorbent [22]

3.5. Optimizing extraction parameters

By DM- μ -SPE procedure, the separation/extraction of thallium in water, wastewater and urine samples was achieved by a novel Fe_3O_4 -ATPyHS@GO adsorbent between 4-300 $\mu\text{g L}^{-1}$ thallium concentration. For the efficient extraction of thallium based on Fe_3O_4 -ATPyHS@GO adsorbent, the extraction conditions must be optimized. So, the effective parameters such as pH, the amount of adsorbent, the eluent, the sample volume, and the adsorption capacity must be studied.

3.5.1. pH effect

The pH of extraction of thallium in water and urine samples must be evaluated and optimized. The favorite pH cause to increase the adsorption of thallium ions by the Fe_3O_4 -ATPyHS@GO adsorbent. So, the different pH between 2-11 was examined for thallium extraction in water and urine samples by adjusting pH with different buffer solutions. The results showed us, the maximum extraction of the Fe_3O_4 -ATPyHS@GO adsorbent for Tl(I) was obtained at pH of 4-7. Also, the recoveries for thallium were decreased at acidic pH less than 4 and basic pH more than 7. So, the pH 5 was selected as the optimal pH for extraction of thallium in water and urine samples by the Fe_3O_4 -ATPyHS@GO adsorbent (Fig.7). The mechanism of extraction of thallium was occurred by the dative bond of thiol

group [$2(\text{Ti}^+) \dots\dots\dots^2:\text{SH-ATPyHS@GO-Fe}_3\text{O}_4$] with the positively charged of thallium(Tl^+) at optimized pH. In addition, the thallium ions participated ($\text{Tl}(\text{OH})$) at more than pH 7.5.

3.5.2. Amount of Fe_3O_4 -ATPyHS@GO adsorbent

For high extraction of thallium in water/urine samples, the amount of the Fe_3O_4 -ATPyHS@GO adsorbent evaluated at thallium concentration between 4-300 $\mu\text{g L}^{-1}$. For this purpose, the various amount of the Fe_3O_4 -ATPyHS@GO adsorbent between 5-50 mg were studied for Tl(I) extraction in water and standard solutions by the DM- μ -SPE method. As Figure 8, the best recovery for thallium extraction was created by 20 mg of Fe_3O_4 -ATPyHS@GO adsorbent. So, 25 mg of the Fe_3O_4 -ATPyHS@GO adsorbent was used for further work.

3.5.3. Effect of eluents

The various eluents such as HNO_3 , H_2SO_4 , NaOH and CH_3COOH were used for back extraction thallium ions from the Fe_3O_4 -ATPyHS@GO adsorbent. In acidic and basic pH, the dative bonding between the thiol group (HS) and thallium (Tl) was started to dissociate ($4 > \text{pH} > 6$). So, after break down the bonding, the thallium ions released in eluent solution by elution. At pH more than 7, the thallium participated as thallium hydroxyl (Tl-OH)

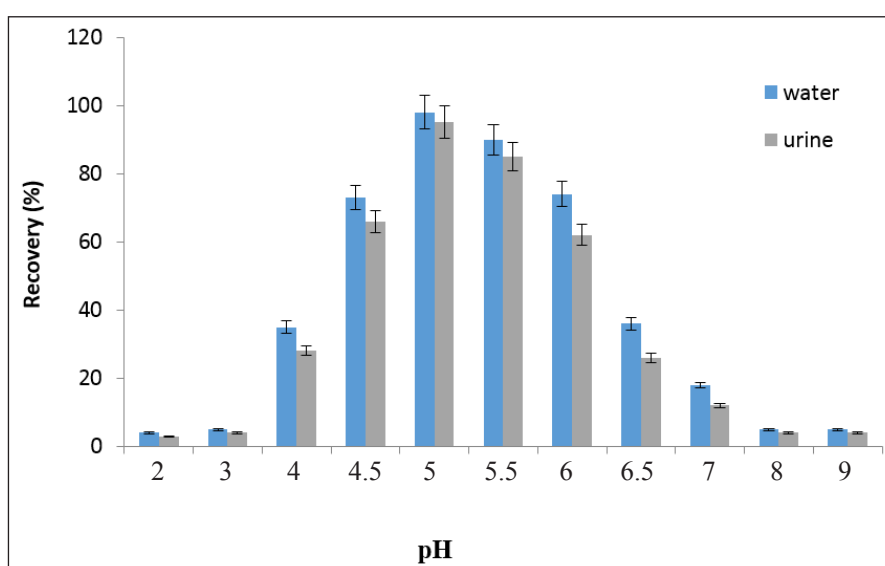


Fig.7. The effect of pH on thallium extraction in water and urine samples by Fe_3O_4 -ATPyHS@GO adsorbent

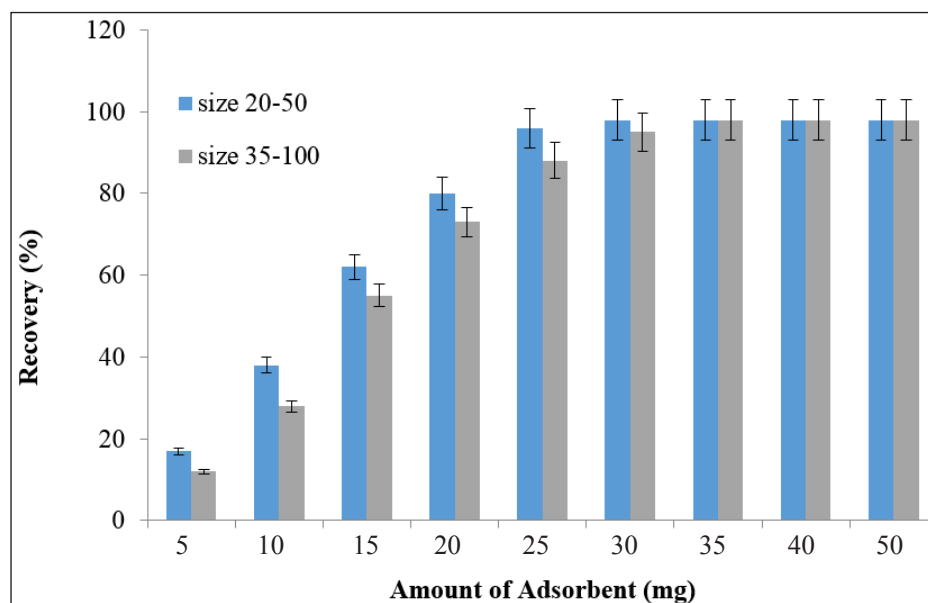


Fig.8. The effect of amount of Fe₃O₄-ATPyHS@GO adsorbent on thallium extraction in water and urine samples by the DM-μ-SPE method

and in low pH, the bonding of Tl-SH dissociated. Due to results, the HNO₃ and NaOH has more recovery as compared to H₂SO₄ and CH₃COOH. The different acid solution with different volume and concentration was used for back extraction Tl(I) in water and urine samples (0.2-2.0 mol L⁻¹, 0.1-0.5 mL) by the DM-μ-SPE procedure. Due to results, the Tl ions were completely back-extracted from the Fe₃O₄-ATPyHS@GO adsorbent by nitric acid and

NaOH solutions more than 1.0 mol L⁻¹ and 0.1 mol L⁻¹, respectively. Therefore, 0.1 mol L⁻¹ of NaOH was used as an optimum eluent for this study. Also, the effect of different volumes of eluents from 0.1 mL to 0.5 mL for thallium was checked. Therefore, 0.5 mL of NaOH (0.1 M) selected as optimum elution (Fig. 9). Also, the more concentration of NaOH (M>0.2) caused to the thallium participation (Tl-OH).

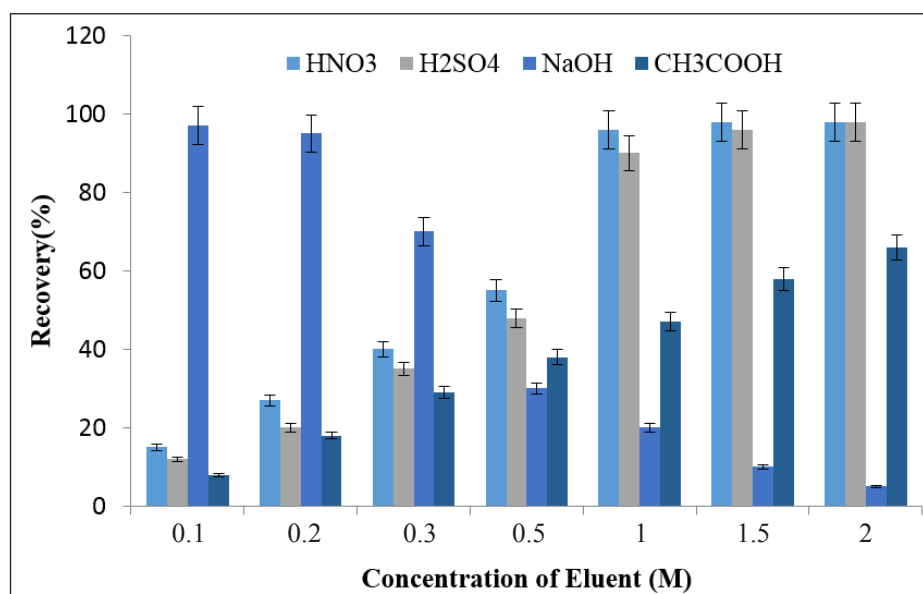


Fig.9. The effect of eluent concentration on thallium extraction in water and urine samples by the Fe₃O₄-ATPyHS@GO adsorbent

3.5.4. Effect of sample volume

The main factor for efficient extraction of Tl ions from water/urine samples is sample volume. The effect of different volumes between 10-200 mL for Tl extraction based on the $\text{Fe}_3\text{O}_4\text{-ATPyHS@GO}$ adsorbent was studied and optimized in water and urine samples ($4\text{-}300\ \mu\text{g L}^{-1}$). By results, the high recovery (%) was occurred for 55 mL for urine and 70 mL for water samples. So, 50 mL of sample volume was used for further work by the DM- μ -SPE procedure (Fig. 10).

3.5.5. Effect of sonication time

The dispersion of $\text{Fe}_3\text{O}_4\text{-ATPyHS@GO}$ adsorbent increased the interaction between thiol group (HS) and thallium ions at pH 5. By uniform dispersion of the $\text{Fe}_3\text{O}_4\text{-ATPyHS@GO}$ adsorbent, the chemical adsorption of thallium occurred. Therefore, the extraction recovery increased due to physical adsorption of GO and chemical bonding of HS group in $\text{Fe}_3\text{O}_4\text{-ATPyHS@GO}$ adsorbent. Moreover, the sonication times was effected on extraction rate. The various sonication times (1-10 minute) was used and the recoveries obtained. The best recoveries were achieved at the sonication time of 2.5 min. Therefore, 3.0 min was used as the optimum time for thallium extraction in water and urine samples. After sonication, the magnetic adsorbent (Tl- $\text{Fe}_3\text{O}_4\text{-ATPyHS@GO}$) was collected from the liquid samples by extra magnet accessory.

3.5.6. The adsorption capacity

The $\text{Fe}_3\text{O}_4\text{-ATPyHS@GO}$ adsorbent was dispersed in water samples and the extractions of thallium ions from liquid samples were followed many times and re-usage of adsorbent calculated. The results showed, the $\text{Fe}_3\text{O}_4\text{-ATPyHS@GO}$ adsorbent can be used for 18 extraction cycles at pH of 5.0. The absorption capacities (AC) of the $\text{Fe}_3\text{O}_4\text{-ATPyHS@GO}$ adsorbent depended on the BET, the function group and size of adsorbent. In batch system, 25 mg of the $\text{Fe}_3\text{O}_4\text{-ATPyHS@GO}$ nanoparticles was used in 50 mL of thallium solution ($5\ \text{mg L}^{-1}$; ppm) at pH 5.0. After 10 minutes' sonication, the AC of adsorbent calculated by F-AAS. The adsorption capacities of the $\text{Fe}_3\text{O}_4\text{-ATPyHS@GO}$ adsorbent for Tl ions were obtained $137.5\ \text{mg g}^{-1}$.

3.5.7. Interference of coexisting ions

The effect of main coexisting ions on thallium extraction based on the $\text{Fe}_3\text{O}_4\text{-ATPyHS@GO}$ adsorbent was evaluated in water and urine samples by the DM- μ -SPE procedure. So, the effect of various concentrations of interfering ions (1-3 ppm) was studied for 50 mL of water samples by proposed procedure at pH 5.0. The main concomitant ions in water and urine were selected and used for thallium extraction by the $\text{Fe}_3\text{O}_4\text{-ATPyHS@GO}$ adsorbent. The results showed that the interference coexisting ions do not affect on the thallium extraction in optimum conditions (Table 2).

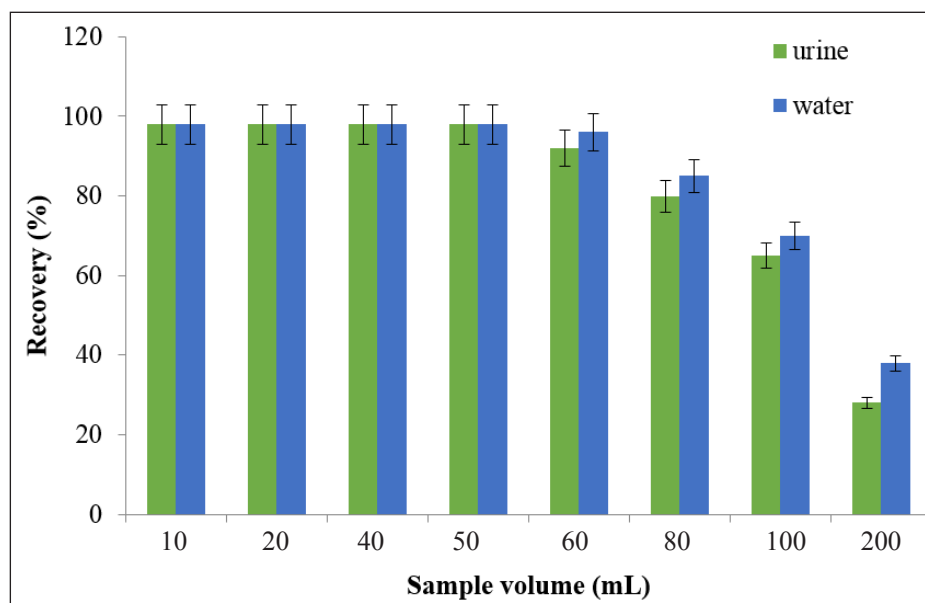


Fig.10. The effect of sample volume on thallium extraction in water and urine samples by the $\text{Fe}_3\text{O}_4\text{-ATPyHS@GO}$ adsorbent

Table 2. The effect of interferences ions on extraction of thallium in human urine and water samples by the DM-μ-SPE procedure

Interferences ions	Mean ratio (C ₁ /C _{T(0)})	Mean ratio (C ₁ /C _{T(0)})	Recovery (%)	Recovery (%)
	Urine	Water	Urine	Water
Mo ²⁺ , Ni ²⁺ , Co ²⁺ , Mn ²⁺	400	650	98.1	97.0
Zn ²⁺ , Cu ²⁺	700	900	96.5	98.3
Pb ²⁺ , Cd ²⁺ , V ³⁺ , Cr ³⁺	550	700	98.6	99.2
Br ⁻ , F ⁻ , Cl ⁻ , I ⁻ , NO ₃ ⁻	900	1200	97.9	98.5
Na ⁺ , K ⁺ , Ca ²⁺ , Mg ²⁺	1000	1300	97.3	98.8
Se ⁴⁺	350	400	97.1	97.6
Al ³⁺ , Be ⁺²	600	600	97.4	98.7
CO ₃ ²⁻ , PO ₄ ³⁻ , SO ₄ ²⁻ , NH ₄ ⁺	800	950	97.7	98.6
Hg ² , Ag ⁺	200	300	96.8	97.4
Sn ²⁺	500	700	98.2	97.9

3.5.8. Validation in real samples

The DM-μ-SPE procedure was used for extraction and determination of thallium in water and urine samples. The validation of results for the Fe₃O₄-ATPyHS@GO adsorbent were shown in Table 3. For validation, the real samples were spiked to different concentration of standard solutions of thallium and process continued by the DM-μ-SPE procedure at

pH 5.0 (Table 3). As Table 3, the efficient extraction and high recovery for thallium ions were obtained in water and human urine samples by nanoparticles of the Fe₃O₄-ATPyHS@GO adsorbent. Moreover, the standard reference materials were prepared in water and urine samples with ICP-MS analyzer for validating of the DM-μ-SPE procedure based on the Fe₃O₄-ATPyHS@GO adsorbent (Table 4).

Table 3. Validation of methodology for thallium ions in water and urine samples based on Fe₃O₄-ATPyHS@GO adsorbent by spiking of real samples

Sample*	Added (μg L ⁻¹)	*Found (μg L ⁻¹)	Recovery (%)
^a Well water	---	56.4 ± 2.4	---
	50	104.6 ± 4.5	96.4
^b Wastewater	---	146.6 ± 7/5	---
	150	294.3 ± 13.4	98.5
Wastewater ^c	---	122.9 ± 5.9	---
	100	225.7 ± 11.2	102.8
^v Urine	---	4.7 ± 0.2	---
	5	9.6 ± 0.5	98.0
Urine ^v	---	11.9 ± 0.4	---
	10	21.6 ± 0.9	97.0
^v Urine	---	28.9 ± 1.3	---
	30	59.8 ± 2.7	103

*Mean of three determinations of samples ± confidence interval (P = 0.95, n = 10)

^aWell water prepared from Varamin garden, Tehran, Iran

^bWastewater prepared from chemical factory, Karaj, Iran

^cWastewater prepared from petrochemical factory, Arak, Iran

^vUrine prepared from workers from car, chemical and paint factories, Iran

Table 4. Validation of D- μ -SPE procedure for thallium determination in water and urine samples by ICP-MS (certified reference materials, CRM, n=10)

Sample	ICP-MS ($\mu\text{g L}^{-1}$)	Added	Found* ($\mu\text{g L}^{-1}$)	Recovery (%)
CRM1	25.3 \pm 0.5	-----	24.9 \pm 1.2	-----
		20.0	44.3 \pm 1.9	97.0
CRM 2	62.7 \pm 0.7	-----	64.1 \pm 2.8	-----
		50.0	113.2 \pm 5.2	98.2
CRM 3	5.1 \pm 0.2	-----	4.8 \pm 0.2	-----
		5.0	9.9 \pm 0.4	102
CRM 4	6.4 \pm 0.2	-----	6.2 \pm 0.3	-----
		5.0	11.0 \pm 0.5	96.0

*Mean of three determinations of samples \pm confidence interval (P = 0.95, n = 10)

CRM1: Thallium concentration in Water by ICP-MS (25.3 $\mu\text{g L}^{-1}$)

CRM2: Thallium concentration in Wastewater by ICP-MS (62.7 $\mu\text{g L}^{-1}$)

CRM3: Thallium concentration in urine by ICP-MS (5.1 $\mu\text{g L}^{-1}$)

CRM4: Thallium concentration in urine by ICP-MS (6.4 $\mu\text{g L}^{-1}$)

4. Conclusions

A simple and reliable method was used for preconcentration, separation and determination of Tl (I) in human urine and water samples by DM- μ -SPE procedure. The proposed method was developed based on magnetic Fe₃O₄-ATPyHS@GO adsorbent at pH 5.0 without any organic chelating agent and organic solutions. The proposed method based on the Fe₃O₄-ATPyHS@GO adsorbent can be considered for Tl extraction in liquid phase as a low cost, efficient, reusability and fast separation phase. The newly developed method was low interference, easy usage for sample preparation in human urine samples and also provides low LOD (0.9 $\mu\text{g L}^{-1}$), RSD (1.8-2.1%) values as well as good PF (50) and quantitative recoveries more than 95% for thallium extraction in water and urine human matrixes. So, the proposed method based on magnetic nanoparticles and thiol groups on the Fe₃O₄-ATPyHS@GO adsorbent can be considered as a fast sample preparation technique with low amount of adsorbent for thallium separation and determination by F-AAS.

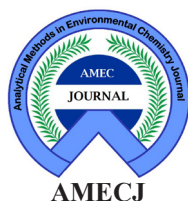
5. Acknowledgements

The authors wish to thank the Department of Chemistry, Shahid Bahonar University of Kerman, Kerman, Iran and Department of Chemistry of Islamic Azad University, Kerman, Iran.

6. References

- [1] T.S. Lin, J.O. Nriagu, Thallium in the environment, New York: Wiley, pp.31-44,1998.
- [2] C. Yang, Y. Chen, P. Peng, X. Chang, C. Xie, Distribution of natural and anthropogenic thallium in the soils in an industrial pyrite slag disposing area, *Sci. Total Environ.*, 341 (2005) 159–172.
- [3] A. Vaněk, Z. Groesslova, M. Mihaljevic, Thallium contamination of soils/vegetation as affected by sphalerite weathering: a model rhizospheric experiment, *J. Hazard. Mater.*, 283 (2015) 148–156. <https://doi.org/10.1016/j.jhazmat.2014.09.018>.
- [4] M. Sadowska, E. Biaduń, B. Krasnodebska-Ostrega, Stability of Tl(III) in the context of speciation analysis of thallium in plants, *Chemosphere*, 144 (2016) 1216–1223.
- [5] Z. Ning, L. He, T. Xiao, L. Márton, High accumulation and subcellular distribution of thallium in green cabbage, *Int. J. Phytoremed.*, 17 (2015)1097–1104.
- [6] B. Krasnodebska-Ostrega, Tl I and Tl III presence in suspended particulate matter: speciation analysis of thallium in wastewater, *Environ. Chem.*, 12 (2015) 374–379.
- [7] P. Cvjetko, I. Cvjetko, M. Pavlica, Thallium toxicity in humans, *Arch. Ind. Hyg. Toxicol.*, 61 (2010) 111–119. <https://doi.org/10.2478/10004-1254-61-2010-1976>.

- [8] J.M. Wallace, Kale and thallium: insights from your nutrition team. *Permaculture solutions for healing*, 2015.
- [9] A. Lansdown, *The carcinogenicity of metals: human risk through occupational and environmental exposure*, Cambridge: Royal Society of Chemistry, pp. 323–330, 2013.
- [10] Z. Groesslova, A. Vanek, M. Mihaljevic, V. Ettler, M. Hojdová, T. Zádorová, Bioaccumulation of thallium in a neutral soil as affected by solid-phase association, *J. Geochem. Explor.*, 159 (2015) 208–212.
- [11] T. Wojtkowiak, B. Karbowska, W. Zembrzusi, M. Siepak, Z. Lukaszewski, Miocene colored waters: a new significant source of thallium in the environment, *J. Geochem. Explor.*, 161 (2016) 42–48. <https://doi.org/10.1016/j.gexplo.2015.09.014>.
- [12] F.S. Hussain, N.S. Hussain, Clinical utility of thallium-201 single photon emission computed tomography and cerebrospinal fluid epstein-barr virus detection using polymerase chain reaction in the diagnosis of AIDS-related primary central nervous system lymphoma, *Cureus.*, 8 (2016) e606.
- [13] L. Osorio-Rico A. Santamaria S. Galván-Arzate, Thallium toxicity: general issues, neurological symptoms, and neurotoxic mechanisms, *Adv. Neurobiol.*, 18 (2017) 345-353.
- [14] V. Yu, M. Juhász, A. Chiang, N. Atanaskova Mesinkovska, Alopecia and associated toxic agents: A systematic review, *Skin Appendage Disord.*, 4 (2018) 245-260.
- [15] HY. Yu, C. Chang, F. Li, Q. Wang, M. Chen, J. Zhang, Thallium in flowering cabbage and lettuce: Potential health risks for local residents of the Pearl River Delta, South China, *Environ. Pollut.*, 241 (2018) 626-635.
- [16] B. Štádlarová, M. Kolrosová, J. Dědina, S. Musil, Atomic fluorescence spectrometry for ultrasensitive determination of bismuth based on hydride generation – the role of excitation source, interference filter and flame atomizers, *J. Anal. At. om.*, 35 (2020) 993-1002.
- [17] B. Karbowska, T. Rębiś, G. Milczarek, Electrode modified by reduced graphene oxide for monitoring of total thallium in grain products, *Int. J. Environ. Res. Public Health*, 15 (2018) 653.
- [18] L. Nyaba, T. S. Munonde, Magnetic Fe₃O₄@Mg/Al-layered double hydroxide adsorbent for preconcentration of trace metals in water matrices, *Sci. Reports*, 11(2021) 2302.
- [19] L. Nyaba, B. Dubazana, A. Mpupa, P. N. Nomngongo, Development of ultrasound-assisted dispersive solid-phase microextraction based on mesoporous carbon coated with silica@iron oxide nanocomposite for preconcentration of Te and Tl in natural water systems, *Open Chem.*, 18 (2020) 412–425.
- [20] T. Kusutaki, M. Furukawa, Preconcentration of Pb with aminosilanized Fe₃O₄ nanopowders in environmental water followed by electrothermal atomic absorption spectrometric determination, *Chem. Eng.*, 3 (2019) 74.
- [20] W.S.J. Hummers, R.E. Offeman, Preparation of graphitic oxide, *J. Am. Chem. Soc.*, 80 (1958) 1339.
- [21] S. Khodabakhshi, F. Marahel, A. Rashidi, M. Khaleghi Abbasabadi, A green synthesis of substituted coumarins using nano graphene oxide as recyclable catalyst, *J. Chin. Chem. Soc.*, 62 (2015) 389-392.
- [22] H. Shir Khanloo, M. K. Abbasabadi, F. Hosseini, A. Faghihi, Nanographene oxide modified phenyl methanethiol nanomagnetic composite for rapid separation of aluminum in wastewaters, foods, and vegetable samples by microwave dispersive magnetic micro solid-phase extraction, *Food Chem.*, 347 (2021) 129042.
- [23] M.K. Abbasabadi, A. Rashidi, S. Khodabakhshi, Benzenesulfonic acid-grafted graphene as a new and green nano adsorbent in hydrogen sulfide removal, *J. Nat. Gas Sci. Eng.*, 28 (2016) 87-94.
- [24] M. Khaleghi-Abbasabadi, D. Azarifar, Magnetic Fe₃O₄-supported sulfonic acid-functionalized graphene oxide (Fe₃O₄@GO-naphthalene-SO₃H): a novel and recyclable nanocatalyst for green one-pot synthesis, *Res. Chem. Intermed.*, 45 (2019) 2095-2118.



A review: Effects of air, water and land dumpsite on human health and analytical methods for determination of pollutants

Ihenetu Stanley Chukwuemeka^{a,*}, Victor Obinna Njoku^a, Chinweuba Arinze^b,
Ibe Francis Chizoruo^a, and Ekeoma Nmesoma Blessing^c

^a Chemistry Department, Imo State University Owerri, Imo State Nigeria

^b Chemistry Department, Chukwuemeka odimegwu Ojukwu University Uli, Anambra Nigeria

^c Medicine and surgery Department, Gregory University, Uturu Abia State, Nigeria

ARTICLE INFO:

Received 26 May 2021

Revised form 28 Jul 2021

Accepted 21 Aug 2021

Available online 30 Sep 2021

Keywords:

Environment pollutants,

Water,

Air and soil,

Analytical chemistry methods,

Human health

ABSTRACT

Environment pollutants are found here and there in developing countries and these contaminations affect the environment adversely. This is done by pecculation of solid and liquid substances in the dumpsites and industrial pollutions into the soil which form toxic chemicals as well as evaporation of gases into the atmosphere. Few remediation of pollution which includes incineration which is the waste treatment process that involves the combustion of organic substances contained in waste material, the waste handling practices, the recycling resource recovery, the avoidance and reduction methods, the adsorption based on nanotechnology and the bioremediation technology which appears as a cost-effective and environmental friendly approach for cleanup. Recently researches shows that various chemicals (VOCs, BTEX, heavy metals) that might be delivered into the air or water can cause unfriendly health effects which was analyzed based on sample treatments (solid phase extraction: SPE, the liquid-liquid microextraction: LLME, the magnetic solid phase extraction: MSPE) and instruments such as ET-AAS, F-AAS and GC-FID methods. The related weight of disease can be substantial, and interest in research on health effects and intervention in explicit populations and openness circumstances is significant for the development of control systems. Pollution control and determination is thusly a significant segment of disease control, and health experts and analytical chemistry specialists need to foster associations with different areas to recognize and carry out need interventions.

1. Introduction

The environment pollution in waters and the dumpsite in soil can be described as a portion of land where waste materials and discarded. In Africa, thousands and tons of wastes are generated daily in many ways [1]. The indiscriminate and unprotected disposal of waste can instigate environmental

degradation through introducing various toxicants, including heavy metals in the soil, air and water. Open dumping of municipal solid waste is a common practice in Nigeria. Chemical industries and dumpsites are important pollution sources in the environment (VOCs and heavy metals, organic and inorganic pollutants, toxic gas, organic cells, viruses) and can cause various diseases in the human body. Traditionally, dumpsites have remained the utmost regular method of waste dumping in many places around the world both in

*Corresponding Author: [Ihenetu Stanley Chukwuemeka](mailto:Ihenetustanley@yahoo.com)

Email: Ihenetustanley@yahoo.com

<https://doi.org/10.24200/amecj.v4.i03.147>

urban and rural areas. Most of the dumpsites are situated within the locality of living communities and wetlands. Some of chemical factories, oil company and petrochemical industries are located close to rivers, well waters, the agricultural soil where human activities are carried out [1]. In addition, the environmental pollutants must be removed from wastewater, water and air based on nanosorbents by chemical and physical adsorption process. Waste can be a strong material, fluid, semi-strong or holder of vaporous material [2]. Recently, the different adsorbent based on nanotechnology have positive effected on decreasing of pollutants from environment matrixes.

2. Environment pollutions

2.1. VOCs and heavy metal pollutions in water, soil, air

Volatile organic compounds (VOCs) are compounds that have a high vapor pressure and low water solubility. Numerous VOCs are human-made chemicals that are utilized and delivered in the assembling of paints, drugs, and refrigerants [3]. VOCs regularly are organic solvents, like trichloroethylene; fuel oxygenates, for example, methyl tert-butyl ether (MTBE); or side-effects delivered by chlorination in water treatment, like chloroform. VOCs are regularly parts of petrol fuels, pressure driven liquids, acetones, and cleaning specialists. VOCs are shared conviction water impurities. Volatile organic compounds (VOCs) are emitted as gases from certain solids or liquids. VOCs include a variety of chemicals, some of which may have short- and long-term adverse health effects. Concentrations of many VOCs are consistently higher indoors (up to ten times higher) than outdoors [4]. VOCs are emitted by a wide array of products numbering in the thousands. Examples include: paints and lacquers, paint strippers, cleaning supplies, pesticides, building materials and furnishings, office equipment such as copiers and printers, correction fluids and carbonless copy paper, graphics and craft materials including glues and adhesives, permanent markers, and photographic solutions [3-4]. A heavy metal is

characterized as a metal with a density higher than 5 g cm^{-3} (i.e., specific gravity more noteworthy than 5). The water treatment of explosive and heavy metals co-contaminated soil was evaluated [5]. According to previous references, the expression of heavy metals is frequently utilized as a gathering name for metals and semimetals (metalloids) that have been related with pollution and potential toxicity or ecotoxicity [6]. Very as of late, we have proposed a more extensive definition for the term, and heavy metals have been characterized (natural occurring metals having atomic number more prominent than 20 and an essential density more noteworthy than $5 \text{ g} \times \text{cm}^{-3}$). Also, determination of heavy metals in soil, vegetables and wastewater based on DLLME was obtained by the solidified deep eutectic solvent coupled to GFAAS [6]. Heavy metal harmfulness can have a few health impacts in the body. Heavy metals can harm and modify the working of organs like the brain, kidney, lungs, liver, and blood. Heavy metal harmfulness can either be acute or chronic impacts. Long haul openness of the body to heavy metal can dynamically prompt solid, physical and neurological degenerative cycles that are like diseases like Parkinson's disease, different sclerosis, strong dystrophy and Alzheimer's disease. Likewise, chronic long haul openness of some heavy metals might cause cancer [7]. Many different analytical procedures and sample preparation have been reported for VOCs and heavy metal analysis in water and human samples. The liquid-liquid extraction (LLE), supported liquid extraction (SLE), and solid-phase extraction (SPE) have existed for decades and if you're doing organic sample preparation, you're probably quite familiar with at least one of these techniques [8]. The micro solid-phase extraction (MSPE) and dispersive SPE is a technique which separates analytes, using physical or chemical adsorption interactions with a solid media. The media is mounted on a sorbent material in the form of either a disk or cartridge. The analytes are absorbed on the media as the sample passes through the sorbent material such as zeolites, silica (MSN.MCM), CNTs (MWCNTs, SWCNTs), graphene (NG, NGO, NG-COOH)

and MOF. The analytes are then eluted from the media using a solvent (HNO_3 , NaOH) in which the analytes are soluble and this solution is retained for analysis before determination by F-AAS, ET-AAS, GC-FID, GC-Mass and the UV-Vis spectrometry [8]. SPE is one of the most widely used sample preparation techniques. In SPE, an aqueous sample is passed through a short column containing a suitable solid sorbent, and the solutes are adsorbed onto the column. Afterwards, small amounts of organic solvents of high elution strength are used to recover the analytes from the sorbent, which leads to their enrichment [9]. Solid phase extraction utilizes small amounts of solvent and generates little waste. As a result, it is considered an ecofriendly technique. SPME was introduced by Ayotamuno et al [10]. According to the GAC guidelines, it is a green extraction procedure because it avoids the use of organic solvents and combines extraction, enrichment and sample injection into a single step. Analytes partition between the sample matrix and the SPME fiber coating when the fiber is immersed directly in the sample (direct immersion, or DI-SPME), or between the sample headspace and the fiber coating when the fiber is placed in the space above the BTEX sample (HS-SPME/GC-FID) [10]. Partitioning continues until equilibrium is established between all phases involved. When the extraction process is completed, the SPME fiber is transferred directly to the analytical instrument of choice, typically a gas chromatograph, where analyte desorption takes place. The major advantages of SPME include low cost, simplicity, elimination of the solvent disposal costs, short sample preparation time, reliability, sensitivity, and selectivity [11]. Liquid-liquid extraction (LLE) uses huge volumes of solvents that are regularly risky according to an environmental viewpoint and the cycle is dreary and tedious. During the previous decade, this method has gone through a dynamite change with regards to high-throughput screening with the presentation of miniaturized conventions alongside progressive film based and strong help based advancements. The least difficult procedure is the utilization of the 96-well plate design related

to a liquid dealing with robotic framework; it follows a similar standard as mass scale LLE [12].

2.2. Environment pollution and human health

Effects of environment pollutants and disproportionate dumpsite on human health is overwhelming and numerous to mention, especially in developing cities with the high range and production of plastic materials all over the place. All dumpsite is inclined to discharge pollutants to immediate water bodies and to the air by way of leachates and dumpsite gases correspondingly. Industrialization, population growth and unplanned urbanization have partially or totally turned our environment to dumping sites for waste materials. As many water resources have been rendered hazardous and unfit to man and other living systems as a result of indiscriminate dumping of refuse. In Nigeria, contamination and effluence of the underground and surface water by solid wastes is under disseminate thereby making them inappropriate for man's use [13]. As waste management facilities are deficient in many highly populous areas in most developing and underdeveloped countries owing to the cost and lack of implementation of pertinent enactment. Poor regional and urban planning, lack of implementation of pertinent laws and announcements on waste dumping, lack of systematized landfill sites play a role to the occurrence of dumpsites within people's inhabitations in developing countries. The surface run off and leachates from dumpsites are sources of fresh water contamination. The danger pose by leachates from metropolitan dumpsites depends on the waste conformation, amount, life span and time, temperature, moisture, obtainability for oxygen, soil morphology, and the comparative distance of the locations to the living community and water body. The pollution of soil with heavy metals even at low concentrations are identified to have possible impact on environmental quality and human health as well as professing a long term danger to groundwater and ecosystems [14]. Landfill leachates have been reported to contain a wide range of metals. Source of these

heavy metals ranges from industrial to municipal generation, automobiles, agricultural and domestic practices. The conventional credence that wastes are occasionally hazardous to health cannot be overemphasized. Hazardous waste can cause and has caused pollution, damage to health and even death. Exposure to multiple chemical combinations in populations living near waste dump sites has led to series of human health disorders. It has been reported that heavy metals, VOCs and anions in dump sites leachates can initiate chromosomal disorder and inhabitants in the locality of landfill sites are disposed to mutagenic effects. The degree of contamination growing from percolation of leachates is established by a number of components that include the physicochemical properties of the leachates and soil and the hydrological condition of the surrounding location [15].

2.3. Wastewater pollution

There are four main treatment steps in the wastewater treatment process. The preliminary treatment removes all large and settleable solids from the wastewater. Secondary treatments use accelerated microbiological growth to remove organic pollutants. The tertiary treatment utilizes a combination of chemical and biological processes to reduce nutrient loading in the wastewater. The quaternary treatment removes particularly difficult emergent pollutants, like pharmaceutical compounds or other complex molecules which was used by different organic and inorganic adsorbents such as silica (MSN.MCM) and ionic liquids(ILs). Analytical testing based on instruments at each step is required to monitor key chemical parameters like the nitrogen compounds, the malondialdehyde, the formaldehyde, the phosphates, and the chlorine [16]. Monitoring silicate, calcium, and magnesium content is imperative as they form scale deposits, leading to higher maintenance costs and downtime which was determined as mg L^{-1} with atomic absorption spectrometry (FAAS, ETAAS). As the primary treatment, the treatment of wastewater by a physical or potentially chemical interaction including settlement of suspended solids, or

other cycle in which the Biological Oxygen Demand (BOD) of the approaching wastewater is decreased by essentially 20% before release, and the total suspended solids content is diminished by basically half. The secondary treatment followed with the post-primary treatment of wastewater by an interaction by and large including biological or other treatment with a secondary settlement or other cycle, bringing about a BOD reduction of basically 70% and the Chemical Oxygen Demand (COD) reduction of essentially 75% [17]. Due to the tertiary treatment of public wastewater, the treatment of nitrogen or potentially phosphorus, and additionally some other poison influencing the nature of a particular utilization of water was evaluated (the microbiological pollution and shading). For organic pollution, the treatment efficiencies that characterize a tertiary treatment are the accompanying: organic pollution reduction of essentially 95% for BOD, 85% for COD, the nitrogen reduction of essentially 70%, the phosphorus reduction of essentially 80% and the microbiological reduction accomplishing a waste coliform thickness of < 1000 of every 100 ml. Moreover, explicit industrial effluents might require extra treatment for explicit determinants that may not be normal in many wastewaters [18,19].

2.4. Environment pollution sources

Pollution is the defilement of the environmental natural surface or underground water (domestic waste water, industrial, nitrates from fertilizer) or soil (with fertilizers, pesticides, radioactive wastes, etc.). Presently, about 82% of lands are polluted by the products of petroleum source (hydrocarbons, solvents etc.) used as an energy foundation in the oil industry, in addition, the chemicals were used in various industries and their wastewaters may be included the different pollutants such as, BTEX, VOCs, mercury, arsenic, nickel and vanadium which was determined by analytical methods [19]. There is a diversity of pollutants influencing water bodies, air, soil and subsoil, such as fuel and oil products, crude oil, hydrocarbon residues, other products resulting from the operation (unsaturated

and saturated aliphatic hydrocarbons, and the polycyclic and monocyclic aromatic). It also stances risks to human health, biological environment and vegetation, aromatic compounds having a strong attribute of carcinogenic and mutagenic and, not slightest, influence the environment security, presenting hazards of fire and explosion, when the floating oil reach the groundwater in the basement of various buildings [20]. Accidental oil pollution has turn out to be a common phenomenon nowadays that can cause environmental and social disasters. Potential causes of direct pollution of soil and subsoil can be enclosed by tanks, separators old from wastewater treatment plants, underground pipelines, slurries, settling basins and waste pits of tar, ramp CF loading and unloading, sewerage networks etc. Solid residues, unstored corresponding, which can contaminate the soil, come from: solid impurities concerned in crude oil, sewage sludge from different wastewater treatment plants, solid waste from cleaning of incinerator ash sludge and the maintenance, powder catalyst. Most oil pollution sources come from anthropogenic sources, but there are also some natural sources that pollute the soil and the water bodies [20]. Dumpsite generally contaminates the immediate environment where they are found and they carry hazardous organisms which affects both the environment and the inhabitants of this environment where they are found on. Dumpsite causes various diseases and it increases air borne diseases as well [21].

2.5. Soil pollution

Soil pollution is the change in the composition of soil properties is different characteristics. It involves the building up of toxic persistent substances, slats, radioactive materials, toxic chemicals and other disease causing agents in the soil which have adverse effects on the soil and probably has an adverse effect on plant growth and animal health. Soil comprises of a solid phase (organic matter and minerals matter) as well as an absorbent phase that grasps gases and water [22]. Soil is the mixture of minerals, organic matter, gases, liquids, and the countless organisms that together support life on

earth [22]. The organic portion, which is obtained from the decayed remnants of plants and animals, is concentrated in the dark topmost topsoil. The inorganic fraction made up of rock fragments, was formed over thousands of years by physical and chemical weathering of bedrock. Productive soils are indispensable for agriculture to furnish the world with adequate food. In a general wisdom, soil pollution definition is the existence of unhealthy chemicals (pollutants or contaminants) in soil in extreme enough concentrations to be of danger to human health and the ecosystem. In additionally, yet when the levels of contaminants in soil are not of peril, soil pollution may take place simply due to the fact that the levels of the contaminants in soil surpass the levels that are naturally present in soil (in the situation of contaminants which occur naturally in soil). Soil pollutants comprise a large variability of contaminants or chemicals (organic and inorganic), which may possibly be both naturally- occurring in soil and man-made. In both cases, the main soil pollution instigates are the human activities which might be leaks and spilling of oil, manufacturing process and dumping of toxic materials and substances in the soil [23]. The heavy metals in soil were determined by the Atomic Absorption Spectrophotometer (AAS, Perkin Elmer 2380) [24]. The Analytical methods for removal VOCs and heavy metals from soil were used by different methodology (Figure 1-3).

2.5.1. In situ soil vapour extraction

Volatile and some semi-volatile organic compounds (VOCs and Semi-VOCs) can be eliminated from unsaturated soils by a cycle known as soil vapor extraction (SVE). SVE as an in situ tidy up measure permits contaminated soil to be remediated without unsettling influence or unearthing [25]. Soil vapor extraction (SVE) is an in situ unsaturated (vadose) zone soil remediation technology in which a vacuum is applied to the soil to induce the controlled progression of air and eliminate volatile and some semi-volatile contaminants from the soil. The gas leaving the soil might be blessed to receive recuperate or obliterate the contaminants.

The disadvantage in the utilization of SVE for remediation of contaminated site is that SVE cannot eliminate heavy oils, metals, PCBs, or dioxins from contaminated soil; it is just powerful for remediation of soil contaminated with VOCs and Semi-VOCs. Since the interaction involves the continuous progression of air through the soil, notwithstanding, it regularly advances the in situ biodegradation of low volatility organic compounds that might be available [26].

2.5.2. Excavation

Excavation (evacuation) is a crucial remediation strategy including the expulsion of debase soil/media, which can be dispatched off-site for treatment and additionally removal, or treated nearby when pollutants are manageable to solid remediation procedures [26]. Bioremediation is one of the most viable options for remediating soil contaminated by organic and inorganic compounds

considered detrimental to environmental health [27].

2.5.3. bioremediation strategy and digestion process (Determination in soil)

Biostimulation of indigenous microbes is a bioremediation strategy mostly used for remediation of contaminated soil. This involves addition of nutrients, either organic or inorganic, to enhance the activities of indigenous microbes [27]. The soil sample was digested with $\text{HNO}_3/\text{H}_2\text{O}_2$ by micro wave accessory. At $200^\circ\text{C}/\text{UV}$ irradiation, the sample digested and organic compound convert to SO_x and NO_x and CO_x and exit as gas from head of microwave tube under hood conditions. The inorganic compounds determined in remained solution by FAAS. Also by headspace microwave, the VOCs extracted by new technique and online determined by GC-FID.

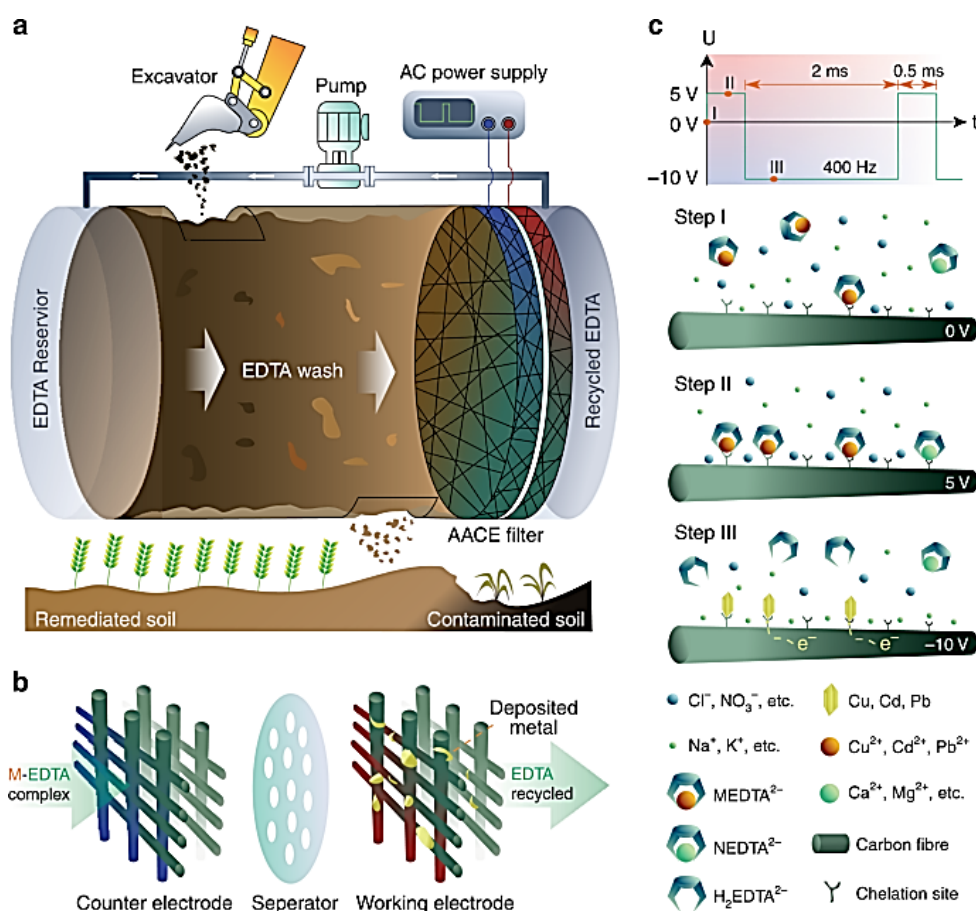


Fig. 1. Remediation of heavy metal contaminated soil by asymmetrical alternating current electrochemistry [28]

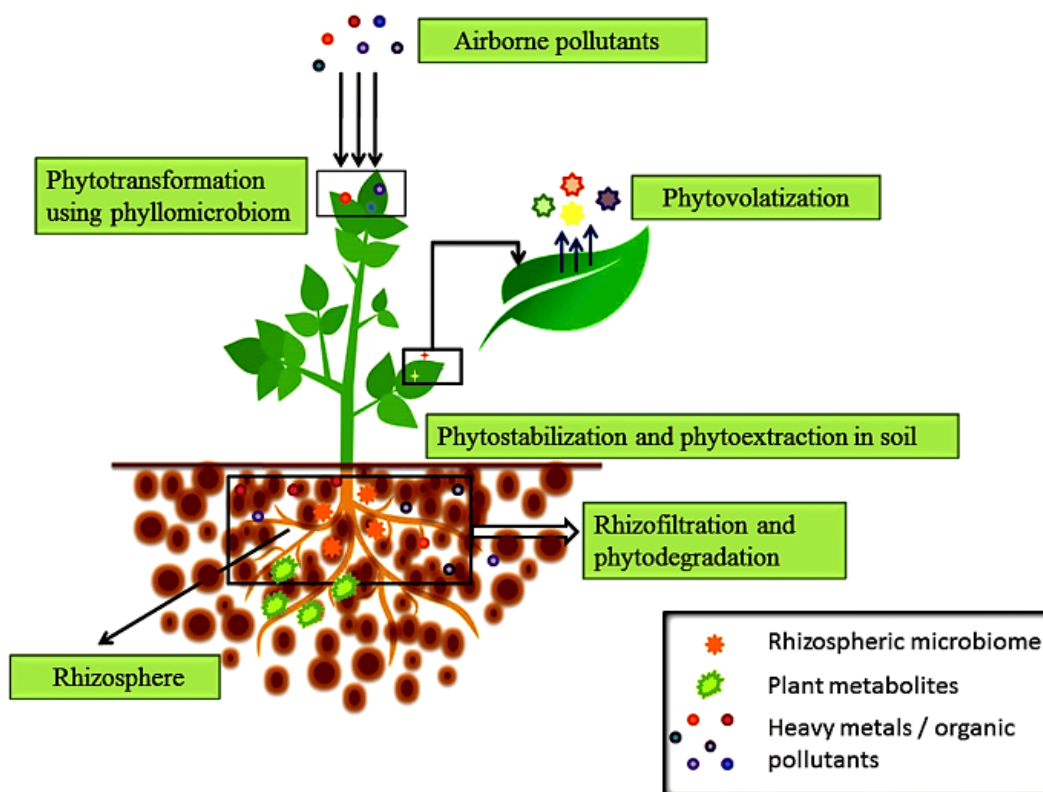


Fig.2. Biological-based methods for the removal of volatile organic compounds (VOCs) and heavy metals



= pressure
(correlates with sample weight)

Fig.3. Microwave digestion methods for determination heavy metals and VOCs in soil

3. Soil Pollutants, Analysis and Health Effect

3.1. Soil pollutant

There are several ways in which soil can be polluted with dumpsite, one of the ways can be through seepage from landfill. When toxic materials are buried under the soil in a portion of land that will be used for agricultural practices, the dump will invariably turn out to be noxious to any crop or plant that is around the vicinity. Before a landfill will be used for agricultural or economical practices, it should be properly treated. After treatment the soil pollutant such as heavy metal and BTEX, VOCs must be determined by analytical methods. Percolation of contaminated water into the soil is another way of polluting the soil which many communities and societies are not aware of it. Moreover, the contaminated water (pollutant) into the soil measured by the different analysis instruments. Also, solid waste seepage is one of the common way of soil pollution, which people neglect without knowing the implication on the soil [28]. The most common chemicals involved in causing soil pollution include solvents from companies, pesticides from manufacturing industries. As HSE role, the pollutants in soil of near chemical industries controlled by chemistry analyzers (AAS, UV-Vis and GC-FID). Soil pollution is instigated by the presence of human-made chemicals or other alteration in the natural soil environment. It is characteristically set off by agricultural chemicals, industrial activity, or improper disposal of waste. The most common chemicals engrossed are petroleum hydrocarbons, polynuclear aromatic hydrocarbons which include benzo (a) pyrene) and naphthalene, lead, pesticides, and other toxic heavy metals. Contamination is concurrent with the amount of industrialization and concentration of chemical usage. The dread over soil contamination stems principally from health risks, from direct interaction with the contaminated soil, depletes from the contaminants, and from optional contamination of water sources within and underlying the soil. Mapping of contaminated soil areas and the resulting cleanup are tedious and costly

errands, requiring expansive measures of geology, hydrology, and chemistry, computer modeling skills, and GIS in Environmental Contamination, alongside an energy about the historical backdrop of industrial chemistry [29]. The effects of dumpsite with regards to agricultural activities include; reduced soil fertility, reduced nitrogen fixation, larger loss of soil and nutrients, deposition of silt in tanks and reservoirs, reduced crop yield, imbalance in soil fauna and flora. The major hinge on the effects of dumpsite encourages the failure of high crop yield and other activities carried out on the soil. Many farmers complain of low yield and the stunted growth of agricultural products without prior knowledge of the effects of regular dumping of garbage and other chemicals on dumpsites located close to their agricultural farm lands [29]. The TLV of heavy metal and VOCs in soil were reported by FDA, EPA and WHO organizations. The levels of heavy metals in the growing soil were highest for Fe, Zn, Pb, and Cu. In the soil samples, the Fe content ranged from 2760.1 to 2833.07 mg per 100 g dry soil, Cu ranged from 15.5 to 20.13 mg per 100 g, Zn ranged from 305.95 to 308.25 mg per 100 g, and Pb ranged from 224.48 to 230.39 mg per 100 g. The more content of heavy metals in soil caused to toxic for human, foods and vegetables [29]. The industrial activity such as chemical factory, paint factory Oil Company caused to dispersed different pollutions such as VOCs and heavy metals (Hg, As, Ni, Co, V, Cd, Al, Mn) from their wastewaters to soils. Chemical and allied industries comprise of basic chemical manufacturing industries like inorganic/organic chemicals, food industries, bulk petrochemicals, pharmaceutical products and their intermediates, polymers and their derivatives, agricultural chemicals, acids, alkali, dyes, paper and pulp, and fertilizers [30]. The chemical industries have significant impact on the environment due to pollution issues. Wastewater from chemical industry contains mainly organic and inorganic pollutants. These pollutants are toxic, mutagenic, carcinogenic, and mostly nonbiodegradable. Complete treatment of effluents generated in the various chemical industry units in effluent treatment plant is essential

and the principles of process intensification (PI) can be used for the effluent treatment. Several physical, chemical, and biological processes have been considered for treatment of wastewater obtained from chemical, biological, food, pharmaceutical, pulp and paper, dye and textile industries. The choice of methods for treatment of wastewater is based on the type, nature, and concentration of contaminants. The treated effluent should be eco-friendly and reusable [30].

3.2. Analytical Method in Soil

For sample preparation of soil, the various analytical procedure was used. As the VOCs analysis, the soil directly analyzed by head space solid phase extraction coupled to gas chromatography spectrometer based on FID or mass detectors. In addition, for heavy metals analysis, the soil samples were oven-dried at 105°C for 10 hours until constant weight was attained and then, the soil samples digested. For soil sample, 1 g was digested in 10 mL of 1:1 HNO₃ and heated to 95°C to dry

and thereafter refluxed for 10 minutes without boiling. After cooling, 5 mL of concentrated HNO₃ was once again added and refluxed for 30 minutes till brown fumes were produced. The process of adding 5 mL of concentrated HNO₃ was repeated over and over till white fumes appeared. The solution was vaporized to about 5 on mantle set at 95°C with a watch glass over it. After cooling the resulting sample, 2 mL of H₂O and 3 mL of 30% H₂O₂ were added and the solution was placed on the heating mantle to start the oxidation of peroxide until effervescence subsided. Finally, the heavy metals determined by the Atomic Absorption Spectrophotometer (AAS, Perkin Elmer 2380) [24]. Due to Table 1, the Various analytical methods for determination pollutants in soil and water samples.

3.3. Effect of Soil Pollutants on Human Health

There are different routes in which soil or land pollution can affect human health either by short term or long term exposure. When consumed some of this harmful chemicals enters the digestive

Table 1. Various analytical methods for determination pollutants in soil and water samples

Sample	Pollutant	Instrument	method	Ref
Water	VOCs	GC-MS	SPE	[3]
Soil	Toxic chemical			
Water	VOCs	GC-MS	Nanotechnology over conventional treatment technologies	[2]
Air	Pesticides	F-AAS	Adsorption	
	Heavy metals	HPLC		
	Phenols			
Water	Trichloroethylene (TCE)	GC-MS	LLME-SPME	[4]
Soil	Heavy metals	F-AAS ET-AAS	SCWEP	[5]
Soil, Water, municipal wastewater	Heavy metals	CE-UV	DLLME SDES	[6]
Water	Heavy metals	AAS/SPME	Adsorption based on (CNMs), (MNPs), (NIPs), (N-MOFs), (SiNPs)	[9]
Soil				
Soil and water	VOCs Malondialdehyde Formaldehyde	HPLC-UV	VALLME-HDES	[16]
Water	Aromatic hydrocarbons	GC-MS	Pretreatment techniques HS-SPME	[24]
Soil				
Air				
Soil	Hydrocarbon	GC-MS	SVE	[25]

LLME-SPME: Liquid-liquid microextraction assisted solid phase microextraction, SCWEP: subcritical water extraction process, DLLME: Dispersive liquid-liquid microextraction, SDES: Solidification of deep eutectic solvent, CNMs: Carbon nanomaterials, MNPs: magnetic nanoparticles, NIPs: Nano-imprinted polymers, N-MOFs: Nano-based metal-organic frameworks, SiNPs: Silica nanoparticles, SPME: Solid phase microextraction, VALLME-HDES: Vortex-assisted liquid-liquid microextraction based on hydrophobic deep eutectic solvent, HS-SPME: Head space solid phase microextraction, SVE: Soil vapor extraction

system, they are absorbed and taken to the liver, these chemical will only be broken down by the liver to certain extent in some cases these chemicals which are not fully absorbed remains in the guts which can be toxic on the gut lining. Direct contact of contaminated soil to the skin can lead to skin damage for example chromium which is a soil pollutant, when this chemical is absorbed by the skin it causes skin irritation [31]. Arsenic (AsIII and AsV); which includes pesticides, coal burning and wood preservative from preservative and agro chemicals etc, which can be consumed through ground water by absorption of the soil content into the water. Intake of this over a long time leads to GIT diseases, cardiovascular dysfunction and liver damage. As Figure 4, Dioxin includes the polychlorinated dibenzodioxins (PCDD) and the polychlorinated dibenzofurans (PCDF) from waste recycling industry and paper industry which

is consumed through contaminated foods such as meat, fish and dairy product which damages to the immune system and also carcinogenic. Also, cadmium (Cd^{2+}) can be gotten from pigments, sewage sludge, water pipes etc. it is mainly consumed by animals but are harmless to animal health, can affect human consuming animal product and cause to MS and cancer. Fluoride as a high level of fluoride consumption in drinking water leads to joint stiffness and pains, it causes calcification of ligaments and tendons and also leads to osteosclerosis. Mercury (Hg) consumed by consumption of contaminated food (Sea Fish as organic mercury $\text{C}_2\text{H}_5\text{-Hg}$ and $\text{CH}_3\text{-Hg}$) or metallic mercury (mercury cell, vapor from petrochemical industries) leads to damage of the central nervous system(CNS), organ damage such as the liver and kidney, it also causes teratology in a fetus and poor brain development [32].

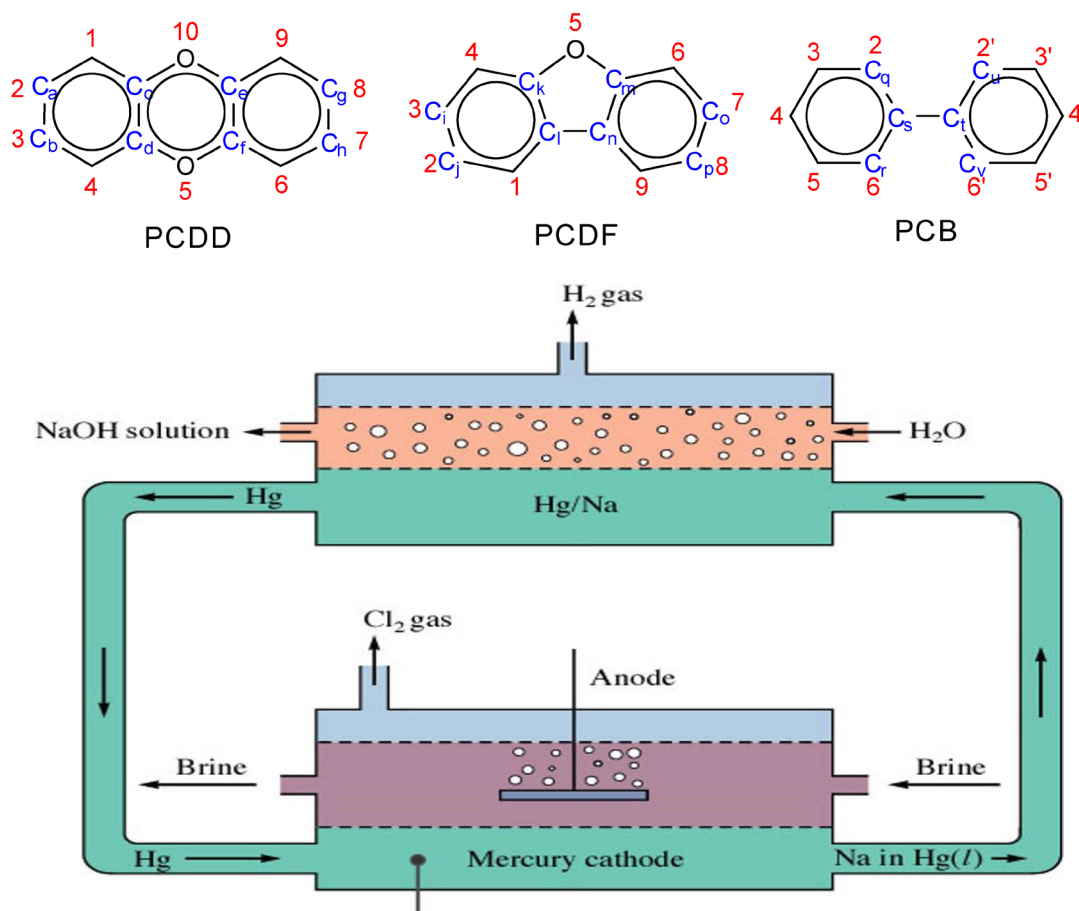


Fig. 4. Mercury cell (production NaOH and Chlorine), dibenzodioxins (PCDD) and polychlorinated dibenzofurans (PCDF) [32]

4. Water Pollutants, Analysis and Health Effect

4.1. Water pollutants

Water contamination is an animated change in the nature of the water, which makes it unbefitting or hazardous as concerns food, agriculture, human and animal health, fishing, and industry or recreation interest. The chemical hazards are the Copper, Manganese, Lead, Cadmium, Phosphate, Nitrate and so on, as the public health concern, the ground water ought to be liberated from physical and chemical hazards. Individuals in and around the dumping site are relying on the ground water for drinking and other homegrown purposes. Other high-hazard bunch incorporates population living near a waste dump and those, whose water supply has gotten polluted either because of waste dumping or leakage from landfill sites expands danger of injury, and disease [33] Water is one of the determinants of human earth framework. Diseases may jump up through water contamination, particularly groundwater tainting, and quickly spread past human desire as a result of its stream instrument. One of the main considerations that make the earth tenable for humans is the presence of water. Framing the significant segment of plant and animal cells, it is the premise of life and thusly the advancement of water assets is a significant segment in the coordinated improvement of any territory [33]. Most water pollution does not continuously begin in the water itself. Practically every human activity has a consequence on the quality of the water environment. Dumpsites that are seen in water ways and places that are close to water bodies run off to the water bodies

during rainfall and assimilation to the soil which eventually find it way to the water bodies. The causes of water pollution nevertheless, relatively surprisingly sometimes include: Sewage from household and from close industries that channel their sewage directly or indirectly to the water bodies, nutrients for agricultural farms that are dumped close to water bodies are also an avenue for water contamination and pollution, Heavy metals, the xenobiotic compounds in wastewater, Land or air pollution are also part of the notifiable avenue for water contamination. [34]. The amount of debris in some waste sites as seen in Owerri in groups (Table 2).

4.2. Analytical method in Water

For determination of heavy metals in water sample preparation was used. First, 2 mL of concentrated HNO₃ and 5 mL of concentrated HCl to a 100 mL aliquot of collected water sample. The solution was covered with a watch glass and heated at 95°C till volume reduced to 15 mL before being allowed to cool. Thereafter, the final volume was adjusted to 100 mL with reagent water and replicates were processed on a routine basis to determine precision. The concentrations of Cu, Zn, Fe, and Pb in the filtrate of water were estimated using the AAS. For determination VOCs any reagents have not added to water samples. The metal concentration in the water decreases in the following sequential order: As > Pb > Zn > Cu = Al = Cr > Cd = Hg. Also, in the sediment, the sequential order is as follows: Cr > Zn > Cu > Pb > As > Cd > Hg [35]. For evaluation of surface and groundwater on land and coastal sea waters, we usually selected the heavy metals (Cd,

Table 2. The amount of debris in some waste sites as seen in Owerri in groups

Material	Highly seen	Moderately seen	Not seen
Plastics	√		
Rubber	√		
Cloth		√	
Glass/ceramics		√	
Paper/cardboard	√		
Metal	√		
Wood		√	
Other		√	

Hg, Pb) as priority hazardous substances, and then, the heavy metals (Cu, Zn, As, Cr) were chosen as specific pollutants. Aluminum was chosen as toxic to a wide range of aquatic ecosystems [36]. Due to the Hazardous Substances in Water, the chemical and ecological status were determination with environmental quality standards(EQS) for priority hazardous substances (PHS) and specific pollutants (SP). According to EQS, the values of metals in the surface waters for cadmium, mercury, copper, chromium, zinc were obtained 0.04, 0.0025, 1.0, 1.2, zinc $\mu\text{g L}^{-1}$, respectively [35]. Nsibande et al used fluorescence detection of pesticides based on quantum dot (CQDs) in water samples [37]. Cao et al reported Metal-organic framework (MOF) for extraction insecticides in water samples by dispersive solid phase extraction (DSPE) [38]. Selahle and Kachangoon used magnetic solid phase extraction (MSPE) based on porphyrin organic polymer and hydrophobic deep eutectic solvent(HDES) based DLLME for determining of insecticide in water [39, 40]. Bessonova and Ykowska reported the role of ionic liquids for determination of pesticides and VOCs in waters by DLLME [41, 42]. Also, the determination pesticide, heavy metals and VOCs in waters followed by DLLME –GC-MS and HPLC-MS/MS [43,44]. Moreover, the analytical methods for determination heavy metals and other pollutants in waters followed by zeolitic imidazolate framework (ZIF-7) based on MSPE and the biosensors in waters [45-48]. Recently. The researchers used SPE, MSPE, LLME, LLE, Liquid-phase membrane extraction (LPME) for metal, pesticides, carboxylic acids, phenol in water matrixes [49-52]. Also many metals and VOCs were determined by different ionic liquids and adsorbents (Table 3 and 4). Cloud point extraction (CPE) has been utilized for the preconcentration of cobalt, mercury and nickel, after the arrangement of a complex with 1-(2-thiazolylazo)-2-naphthol (TAN), and later examination by flame atomic absorption spectrometry utilizing octylphenoxypolyethoxyethanol (Triton X-114) as surfactant. The chemical factors influencing the detachment stage and the viscosity influencing the detection cycle were enhanced. Under the ideal

conditions, preconcentration of just 50 ml of sample within the sight of 0.05% Triton X-114 permitted the detection [53]. The current work depicts a straightforward, dependable analytical strategy that satisfies the assurance of benzene and toluene, in environmental water samples. The technique depended on the cleanse of BTEX (a gathering of unstable natural mixtures (VOCs)) from water samples to a particular volume of acetonitrile preceding making the analysis by superior liquid chromatography outfitted with a photo diode array detector. The created method was upgraded utilizing full factorial design, and the subsequent ideal boundaries were applied in the examinations of approval which affirm method dependability; recuperation was somewhere in the range of 94 and 106% with a maximum relative inclination of 5.9%, relative standard deviation was under 7.7% ($n = 10$), and cut off of detection varied from 0.18 to 0.6 $\mu\text{g L}^{-1}$ [53].

4.3. Effect of Water Pollutants on Human Health

Since water have a wide range of usage all over the world, the contaminated water makes gives ill damages and causes serious health damage. Poor or developing countries or communities are at risk because their homes are often close to polluting industries. Water borne pathogens are present in the water due to fecal contamination and consumption of untreated water. This lead to bacteria diseases, pollutant, viral diseases and parasitic diseases which was explain as below text.

Bacteria: such as typhoid which is caused by *Salmonella typhimurium* bacteria, which mostly infects the lining of the gastrointestinal tract leading to constipation or diarrhea including high fever it also affects organs such as the liver and spleen. Cholera caused by *vibrio cholerae* , and Dysentary caused by *shigella*, *campylobacter*, *E. coli* and salmonella bacteria species which leads to intestinal infection causing dehydration, excessive expulsion of water, blood and nutrient through vomiting and excretion , this leads to body weakness and stomach pains [75].

Table 3. Determination of heavy metal pollutants in water samples using ionic liquids or adsorbent

Metal	Sample	preparation method	Analysis	ILs	Volume (mL)	Heavy metal interferences	Recovery (%)	Ref.
Co ²⁺	Tap and lake Water	ISFME	FAAS	[HMIM][BF ₄] and NaPF ₆	5.0	Mn ²⁺ , Cd ²⁺ , Ni ²⁺ , Zn ²⁺	97.8	[54]
As ³⁺	Industrial wastewater	LLME	LC-MS	[HMIM][PF ₆]	20	Cu ²⁺ , Zn ²⁺ , Cd ²⁺	More than 95%	[55]
Co ²⁺	Mineral, tap, and river water	DLLME	F-AAS	[HMIM][PF ₆] with [HMIM][Tf ₂]	10	Ni ²⁺ , Mn ²⁺ , Cu ²⁺ , Zn ²⁺ , Cd ²⁺ , Fe ³⁺ , Al ³⁺ , Rh ²⁺ ,	100.3	[56]
Cd ²⁺	Lake and waste water	DLLME	F-AAS	[BMIM][PF ₆] with PAN	15	Fe ³⁺ , Zn ²⁺ , Pb ²⁺ , Na ⁺ , K ⁺ , Ca ²⁺ and	99.3	[57]
Cu ²⁺	River and lake water	IL-UADLLME-SAP	LC	Cyphos IL	15	Mn ²⁺ , Zn ²⁺ , Cd ²⁺ , Sn ²⁺ , Pb ²⁺ ,	99.5	[58]
Ni ²⁺	Tap and mineral water	DLLME	UV-Vis	[HMIM][Tf ₂ N] and PAN	10	Pb ²⁺ , Cr ³⁺ , Al ³⁺ , Sb ³⁺ , Cu ²⁺ , Cd ²⁺ ,	98.0	[59]
Cr ³⁺	Mineral, sea, and river water	LLME	F-AAS	[BMIM][BF ₄] and DPC	10	Zn ²⁺ , Co ²⁺ , Cu ²⁺ , Ni ²⁺ , Cd ²⁺ , Bi ³⁺ ,	98.4	[60]
Pb ²⁺	Ground and surface water	UA-ILDME	F-AAS	[BMIM][PF ₆] with Dithizone	10	Co ²⁺ , Ni ²⁺ , Zn ²⁺ , and Cd ²⁺	98.3	[61]
Cd ²⁺	river, and well water	UA-MR- IL-DLLME	F-AAS	[BMIM][PF ₆] and APDC	10	Mn ²⁺ , Cu ²⁺ , Zn ²⁺	99.4	[62]
Cd ²⁺	Water	SFM-μ-SPE	AT-FAAS	CNTs@DHSP	20	Ni ²⁺ , Mn ²⁺ , Cu ²⁺ , Zn ²⁺ , Al ³⁺ , Hg ²⁺	98.0	[63]
Se ⁴⁺	Water	SPE	F-AAS	Dried activated sludge (DAS)	100	Ni ²⁺ , Co ²⁺ , Cu ²⁺ , Zn ²⁺ , Hg ²⁺ , Mn ²⁺	96.0	[64]
Ni ²⁺	Water	USA-D-μ-SPE	ET-AAS	(BDC) ₂ (DABCO) (MOF)	25	Ag ⁺ , Cu ²⁺ , Mg ²⁺ , Co ²⁺ , Pb ²⁺ , Zn ²⁺	98.8%	[65]

IL-HLLME: Ionic liquid for homogeneous liquid-liquid microextraction

LLME: Liquid-liquid microextraction

DLLME: Dispersive liquid-liquid microextraction

IL-UADLLME-SAP: Ionic liquid - Ionic liquid ultrasound-assisted dispersive liquid-liquid microextraction based on solidification of the aqueous phase

UA-MR- IL-DLLME: Ultrasound-assisted magnetic retrieval-linked ionic liquid dispersive liquid-liquid microextraction

SFM-μ-SPE: Syringe filter membrane- micro solid-phase extraction

Pollutant: The diseases of air pollution include the ischemic heart disease(IHD), the respiratory infections(RI), the chronic obstructive pulmonary disease (COPD), cancer. Heavy metals such as Hg, V, Ni, Co and Pb created autoimmune diseases in human. The autoimmune disease may indicate

the production of autoantibodies, infiltration of destructive inflammatory cells into different target organs. The most of autoimmune diseases is due to extra concentration heavy metals in the environment which is produced by industrial pollutants. Also, the volatile organic compounds (VOCs) are entered

Table 4. Determination of VOCs pollutants in water samples using ionic liquids or adsorbent

VOCs	Sample	preparation method	Analysis	ILs	Volume (mL)	LOD($\mu\text{g/L}$)	Recovery (%)	Ref.
Benzene	PTI	LTTMs	GC-FID	Sulfolane IL	-----	-----	98.25	[66]
DDD	Rain water	DLLME	HPLC	[BMIM][PF ₆] and [HMIM][PF ₆]	5.0	0.35	96.3	[67]
Estradiol benzoate (EB)	River water	DLLME	HPLC	BMIM][BF ₄] and [NH ₄][PF ₆]	160	0.045	105.1	[68]
Phenol	Water	LE	Color reaction	[BMIM][Tf ₂ N] [HMIM][Tf ₂ N]	10	-----	99.9	[69]
BTEX	Water	CPBDDE	Voltammetry	Carbon Nanoadsorbent	10	3.0×10^{-7} mol L ⁻¹	98.9-99.4	[70]
Ethanol, Heptane	Water	Solvent extraction	GC	Nanostructure	-----	0.023	95.4-102%	[71]
Xylene	Water	Solid liquid separation	GC	MOF/ zeolites	15	-----	95%	[72]
Benzene	Water	D – μ -SPE	SHS-GC-MS	CNTs@PhSA	-----	-----	96.8-102	[73]
Benzene Toluene	Water	SPE	HS-GC	CuONPs	-----	-----	98.7%	[74]

CPBDDE: Cathodically pretreated boron-doped diamond electrode

LTTMs: Low transition temperature mixtures

PTI: Petrochemical industry

from environment to the human body and caused to cancer. VOCs as hazardous chemicals can cause to irritation, headaches, fatigue, nausea and dizziness problems. High concentrations of VOCs cause lungs cancer and damage the liver, kidney and CNS. Viral: such as viral hepatitis A caused by hepatitis A virus which infects the liver leading to jaundice in some part of the body especially the sclera, loss of appetite, fatigue and high fever. Poliomyelitis caused by poliomyelitis virus leading to sore throat, fever and paralysis of the limbs. Gastro enteric diseases caused by rotavirus, adenovirus and other viruses that are found in water contaminants.

Parasitic: which includes tapeworm intestinal infestation, pinworms and round worms (*Ascaris lumbricoids*) the eggs of this parasitic worms are harmful to the human health, when their eggs consumed through contaminated water or

ingested through contaminated food infects the gastrointestinal system, digested eggs produces live parasitic worms inside the body system, these worms begin to compete for nutrient causing abdominal pains and discomforts, retarded growth and body weakness [76].

5. Air Pollutants, Analysis and Health Effect

5.1. Air pollutants

Air contaminant or poison is a waste matter that pollutes the air. Any material or chemical waste product, which adjudicates the air and other natural reserves harmful or generally impracticable. There are several factor that promote the severity of air pollution, they include its persistence, chemical nature and the concentration. Solid waste makes a few noxious gases, for example, Hg^o, VOCs,

BTEX, H₂S, suspended Sulfur Dioxide (SO₂), oxides of Nitrogen (NO_x), Carbon Monoxide (CO), Respirable Suspended Particulate Matter (RSPM) and Suspended Particulate Matter (SPM). The residue delivered from different sources can create a gathering of sicknesses going from a straightforward cold to hazardous illnesses like cancer [77].

5.2. Analytical Methods in Air

Benzene, Toluene, Ethylbenzene and Xylenes isomers (BTEX) are a group of highly volatile gaseous pollutants frequently found in indoor and outdoor air. It is known from the literature that these compounds have a negative impact on the environment since they contribute to the formation of ozone and other photochemical oxidants. Moreover, BTEX are either known for being, or suspected to be, irritants, neurotoxins, allergens or carcinogens and their exposure on a long term basis presents a serious threat to the human health. Therefore, implementing effective strategies for pollution control is of paramount importance to limit human exposure and prevent the environment degradation [78]. These days, various techniques dependent on physicochemical or biological cycles have been produced for gaseous pollutant's expulsion like thermal, plasma, synergist or photocatalytic oxidation, condensation, membrane division, biological degradation, absorption and adsorption. Notwithstanding, the pollutant fixation in indoor air or mechanical conditions is generally low, running from sub ppb level to 100 of ppm. It is qualified to make reference to that not all evacuation techniques can be successful at such low focus ranges. Moreover, a portion of these methods are costly or require normal upkeep restricting their utilization at homegrown scale. Among them, adsorption has been shown to be a method that displays a decent trade off among cost and proficiency for BTEX evacuation at low fixations [78]. Since BTEX focuses are typically exceptionally low, the combination of preconcentration gadgets is for the most part expected to expand the affectability of these

methods. Along these lines, in the referenced pre fixation unit, an adsorbent is utilized to trap pollutant particles and concentrate the example that is destined to be, thusly, dissected by ordinary gas chromatography. The adsorbent prerequisites in pollutant evacuation just as gas investigation incorporate a negligible leap forward, huge adsorption limit, thermal solidness and selectivity to the designated pollutants. Furthermore, the desorption temperature ought to be moderate to empower a powerful, modest and quick adsorbent recovery [79]. Carbon monoxide (CO) has a characteristic infrared absorption near 4.6 μ m. The absorption of infrared radiation by the carbon monoxide molecule can therefore be used to measure the concentration of carbon monoxide in the presence of other gases. The Non-dispersive infrared photometry method [NDIR] is based on this principle. Most commercially available NDIR analyzers incorporate a gas filter to minimize interferences from other gases. They operate at atmospheric pressure, and the most sensitive analyzers are able to detect minimum carbon monoxide concentrations of about 0.05 mg m⁻³ (0.044 ppm). Interferences from carbon dioxide and water vapour can be dealt with so as not to affect the data quality. Also, the another sensitive method for measuring low background levels of carbon monoxide (CO) is gas chromatography. This technique is an automated, semi-continuous method in which carbon monoxide is separated from water, carbon dioxide and hydrocarbons other than methane by a stripper column. Carbon monoxide and methane are then separated on an analytical column, and the carbon monoxide is passed through a catalytic reduction tube, where it is converted to methane. The carbon monoxide (converted to methane) passes through a flame ionization detector, and the resulting signal is proportional to the concentration of carbon monoxide in the air. This method has been used throughout the world. It has no known interferences and can be used to measure levels from 0.03 to 50 mgm⁻³ (0.026 to 43.7 ppm). Nitrogen oxides are one of the primary pollutants

just as the evaluation standards of the air quality. Nitrogen oxides (NO) in the atmosphere adversely affect people principally through the respiratory system, which might cause intense and constant health issues. In this manner, the investigation of examination and detection methods for nitrogen oxides will be critical. There are numerous methods for the determination of nitrogen oxides like ion chromatography, chemiluminescence, fluorescence, and colorimetric micro determination. Among these methods, the fluorescence strategy has attracted a lot of consideration and been applied generally for the location of nitrite for the high sensitivity, selectivity, low limit of recognition and straightforward activity. As per the writing, NO_2 —natural colors and NO_2 - KBrO_3 —natural colors are the fundamental frameworks for the assurance of nitrite by the fluorescence spectrometry. Methods for deciding degrees of sulfur dioxide (SO_2) in the air incorporate ion chromatography, titration, calorimetry, mass spectrometry, conductimetry, amperometric detection, flame photometric detection, and turbidimetry. Ion chromatography is by all accounts the most sensitive of these methods with a detection cutoff of 3 μg per sample for sulfur dioxide. Sulfur dioxide has additionally been estimated in stack gases. Methods for estimating sulfur dioxide in stack gases incorporate beat fluorescence detection and titration. Sulfur dioxide isn't found in water since it is decreased to sulfuric corrosive in water. Colorimetry, titration, and either corrosive distillation (AD) or soluble base extraction (AE) ion exclusion chromatography (IEC) with electrochemical detection (ED) can be utilized to gauge sulfur dioxide in food and beer. The analytical methods in air was shown in (Table 5.)

5.3. Ways of Air pollution

Dumpsite emit poisonous gases which enter the air and become detrimental to man and the environment at large. These surface fires emanate particulate matter, which include black carbon or dust, popularly refers to as smut, which is a short-term climate pollutant with global warming prospective. While drenching such fires is comparatively easy, subsurface fires are not. This happens when biodegradable waste decomposes anaerobically and produces landfill gases. The major constituent of landfill gas— methane — catches fire when it comes in acquaintance with air. Chemical factories, oil company, petrochemical Company and industrial chemical activities caused to relapsed VOCs, BTEX, the metallic and inorganic mercury, H_2S in air [79].

5.4. Effect of Air Pollution on Human Health

Air pollution is determined by presence of particles in the air which are known as pollutants and are presents in large quantities for long periods of time. Such pollutants include particles hydrocarbons, carbon monoxide, carbon(IV) oxide, lead nitrogen oxide(NO) and sulfur oxide. This pollutant when inhaled into the body system either due to long term or short term effect causes serious health implications such as respiratory disorders, cardiovascular dysfunction, neurogenic instability such as and pathological diseases [80].

Carbon Monoxide: When there is exposure to this gas it leads to tiredness, dizziness, headaches, nausea, confusion, and impaired vision. Long term exposures can lead to brain damage, heart dysfunction, breathing difficulties and muscle weakness. When inhaled it combines with

Table 5. The analytical methods in air

Air pollutant	Type	Ref
SO_2	Cu–Ce catalysts supported on activated carbon	[2,88]
Dust, H_2S	Fluorinated MOF	[83-85]
O_3 , Oxidant	Adsorbent	[20, 79]
Hydrocarbons	Metamodel to a spatially-distributed housing stock	[79]
NO , NO_2	2D Hybrid Nanomaterials	[82,78]
CO	Gas sensors	[81]
CO_2	Gas sensors	[81]

hemoglobin in the blood by displacing oxygen and forming carboxyhemoglobin which causes the cell and organs to become hypoxic (lacking of oxygen). The brain and heart consumes large amount of oxygen but due to the toxicity of carbon monoxide the brain and heart cells will lack adequate oxygen for proper functioning [81].

Nitrogen Oxide: Nitrogen oxide are pollutants that mainly affects the respiratory system and causing respiratory metaplasia, short term exposure to this can increase a person chance of respiratory infections and asthma. Long term exposures can lead to chronic lung diseases. When inhales the respiratory airways response effectively leading to allergic reaction causing increase in airway neutrophilia and bronchial hyper responsiveness, it reduces the antioxidant effects of tissues, it replaces type I alveolar epithelial cells and ciliated epithelial cells with more oxidant resistant type II and non-ciliated cells [82].

Sulfur Dioxide: High concentrations of sulfur dioxide causes skin irritation, irritation of mucus membranes of the eyes, nose, lungs etc. it reduces the function of the lungs it makes breathing difficult, people living with asthma and children are sensitive to this [83]. Also, the exposure of NO_2 and SO_2 cause to many diseases such as the respiratory system, skin irritation and irritation of mucus [83-85].

6. Urban Effects for Pollutants

Urban effects of dumpsite have been monitored in developed cities while in some area, the effects of this dumpsite are still overlooked which in turn leads to clogging of drains, Inundation of areas, public health problems, pollution of drinking water sources, foul smell and release of gases, ecological imbalance, release of pollutant gases, release of radioactive rays causing health problems, increased salinity, reduced vegetation and other effects. Pollution runs off into rivers and executes the fish, plants and other aquatic life, crops and grain developed on dirtied soil

may give the contaminations to the customers, contaminated soil may presently don't develop crops and grub, soil structure is harmed (clay ionic structure impaired), consumption of establishments and pipelines, debilitates soil solidness, may deliver fumes and hydrocarbon into structures and basements, may make poisonous tidies, may poison children playing in the region [86].

7. Remediation of Pollution

7.1. Incineration

Incineration is a waste treatment measure that includes the burning of organic substances encased in waste materials. Incineration and other high-temperature waste treatment frameworks are depicted as "thermal treatment". Incineration of waste materials changes over the waste into ash, flue gas, and heat. The ash is generally formed by the inorganic constituents of the waste, and may appear as strong bumps or particulates conveyed by the flue gas. The flue gases must be destroyed of gaseous and particulate contaminations before they are scattered into the environment. In certain conditions, the heat created by incineration can be utilized to deliver electric force. Incineration with energy repositioning is one of a few waste-to-energy (WtE) advances such as pyrolysis, anaerobic digestion and gasification [87]. In certain nations, incinerators manufactured only a couple many years prior frequently did exclude a materials detachment to eliminate dangerous, cumbersome or recyclable materials before burning. This implies that while incineration doesn't totally supplant landfilling, it altogether diminishes the vital volume for removal. Dump trucks frequently diminish the volume of waste in an underlying compressor before conveyance to the incinerator. Then again, at landfills, the volume of the uncompressed trash bin be decreased by around 70% by utilizing a stationary steel compressor, yet with a huge energy cost. In numerous nations, more straightforward waste compaction is a typical practice for compaction at landfills.

Incineration has especially solid advantages for the treatment of certain waste sorts in specialty areas such as clinical wastes and certain perilous wastes where microbes and poisons can be devastated by high temperatures. Denmark and Sweden have been pioneers in utilizing the energy created from incineration for more than a century, in restricted joined heat and force offices supporting region heating plans [88].

7.2. Recycling

Recycling is viewed as a helpful recuperation practice which alludes to the assembly and reuse of waste materials which incorporate beverage holders, water compartment and so forth. The materials from which the things are made can be measure again into new items. Material for recycling may be gathered autonomously from general waste utilizing assortment vehicles and devoted receptacles. In specific spots and networks, the maker of the waste is required to isolate the materials into various receptacles which may be paper canister, plastics container, metals container and so on, prior to its assortment [89]. While I a few spots and networks, every recyclable substance and materials are unloaded in a solitary assortment canister and are sorted later by focal office. The most extreme famous customer items reused comprise of steel from food and aerosol cans, copper such as wire, old steel furnishings or equipment, aluminum such as beverage cans, polyethylene and PET bottles, newspapers, glass bottles and jars, paperboard cartons, light paper and magazines and corrugated fiberboard boxes. The recycling of unpredictable and complex materials such as computers and electronic equipment is more testing, because of the additional destroying and division required [90]. The category of material acknowledged for recycling varies by city and nation. Every city and nation has different recycling programs set up that can deal with the countless sorts of recyclable materials. In any case, exact variety in gathering is reproduced in the resale estimation of the material whenever it is reprocessed [91].

7.3. Resource recovery

Resource recovery is the methodical digression of waste, which was envisioned for disposal, for a precise next use. It is the handling of recyclables to achieve or recover materials and resources, or transform to energy. These actions are accomplished at a resource retrieval facility where the machines or equipment for recovery are readily available. Resource retrieval mechanism is not only environmentally imperative, but it is correspondingly cost effective. It reduces the amount of waste products for disposal, it also saves space in landfills mechanism and preserves natural resources. This method of waste management can be used in developing countries in order to generate and maintain their economy. As an example of how resource recycling can be beneficial, many of the items thrown away contain precious metals which can be recycled to create a profit, such as the components in circuit boards [91].

7.4. Avoidance and reduction methods

This method includes finding possible ways to minimize the generation of waste which will eventually be dumped at the dumpsites. The reduction on the use of plastic, rubber, nylon and polythene will go a long way in waste reduction. An imperative method of waste dump management is the preclusion of waste material being fashioned, also known as waste reduction [53]. Approaches that can be followed to avoid these waste include the reuse of second-hand materials and products, fixing and maintaining of broken items instead of purchasing new ones, trying to produce material sand products that re reusable or refillable for instance cotton instead of plastic shopping bags), aiding consumers to always use products that are reusable and not always disposable such as cutlery etc [92].

7.5. Bioremediation Technology

The bioremediation is seen as the usage of living microorganisms to lower the environmental

pollutants and chemicals into less contaminated and poisonous forms (Fig.5). It makes use of naturally stirring bacteria, fungi or plants to decontaminate substances hazardous to human health and the environment in general. It is also seen as the use of biological systems to reduce the concentrations of crude oil wastes from contaminated soil [93]. Bioremediation approach can be as unpretentious as applying a garden fertilizer to an oil-contaminated soil, or as multifaceted as an engineered treatment “cell” where soils or other media are manipulated, aerated, heated, or treated with various chemical compounds to promote degradation [93].

7.6. Chemical adsorption Process

An adsorbent is an insoluble material covered by liquid on the surface, including vessels and pores. A material is supposed to be adsorbent when it has the ability to contain an unmistakable measure of liquid in little chambers like a wipe. Adsorbents assume an indispensable part in chemical absorption, which happens when a specific substance is caught on a material’s surface. Adsorbents that are equipped for adsorbing carbon dioxide incorporate carbon materials (like initiated carbon and carbon filaments), silica gel, actuated alumina, zeolites

(like 5A and 13), mesoporous silicas (like SBA and MCM), metal-natural frameworks, metal oxides (like calcium oxide and magnesia), particle trade resins, and layered twofold hydroxides, (for example, hydrotalcites). Be that as it may, the adsorbents including physisorption show immaterial adsorption limit with respect to carbon dioxide at high temperatures. The adsorption limit and selectivity are determinants of adsorbent separating the CCS measures [94]. Graphene is a carbon-based nanomaterial with a two-dimensional design, high explicit surface region and great substance strength. It is accessible in different structures, for example, perfect graphene, graphene oxide and decreased graphene oxide. Graphene might be oxidized to add hydrophilic gatherings for heavy metal expulsion. adsorbed chromium onto the outer layer of graphene oxide and the most extreme adsorption limit found was around 92.65 mg/g at an ideal pH of 5. This adsorption of chromium on graphene oxide was observed to be endothermic and unconstrained [95]. The graphene, MWCNTs and nanoparticles of metals such as AgNPs were used for adsorption pollutants from air and water samples by chemical or physical adsorption of adsorbents with high surface area. Ashori et al showed that a novel nanosorbent based on IL@

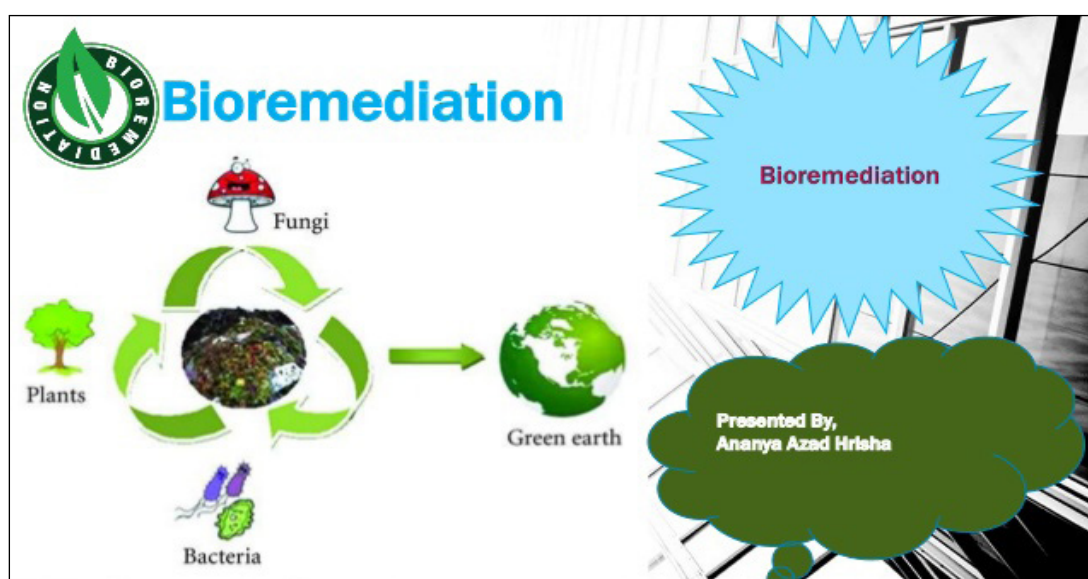


Fig. 5. Bioremediation Technology [92]

MWCNTs for benzene removal from air (Fig. 6a and 6b). Osanloo et al used the AgNPs for removal mercury from air [96]. Shirkhanloo et al used the silver nanoparticles on glassy balls for removal mercury vapor from air [96]. Khaligh et al reported the carboxyl-functionalized nanoporous graphene (NG-COOH) as adsorbent for extraction and speciation of inorganic and organic mercury (Hg (II) and R-Hg ; CH_3Hg^+ / $\text{C}_2\text{H}_5\text{Hg}^+$) in water samples by the US-D-IL- μ -SPE procedure [97]. Mousavi et al showed an amine-functionalized mesoporous silica UVM-7 can be extracted the manganese (II, VII) ions from water samples by the US-D- μ -SPE procedure which

was determined by the AT-FAAS [98]. Rashidi et al used the hybrid nanoadsorbent which was prepared by depositing graphene on the zeolite clinoptilolite by chemical vapor deposition for adsorption of lead(II) and cadmium(II) in water samples by the USA-DMSPE procedure [99]. Rakhatsah et al reported the styrene adsorption in water samples based on task-specific ionic liquid immobilized on multi-walled carbon nanotubes (MWCNTs@[Hemim][BF₄]) which was determined by USA-DCC- μ -SPE procedure coupled to GC-FID. The styrene affected on human body and caused cancer, problem in CNS and liver [100].

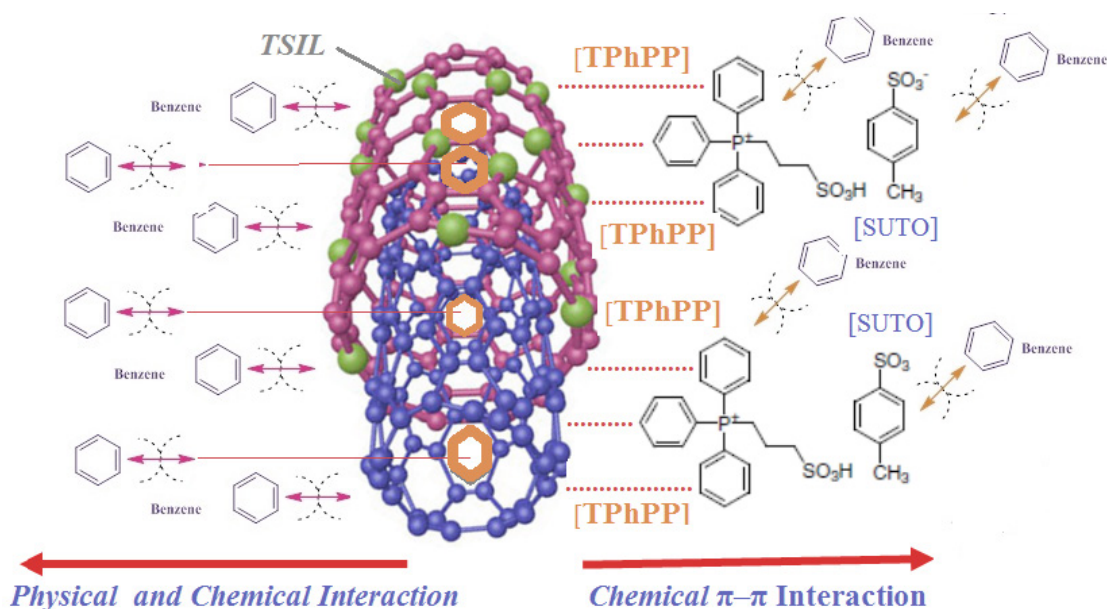


Fig.6a. Adsorption benzene from air by task-specific ionic liquid coated on MWCNTs [101]

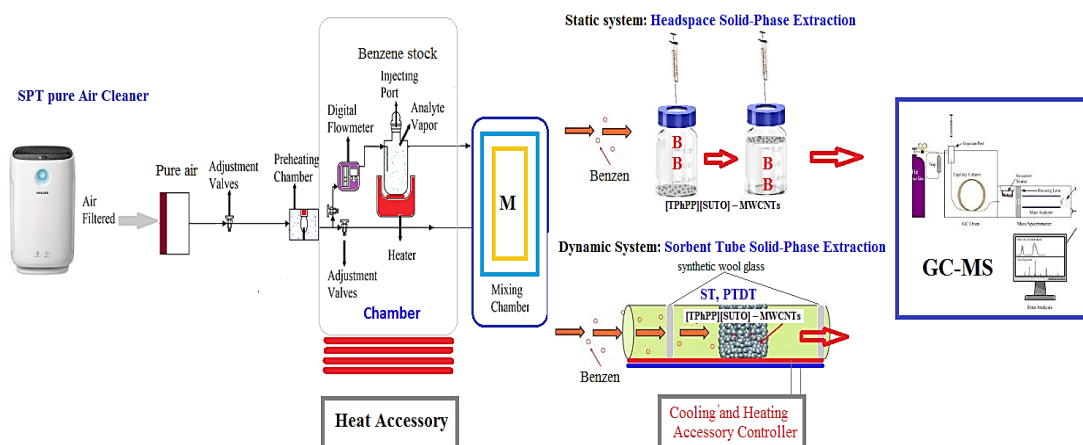


Fig.6b. Mechanism of adsorption benzene from air by task-specific ionic liquid coated on MWCNTs [101]

8. Conclusions

Pollution caused by chemical industries and dumpsite is the most prevalent problem in the environment especially when it comes to soil pollution caused by manmade pollution. The release of waste materials into the environment is receiving worldwide attention. The effect of dumpsite pollution on soil properties was investigated by reviewing studies done in Owerri in Nigeria. The various analytical methods were used for water, soil and air analysis. The pollutant can be removed from environment by different techniques such as Bioremediation, Biodegradation, adsorption, oxidation and reduction.

9. Acknowledgements

The authors wish to thank the Chemistry Department, Imo State University Owerri, Imo State Nigeria; Chemistry Department, Chukwuemeka odimegwu Ojukwu University Uli, Anambra Nigeria and Medicine Department, Gregory University, Uturu Abia State, Nigeria.

10. References

- [1] K. T. Semple, B. J. Reid, T. R. Fermor, Impact of composting strategies on the treatment of soils contaminated with organic pollutants, *Environ. Pollut.*, 112 (2011) 269-283.
- [2] R.K. Ibrahim, M. Hayyan, M.A. Al-saadi, A. Hayyan, S. Ibrahim, Environmental application of nanotechnology; air, soil, and water, *Environ. Sci. Pollut.*, 23 (2016) 13754–13788.
- [3] A. Andrade-Eiroa, M. Canle, V. Leroy-Cancellieri, V. Cerdà, Solid-phase extraction of organic compounds: A critical review (Part I), *TrAC- Trends Anal. Chem.*, 80 (2016) 641–654.
- [4] M. Zhang, P. de B. Harrington, Determination of Trichloroethylene in Water by Liquid–Liquid Microextraction Assisted Solid Phase Microextraction, *Chromatogr.*, 2 (2015) 66–78.
- [5] M.N. Islam, H.Y. Jung, J.H. Park, Subcritical water treatment of explosive and heavy metals co-contaminated soil: Removal of the explosive, and immobilization and risk assessment of heavy metals, *J. Environ. Manag.*, 163 (2015) 262–269.
- [6] M.H. Habibollahi, K. Karimyan, H. Arfaenia, N. Mirzaei, Y. Safari, R. Akramipour, H. Sharafi, N. Fattahi, Extraction and determination of heavy metals in soil and vegetables irrigated with treated municipal wastewater using new mode of dispersive liquid–liquid microextraction based on the solidified deep eutectic solvent followed by GF-AAS, *J. Sci. Food Agric.*, 99 (2019) 656–665.
- [7] F. Giani, R. Mastro, M.A. Trovato, P. Malandrino, M. Russo, G. Pellegriti, P. Vigneri, R. Vigneri, Heavy metals in the environment and thyroid cancer, *Cancers*, 13 (2021) 4052.
- [8] S. Dugheri, A review of micro-solid-phase extraction techniques and devices applied in sample pretreatment coupled with chromatographic analysis, *Acta Chromatogr.*, 12 (2020) 35.
- [9] W. A. Khan, Nanomaterials-based solid phase extraction and solid phase microextraction for heavy metals food toxicity, *Food Chem. Toxicol.*, 145 (2020) 111704.
- [10] W. Setyaningsih, T. Majchrzak, T. Dymerski, J. Namieśnik, M. Palma, Key-Marker volatile compounds in aromatic rice (*Oryza sativa*) Grains: An HS-SPME extraction method combined with GC × GC-TOFMS, *Molecules*, 24 (2019) 4180.
- [11] NR. Biata, KM. Dimpe, J. Ramontja, N. Mketi, PN. Nomngongo, Determination of thallium in water samples using inductively coupled plasma optical emission spectrometry (ICP-OES) after ultrasonic assisted-dispersive solid phase microextraction, *Microchem. J.*, 137 (2018) 214-22.
- [12] SZ. Mohammadi, A. Sheibani, F. Abdollahi, Speciation of Tl(III) and Tl(I) in hair samples by dispersive liquid–liquid microextraction based on solidification of floating organic

- droplet prior to flame atomic absorption spectrometry determination, *Arab. J. Chem.*, 9 (2016) S1510-S5.
- [13] O. B. Ifeoluwa, Harmful effects and management of indiscriminate solid waste disposal on human and its environment in Nigeria: A Review, *Glob. J. Res. Rev.*, 6 (2019) 1-7.
- [14] S. C. Ihenetu, F. C. Ihenetu, G. I. Kalu, Determination of heavy metals and physicochemical parameters of crude oil polluted soil from Ohaji Egbema Local Government in Imo State, *Open J. Yangtze Gas Oil*, 2 (2017) 161-167.
- [15] S. Zhu, J. Zhou, H. Jia, H. Zhang, Liquid-liquid microextraction of synthetic pigments in beverages using a hydrophobic deep eutectic solvent, *Food Chem.*, 243 (2018) 351-356.
- [16] A. Safavi, R. Ahmadi, A. M. Ramezani, Vortex-assisted liquid-liquid microextraction based on hydrophobic deep eutectic solvent for determination of malondialdehyde and formaldehyde by HPLC-UV approach, *Microchem. J.*, 143 (2018) 166-174.
- [17] S. McMichael, P. Fernández-Ibáñez, J. Byrne, A review of photoelectrocatalytic reactors for water and wastewater treatment, *Water*, 13 (2021) 1198.
- [18] D. Alrousan, A. Afkhami, K. Bani-Melhem, P. Dunlop, Organic degradation potential of real greywater using TiO₂ based advanced oxidation processes, *Water*, 12 (2020) 2811.
- [19] R. Ahmadi, G. Kazemi, A. M. Ramezani, A. Safavi, Shaker-assisted liquid-liquid microextraction of methylene blue using deep eutectic solvent followed by back-extraction and spectrophotometric determination, *Microchem. J.*, 145 (2019) 501-507.
- [20] K. Maheep, P. Vijay, Review on solid waste: Its Impact on air and water quality, *J. Pollut. Control*, 8 (2020) 242-252.
- [21] L. O. Odokumaand, A. A. Dickson, Bioremediation of a landfill polluted tropical rain-forest soil, *Global J. Environ. Sci.*, 2 (2003) 29-40.
- [22] A. M. Ramsay, P. J. Warren, A. T. Duke, R. Hill, Effect of bioremediation on the microbial community in oiled mangrove sediments, *Marine Pollut. Bull.*, 41 (2000) 413-419.
- [23] J. Sabate, M. Vinas, A. M. Solanas, Laboratory-scale bioremediation experiments on hydrocarbon-contaminated soil, *J. Int. Biodeter. Biodegr. J.*, 54 (2014) 19-25.
- [24] N. Raza, B. Hashemi, K.H. Kim, S.H. Lee, A. Deep, Aromatic hydrocarbons in air, water, and soil: sampling and pretreatment techniques, *TrAC- Trends Anal. Chem.*, 103 (2018) 56-73.
- [25] C. Labianca, Remediation of a petroleum hydrocarbon-contaminated site by soil vapor extraction: A full-scale case study, *Appl. Sci.*, 10 (2020) 4261.
- [26] M. Schaefer, F. Juliane, The influence of earthworms and organic additives on the biodegradation of oil contaminated soil, *Appl. Soil Ecol.*, 36 (2007) 53-62.
- [27] K. Van Gestel, J. Mergaert, J. Swings, Coosemans, J. Ryckebore, Bioremediation of diesel oil-contaminated soil by composting with biowaste, *Environ. Pollut.*, 5 (2001) 361-368.
- [28] N. Vasudevan, P. Rajaram, Bioremediation of oil sludge- contaminated soil, *Environ. Int.*, 26 (2001) 409-411.
- [29] D. Hou, D. O'Connor, A. D. Igalavithana, Metal contamination and bioremediation of agricultural soils for food safety and sustainability, *Nat. Rev. Earth Environ.*, 1 (2020) 366-381.
- [30] G. Qin, Soil heavy metal pollution and food safety in China: Effects, sources and removing technology, *Chemosphere*, 267 (2021)129205.
- [31] M. Walter, K.S.H. Boyd-Wilson, D. McNaughton, G. Northcott, Laboratory trials on the bioremediation of aged pentachlorophenol residues, *J. Int. Biodeter. Biodegr.*, 3 (2005) 121-130.
- [32] B. A. Wrenn, A. D. Venosa, Health effects of pollution, *Can. J. Microbiol.*, 42 (1996) 252-258.

- [33] K. Yones, F. Kiani, L. Ebrahmi, The effect of land use change on soil and water quality in northern Iran, *J. Mountain Sci.*, 9 (2012) 798–816.
- [34] P. Roccaro, M. Sgroi, F. G. Vagliasindi, Removal of xenobiotic compounds from wastewater for environment protection: Treatment processes and costs, *Chem. Eng. Trans.*, 3 (2013) 32-50.
- [35] Regulation for determining the status of surface waters; ministry of agriculture and rural development, Ministry of health and the ministry of sustainable development and tourism: Podgorica, Montenegro, 1–39, 2019.
- [36] Government of the republic of Montenegro: rulebook on classification and categorization of surface and ground water, 2021. https://www.morskodobro.com/dokumenti/uredba_klasifikacija_kategorizacija_podzemnih_voda.pdf.
- [37] S. A. Nsibande, P. Forbes, Fluorescence detection of pesticides using quantum dot materials e a review, *Anal. Chim. Acta*, 945 (2016) 9–22.
- [38] X. Cao, Z. Jiang, S. Wang, S. Hong, H. Li, C. Zhang, Metal–organic framework UiO-66 for rapid dispersive solid phase extraction of neonicotinoid insecticides in water samples, *J. Chromatogr. B*, 4 (2018) 1077–1078.
- [39] S. K. Selahle, N. J. Waleng, A. Mpupa, P. N. Nomngongo, Magnetic solid phase extraction based on nanostructured magnetic porous porphyrin organic polymer for simultaneous extraction and preconcentration of neonicotinoid insecticides from surface water, *Front. Chem.*, 6 (2020) 8-22.
- [40] R. Kachangoon, J. Vichapong, Y. Santaladchaiyakit, R. Burakham, S. Srijaranai, An eco-friendly hydrophobic deep eutectic solvent-based dispersive liquid–liquid microextraction for the determination of neonicotinoid insecticide residues in water, soil and egg yolk samples, *Molecules*, 12 (2020) 27-85.
- [41] E. A. Bessonova, V. A. Deev, L. A. Kartsova, Dispersive liquid–liquid microextraction of pesticides using ionic liquids as extractants, *J. Anal. Chem.*, 8 (2020) 99-129
- [42] I. Ykowska, J. Ziemblińska, I. Nowak, Modern approaches in dispersive liquid–liquid microextraction (DLLME) based on ionic liquids: A review, *J. Mol. Liq.*, 2 (2018) 319–393.
- [43] A. Szarka, D. Turková, S. Hrouzková, Dispersive liquid–liquid microextraction followed by gas chromatography–mass spectrometry for the determination of pesticide residues in nutraceutical drops, *J. Chromatogr. A*, 3 (2018) 126–134.
- [44] I. Timofeeva, A. Shishov, D. Kanashina, D. Dzema, A. Bulatov, on-line in-syringe sugaring-out liquid–liquid extraction coupled with HPLC-MS/MS for the determination of pesticides in fruit and berry juices, *Talanta*, 3 (2017) 76-117
- [45] M. Nasiri, H. Ahmadzadeh, A. Amiri, Sample preparation and extraction methods for pesticides in aquatic environments: A review, *TrAC – Trends Anal. Chem.*, 123 (2020) 115-172.
- [46] E. A. Songa, J. O. Okonkwo, Recent approaches to improving selectivity and sensitivity of enzyme-based biosensors for organophosphorus pesticides: a review, *Talanta*, 5 (2016) 289–304.
- [47] E. Bulska, A. Ruszczyńska, Analytical techniques for trace element determination, *Phys. Sci. Rev.*, 2 (2017) 1–14.
- [48] S. Zhang, W. Yao, J. Ying, H. Zhao, Polydopamine-reinforced magnetization of zeolitic imidazolate framework ZIF-7 for magnetic solid-phase extraction of polycyclic aromatic hydrocarbons from the air-water environment, *J. Chromatogr. A*, 4 (2016) 18–26.
- [49] L. Praker, B. Schuur, Solvent developments for liquid–liquid extraction of carboxylic acids in perspective, *Sep. Purif. Technol.*, 9 (2019) 35–57.
- [50] N. N. Hidayah, S. Z. Abidin, The evolution of

- mineral processing in extraction of rare earth elements using solid–liquid extraction over liquid–liquid extraction: a review, *Min. Eng.*, 3 (2017) 103–113.
- [51] J. M. Kokosa, Selecting an extraction solvent for a greener liquid phase microextraction (LPME) mode-based analytical method, *TrAC – Trends Anal. Chem.*, 2 (2019) 238–247.
- [52] J. Đorđević, G. T. Vladislavljević, T. Trtić-Petrović, Liquid-phase membrane extraction of targeted pesticides from manufacturing wastewaters in a hollow fibre contactor with feed-stream recycle, *Environ. Technol.*, 3 (2017) 78–84.
- [53] C. Zheng, L. Zhao, X. Zhou, Z. Fu, A. Li, Treatment technologies for organic wastewater, *Water Treat.*, 11 (2013) 250–286.
- [54] M. Hosseini, N. Dalali, S. Moghaddasifar, Ionic liquid for homogeneous liquid-liquid microextraction separation/preconcentration and determination of cobalt in saline samples, *J. Anal. Chem.*, 69 (2014) 1141–1146.
- [55] L. Fischer, T. Falta, G. Koellensperger, Ionic liquids for extraction of metals and metal containing compounds from communal and industrial waste water, *Water Res.*, 45 (2011) 4601–4614.
- [56] M. Mirzaei, N. Amirtaimoury, Temperature-induced aggregation ionic liquid dispersive liquid-liquid microextraction method for separation trace amount of cobalt ion, *J. Anal. Chem.*, 69 (2014) 503–508.
- [57] S. Khan, M. Soylak, T. G. Kazi, Room temperature ionic liquid-based dispersive liquid phase microextraction for the separation/preconcentration of trace Cd^{2+} as 1-(2-pyridylazo)-2-naphthol (PAN) complex from environmental and biological samples and determined by FAAS, *Biol. Trace Elem. Res.*, 156 (2013) 49–55.
- [58] J. Werner, Ionic liquid ultrasound-assisted dispersive liquid-liquid microextraction based on solidification of the aqueous phase for preconcentration of heavy metals ions prior to determination by LC-UV, *Talanta*, 182 (2018) 69–73.
- [59] R. Khani, F. Shemirani, Simultaneous determination of trace amounts of cobalt and nickel in water and food samples using a combination of partial least squares method and dispersive liquid–liquid microextraction based on ionic liquid, *Food Anal. Methods*, 6 (2013) 386–394.
- [60] B. Majidi, F. Shemirani, Salt-assisted liquid-liquid microextraction of Cr(VI) ion using an ionic liquid for preconcentration prior to its determination by flame atomic absorption spectrometry, *Microchim. Acta*, 176 (2012) 143–151.
- [61] S. Nizamani, T. G. Kazi, H. I. Afridi, Ultrasonic-energy enhance the ionic liquid-based dual microextraction to preconcentrate the lead in ground and stored rain water samples as compared to conventional shaking method, *Ultrasonics Sonochem.*, 40 (2018) 265–270.
- [62] L. Yao, X. Wang, H. Liu, Optimization of ultrasound-assisted magnetic retrieval-linked ionic liquid dispersive liquid–liquid microextraction for the determination of cadmium and lead in water samples by graphite furnace atomic absorption spectrometry, *J. Ind. Eng. Chem.*, 56 (2017) 321–326.
- [63] J. Rakhtshah, Separation and determination of cadmium in water samples based on functionalized carbon nanotube by syringe filter membrane- micro solid-phase extraction, *Anal. Methods Environ. Chem. J.*, 4 (2021) 5-15.
- [64] M. Ghazizadeh, Speciation and removal of selenium (IV, VI) from water and wastewaters based on dried activated sludge before determination by flame atomic absorption spectrometry, *Anal. Methods Environ. Chem. J.*, 4 (2021) 36-45.
- [65] N. Motakef Kazemi, Zinc based metal–organic framework for nickel adsorption in

- water and wastewater samples by ultrasound assisted-dispersive-micro solid phase extraction coupled to electrothermal atomic absorption spectrometry, *Anal. Methods Environ. Chem. J.*, 3 (2020) 5-16.
- [66] S. Ma, J. Li, L. Li, X. Shang, S. Liu, C. Xue, Liquid-liquid extraction of benzene and cyclohexane using sulfolane-based low transition temperature mixtures as solvents, experiments and simulation, *Energy Fuels*, 32 (2018) 8006–8015.
- [67] X. Wang, Q. C. Xu, C. G. Cheng, R. S. Zhao, Rapid determination of DDT and its metabolites in environmental water samples with mixed ionic liquids dispersive liquid-liquid microextraction prior to HPLC-UV, *Chromatographia*, 75 (2012) 1081–1085.
- [68] R. Zhang, X. Cheng, J. Guo, H. Zhang, X. Hao, Comparison of two ionic liquid-based pretreatment methods for three steroids' separation and determination in water samples by HPLC, *Chromatographia*, 80 (2017) 237–246.
- [69] O.G. Sas, I. Domínguez, Á. Domínguez, B. González, Using bis(trifluoromethylsulfonyl) imide based ionic liquids to extract phenolic compounds, *J. Chem. Thermodynamics*, 131 (2019) 159–167.
- [70] G. Garcia de Freitas Junior, TM. Florêncio, RJ. Mendonça, GR. Salazar-Banda, Rt. Oliveira, Simultaneous voltammetric determination of benzene, toluene and xylenes (BTX) in water using a cathodically, pre-treated boron-doped diamond electrode, *Electroanal.*, 31(2019) 554-559.
- [71] X. Li, Z. Jia, J. Wang, H. Sui, L. He, OA. Volodin, Detection of residual solvent in solvent extracted unconventional oil ore gangues, *J. Eng. Thermophys.*, 28 (2019) 499-506.
- [72] N. Sun, SQ. Wang, R. Zou, WG. Cui, A Zhang, T. Zhang, Q. Li, ZZ. Zhuang, YH. Zhang, J. Xu, MJ. Zaworotko, Benchmark selectivity p-xylene separation by a non-porous molecular solid through liquid or vapor extraction, *Chem. Sci.*, 10 (2019) 8850-8854.
- [73] S. Teimooria, A. H. Hassanib, M. Panaahie, Extraction and determination of benzene from waters and wastewater samples based on functionalized carbon nanotubes by static head space gas chromatography mass spectrometry, *Anal. Method Environ. Chem. J.*, 3 (2020) 17-26.
- [74] L. Mohammadi, E. Bazrafshan, M. Noroozifar, A. Ansari-Moghaddam, F. Barahuie, D. Balarak, Adsorptive removal of benzene and toluene from aqueous environments by cupric oxide Nanoparticles: kinetics and isotherm studies, *Hindawi, J. Chem.*, 2017 (2017) 206-219.
- [75] N. Ariffin, M. M. Abdullah, M. R. R. Zainol, M. F. Murshed, M. A. Faris, R. Bayuaji, Review on adsorption of heavy metal in wastewater by using geopolymer, In proceedings of the MATEC web of conferences, Ho Chi Minh, Vietnam, 10-23, 2016.
- [76] A. S. Mohammed, A. Kapri, R. Goel, Heavy metal pollution: Source, impact, and remedies. In biomangement of metal contaminated soils; Springer, Berlin/Heidelberg, Germany, 1–28, 2011.
- [77] M. M. Hussain, J. Wang, I. Bibi, M. Shahid, N. K. Niazi, J. Iqbal, I. A. Mian, S. M. Shaheen, S. Bashir, N. S. Shah, Arsenic speciation and biotransformation pathways in the aquatic ecosystem: The significance of algae, *J. Hazard. Mater.*, 4 (2020) 12-27.
- [78] C.Y. Lu, M.Y. Wey, Simultaneous removal of VOC and NO by activated carbon impregnated with transition metal catalysts in combustion flue gas, *Fuel Processing Technol.*, 88 (2007) 557–567.
- [79] J. Taylor, C. Shrubsole, P. Symonds, I. Mackenzie, M. Davies, Application of an indoor air pollution metamodel to a spatially-distributed housing stock, *Sci. Total Environ.*, 667 (2019) 390–399
- [80] Burden of disease from the joint effects of household and ambient air pollution, WHO:

Geneva, Switzerland, 2018.

- [81] A. Molina, V. Escobar-Barrios, J. Oliva, A review on hybrid and flexible CO₂ gas sensors, *Synth. Met.*, 270 (2020) 116602.
- [82] A. Chen, R. Liu, X. Peng, Q. Chen, J. Wu, 2D Hybrid Nanomaterials for Selective Detection of NO₂ and SO₂ using light on and off strategy, *ACS Appl. Mater. Interfaces*, 9 (2017) 37191–37200.
- [83] L. Barelli, G. Bidini, L. Micoli, E. Sisani, M. Turco, 13X Ex Cu zeolite performance characterization towards H₂S removal for biogas use in molten carbonate fuel cells, *Energy*, 160 (2018) 44–53.
- [84] Y. Belmabkhout, P.M. Bhatt, K. Adil, R.S. Pillai, A. Cadiou, A. Shkurenko, G. Maurin, G. Liu, W.J. Koros, M. Eddaoudi, Natural gas upgrading using a fluorinated MOF with tuned H₂S and CO₂ adsorption selectivity, *Nat. Energy*, 3 (2018) 1059–1066.
- [85] H.Y. Zhang, C. Yang, Q. Geng, H.L. Fan, B.J. Wang, M.M. Wu, Z. Tian, Adsorption of hydrogen sulfide by amine-functionalized metal organic framework (MOF-199): An experimental and simulation study, *Appl. Surf. Sci.*, 497 (2019) 143815
- [86] S.T. Magwaza, L.S. Magwaza, A.O. Odindo, A. Mditshwa, Hydroponic technology as decentralised system for domestic wastewater treatment and vegetable production in urban agriculture: A review, *Sci. Total Environ.*, 698 (2020) 134154.
- [87] H. Xiao, Q. Cheng, M. Liu, L. Li, Y. Ru, D. Yan, Industrial disposal processes for treatment of polychlorinated dibenzo-p-dioxins and dibenzofurans in municipal solid waste incineration fly ash, *Chemosphere*, 243 (2020) 12535.
- [88] M.Y. Wey, C.H. Fu, H.H. Tseng, K.H. Chen, Catalytic oxidization of SO₂ from incineration flue gas over bimetallic Cu–Ce catalysts supported on pre-oxidized activated carbon, *Fuel*, 82 (2003) 2285–2290.
- [89] O. Maass, P. Grundmann, Added-value from linking the value chains of wastewater treatment, crop production and bioenergy production: A case study on reusing wastewater and sludge in crop production in Braunschweig (Germany), *Resour. Conserv. Recycl.*, 107 (2016) 195–211.
- [90] J. M. Tobin, J. C. Roux, Mucor biosorbent for chromium removal from tanning effluent, *Water Res.*, 32 (1998) 1407–1416.
- [91] V. Prigione, M. Zerlottin, D. Refosco, V. Tigrini, A. Anastasi, Varese, Chromium removal from a real tanning effluent by autochthonous and allochthonous fungi, *Bioresour. Technol.*, 10 (2009) 2770–2776.
- [92] C. Chen, B. Liang, A. Ogino, X. Wang, M. Nagatsu, Oxygen functionalization of multiwall carbon nanotubes by microwaveexcited surface-wave plasma treatment, *J. Phys. Chem. C*, 113 (2009) 7659–7665.
- [93] K. H. Goh, T.T. Lim, Z. Dong, Application of layered double hydroxides for removal of oxyanions: A review, *Water Res.*, 2 (2008) 1343–1368.
- [94] L. Huang, M. He, B. Chen, B. Hu, Magnetic Zr-MOFs nanocomposites for rapid removal of heavy metal ions and dyes from water, *Chemosphere*, 4 (2018) 435–444.
- [95] D. Park, Y. S. Yun, J. M. Park, The past, present, and future trends of biosorption, *Biotechnol. Bioprocess Eng.*, 15 (2010) 86–102.
- [96] H. Shirkhanloo, M. Osanloo, M. Ghazaghi, H. Hassani, Validation of a new and cost-effective method for mercury vapor removal based on silver nanoparticles coating on micro glassy balls, *Atmos. Pollut. Res.*, (2017) 359–365.
- [97] H. Shirkhanloo, A. Khaligh, H. Zavvar Mousavi, A. Rashidi, Ultrasound assisted-dispersive-ionic liquid-micro-solid phase extraction based on carboxyl-functionalized nanoporous graphene for speciation and determination of trace mercury in water samples, *Microchem. J.*, 130 (2016) 245–254.

- [98] H. Shir Khanloo, A. Khaligh, HZ. Mousavi, A. Rashidi, Ultrasound assisted-dispersive-micro-solid phase extraction based on bulky amino bimodal mesoporous silica nanoparticles for speciation of trace manganese (II)/(VII) ions in water samples, *Microchem. J.*, 124 (2015) 637–645.
- [99] HZ. Mousavi, A.M. Rashidi, Ultrasound-assisted dispersive solid phase extraction of cadmium (II) and lead (II) using a hybrid nanoadsorbent composed of graphene and the zeolite clinoptilolite, *Microchim. Acta*, 182 (2015) 1263-1272.
- [100] J. Rakhtshah, N. Esmaili, A rapid extraction of toxic styrene from water and wastewater samples based on hydroxyethyl methylimidazolium tetrafluoroborate immobilized on MWCNTs by ultrasound-assisted dispersive cyclic conjugation-micro-solid phase extraction, *Microchem. J.*, 170 (2021) 106759.
- [101] R. Ashouri, Dynamic and static removal of benzene from air based on task-specific ionic liquid coated on MWCNTs by sorbent tube-headspace solid-phase extraction procedure, *Int. J. Environ.Sci. Technol.*, 18 (2021) 2377–2390.